THE ROLES OF ORPHAN NUCLEAR RECEPTORS IN THE ENDOCRINE PANCREAS

APPROVED BY SUPERVISORY COMMITTEE

Joyce Repa Ph.D

Jay Horton M.D.

Melanie Cobb Ph.D

Carole Mendelson Ph.D

DEDICATION

I dedicate this dissertation to my parents, Ming-Chi Chuang and Mei-Hui Chiang, who give me endless support and love to allow me to pursue my dream. I also would like to dedicate this work to my lovely wife, Tzuling Cheng for sharing the sacrifices and challenges that are required to accomplish this.

ACKNOWLEDGEMENT

I would like to thank my mentor, Dr. Joyce Repa for her inspiring guidance and advice during my study. What I have learned from her is not only the ability to design and conduct experiments to address a scientific question, but also how to appreciate the complexity and beauty of biomedical science. I would also like to thank my committee members, Dr. Jay Horton, Dr. Melanie Cobb, and Dr. Carole Mendelson for their precious time and suggestions to me. Also, I am grateful for all of our collaborators and friends that share reagents and information with me. Many thanks to former post-doc in the lab, Dr. Ji-Young Cha, who worked tirelessly with me to establish the islet isolation and phenotyping procedures. I appreciate my wife Tzuling Cheng, who is also a graduate student in UTSW for her suggestions in cell-imaging related studies. I would also like to acknowledge the assistances provided by our previous technician, Chun-Mei Yang. Finally, I am grateful to everyone in the Diabetes Center and Hypothalamic Center who generously came to my rescue whenever I needed a protocol, reagent, or advice to successfully accomplish my scientific goals.

THE ROLES OF ORPHAN NUCLEAR RECEPTORS IN THE ENDOCRINE PANCREAS

by

JEN-CHIEH CHUANG

DISSERTATION

Presented to the Faculty of the Graduate School of Biomedical Sciences

The University of Texas Southwestern Medical Center at Dallas

In Partial Fulfillment of the Requirements

For the Degree of

DOCTOR OF PHILOSOPHY

The University of Texas Southwestern Medical Center at Dallas

Dallas, Texas

August, 2008

THE ROLES OF ORPHAN NUCLEAR RECEPTORS IN THE ENDOCRINE PANCREAS

Jen-Chieh Chuang, Ph.D.

The University of Texas Southwestern Medical Center at Dallas, 2008

Supervising Professor: Joyce J. Repa, Ph.D.

The hormone insulin plays a critical role in carbohydrate metabolism of animals. The production and secretion of insulin by beta-cells of the pancreatic islet need to be tightly regulated to maintain proper blood glucose levels in the circulation. Dysfunction of this important endocrine system is responsible for diabetic mellitus. Over the last several years, research has suggested that the function and integrity of beta-cells can be dramatically affected by exposure to and accumulation of lipids. Several Orphan Nuclear Receptors (ONRs) have been identified and characterized in other cell types as "lipid sensors" that respond to elevated cellular lipid levels to regulate gene expression.

Therefore the goal of my thesis research is to evaluate the expression and role of these transcription factors on beta-cell function and glucose metabolism.

First, the complement of nuclear hormone receptors in mouse islets, and representative alpha- and beta- cell lines was determined by quantitative real-time PCR. Many nuclear receptors are expressed in the cells of the islet and several show differential expression levels under varying glucose conditions which suggests these nuclear receptors may be important for normal islet cell function.

Of particular interest to our group LXRβ, and to a lesser extent LXRα, are present in the beta cell of islets, and respond to synthetic LXR agonists to upregulate previously identified target genes. Exposing isolated mouse islets to the synthetic LXR agonist T1317 results in increased glucose-stimulated insulin secretion (GSIS). Incubation of islets from *Lxr*-null mice with this ligand has no effect on GSIS thus suggesting the T-compound effect is mediated by LXR. In addition, oral administration of T1317 to wild type, but not *Lxr*-null mice, altered islet GSIS in vivo and promoted efficient glucose clearance. These results suggest that activation of LXR in islet cells can modify islet function and help to control serum glucose levels. We also identified ChREBP as a novel target gene of LXR in the beta cells of the islet and characterized the importance of the LXR-ChREBP axis in insulin secretion from pancreatic islets.

In addition to LXR, HNF4γ is also an ONR of interest in beta cells. Real-time PCR results suggested that HNF4γ and HNF4α are highly expressed in the pancreatic beta cells. Losing the function of HNF4α in beta cells has been shown to cause a rare form of diabetes called MODY1 (maturity-onset diabetes of the young).

However, the importance of HNF4γ in beta cell function has not been addressed. We found that HNF4α and HNF4γ form a heterodimer in the beta cells of the islet. This interaction may be a novel way of regulating gene expression in the beta cells and may have functional significance in islets.

TABLE OF CONTENTS

PRIOR PUBLICATIONS

Abstract. "*Orphan nuclear receptor expression and action in the endocrine pancreas.*" **J. C. Chuang**, J. Y. Cha, J. J. Repa. ADA 2005 Scientific Sessions, San Diego, CA

Abstract. "*Orphan nuclear receptors of the endocrine pancreas: the role of LXR in insulin secretion.*" J. Y. Cha, **J. C. Chuang**, J. J. Repa. Keystone Islet Biology Symposium 2006

Abstract. "*Identification and characterization of HNF4a/HNF4g heterodimers in beta-cells of the mouse endocrine pancreas.*" **J. C. Chuang**, J. Y. Cha, T. Tanaka, J. Sakai and J. J. Repa. Keystone Nuclear receptor Symposium 2008. *Awarded Keystone Symposia Scholarship.*

Abstract. *Selective and potent PPARd agonist KD3010 improves glucose homeostasis in diabetic db/db mice and potentiates glucose-stimulated insulin secretion (GSIS) in mouse islets.* M.Guha, **J. C. Chuang**, J.J. Repa, E. Gardiner, J. Anderson, U. Banerjee, J. Malecha, A. Kabakibi, G.Oshiro, R.Heyman, S.Noble, A.Shiau, T. Rao. ADA 2008 Scientific Sessions

Submitted. *Nuclear hormone receptor expression in the endocrine pancreas.* **J. C. Chuang**, J. -Y. Cha, J.C. Garmey, R. G. Mirmira, J. J. Repa. Molecular Endocrinology.

Submitted. *ChREBP is a critical effector of glucose-stimulated insulin secretion in the mouse pancreatic islet*. J.-Y. Cha, **J.C. Chuang**, A. Villasenor, K. Uyeda, O. Cleaver, J. J. Repa. Cell Metabolism.

N. Gustavsson, Y. Lao, A. Maximov, **J. C. Chuang**, E. Kostromina, J. J. Repa, C. Li, G. K. Radda, T. C. Sudhof and W. Han. *Impaired insulin secretion and glucose intolerance in synaptotagmin-7 null mutant mice.* Proc Natl Acad Sci U S A, 2008. **105**(10): p. 3992-7.

In prep. *Identification and characterization of HNF4α/HNF4γ heterodimers in beta- cells of the mouse endocrine pancreas.* **J. C. Chuang**, J. Y. Cha, T. Tanaka, J. Sakai and J. J. Repa.

In prep. *Liver X receptor agonism augments glucose-stimulated insulin transcription and secretion in human islets.* T. Ogihara, J. Garmey, **J. C. Chuang**, J. J. Repa. K. L. Brayman. R.G. Mirmira, and C. Evans-Molina.

LIST OF FIGURES

LIST OF TABLES

LIST OF DEFINITIONS

qPCR – quantitative real-time PCR

NHR – Nuclear hormone receptor

ONR – Orphan nuclear receptor

LXR – Liver X receptor

PPAR – Peroxisome proliferator-activated receptor

HNF4α – Hepatocyte nuclear factor 4 alpha

HNF4γ – Hepatocyte nuclear factor 4 gamma

FXR – Farnesoid X-activated receptor

VDR – Vitamin D receptor

LBD – Ligand binding domain

DBD – DNA binding domain

AF-1 – Activation function 1

NLS – Nuclear localization signal

ChREBP – Carbohydrate responsive-element binding protein

ABCA1 – ATP-binding cassette transporter A1

ApoE – apolipoprotein E

SCD-1 – stearoyl CoA desaturase 1

SREBP1c – sterol regulatory element-binding protein 1c

IPGTT – Intraperitoneal glucose tolerance test

EMSA– Electrophoretic mobility shift assay

RIA– Radio immune assay

MODY – Maturity onset diabetes of the young

GSIS – Glucose induced insulin secretion

SAB – secretion assay buffer

Glut2 – Glucose transporter 2

ATP – Adenosine triphosphate

ADP – Adenosine diphosphate

WAT – White adipose tissue

GPCR – G protein-coupled receptor

RGS – Regulator of G-protein signaling

GRK – G protein-coupled receptor kinase

GLP-1 – Glucagon like peptide-1

GIP – Gastric inhibitory polypeptide

ADRA2A – Adrenergic receptor 2, type a

ADRB2A – Adrenergic receptor β2

BRS3 – Bombesin-like receptor 3

CCKAR – Cholecystokinin receptor A

CCKBR – Cholecystokinin receptor A

CNR – Cannabinoid receptor

GRPR – Gastrin-releasing peptide receptor

HCRTR – Orexin receptor

NMBR – Neuromedin B receptor

NPY2R – Neuropeptide Y receptor Y2

OPRD1 – Opioid receptor delta 1

OPRK1 – Opioid receptor kappa 1

P2RY1 – Purinergic receptor P2Y

P2RY14 – Purinergic receptor P2Y14

SSTR2 – Somatostatin receptor 2

TGR5 – G protein- coupled bile acid receptor 1

GCGR – Glucagon receptor

GPRC6A – G protein- coupled receptor 6A

LPC – Lysophosphatidylcholine

OEA – Oleoylethanolamide

CA – Cholic acid

CDCA – Chenodeoxycholic acid

LCA – Lithocholic acid

Syt - Synaptotagmin

CHAPTER ONE

Introduction

Functional anatomy of the endocrine pancreas

The pancreas is a glandular organ nestled next to intestine in the abdominal cavity of vertebrates (Figure 1.1 A). It contains exocrine and endocrine compartments that play important roles in digestive and hormone systems respectively. The exocrine pancreas makes up the majority of the pancreas mass and is composed of acinar cells and ductal cells. These cells synthesize and secret digestive enzymes and bicarbonate through a ductal system to intestine to help the processing of foods in the digestive tract. Specialized endocrine cells can be found embedded in the exocrine compartment and only occupy about 2% of cell mass in the pancreas (Figure 1.1 B). These cells form clusters called islets of Langerhans and are able to produce insulin, glucagon, and some other hormones that are secreted into the bloodstream. Together, these hormones produced by endocrine pancreas work on multiple tissues to maintain blood glucose levels within a narrow range.

In the islets, five distinct cell types have been identified and are characterized by the expression of different peptide hormones secreted from each cell type (Elayat, el-Naggar et al. 1995) (Figure 1.1 D). Beta-cells (β-cell) represent the most abundant cell type (65-80%) in the islet and are responsible for the production of insulin, alpha-cells (α-cell, 15-20%) are located on the periphery of the islet and secret glucagon, delta-cells (δ-cell, 3-10%) secrete somatostatin, pp-cells (3-5%) secrete pancreatic peptide, and the fifth cell type, epsilon-cells (ε-cell) secrete ghrelin. The expression of ghrelin in the islet is

The molecular mechanism of insulin secretion

Insulin secretion is primarily regulated by a feed-forward mechanism driven by the elevation of blood glucose. After a meal, the concentration of glucose in the bloodstream increases quickly and the glucose together with other nutrients are transported to all cells in the body through circulation. In the beta cells of the islet, glucose is transported into the cell by Glut2 (Slc2a2), a low-affinity but high-capacity glucose transporter that rapidly raises intracellular glucose levels to that of the bloodstream (Permutt, Koranyi et al. 1989). Once glucose enters the beta cell, it is metabolized by several enzymes sequentially to generate ATP. The resulting elevation of the ATP/ADP ratio causes the closure of ATP-dependent potassium channels (SUR1/Kir6.2) on the cell membrane and the accumulation of intracellular potassium leading to cell membrane depolarization. Upon depolarization, voltage-dependent calcium channels are opened to allow calcium influx (Ashcroft, Proks et al. 1994), which triggers the exocytosis of insulin-containing secretory vesicles (Figure 1.2). This insulin released in the circulation will then have effects on insulin sensitive tissues to increase the uptake of circulating glucose (muscle, and adipose tissue) and reduce gluconeogenesis (liver). Once the blood glucose level returns to a normal range (~5mM), glucose import into beta cell will decrease and the downstream events that lead to the secretion of insulin will be terminated.

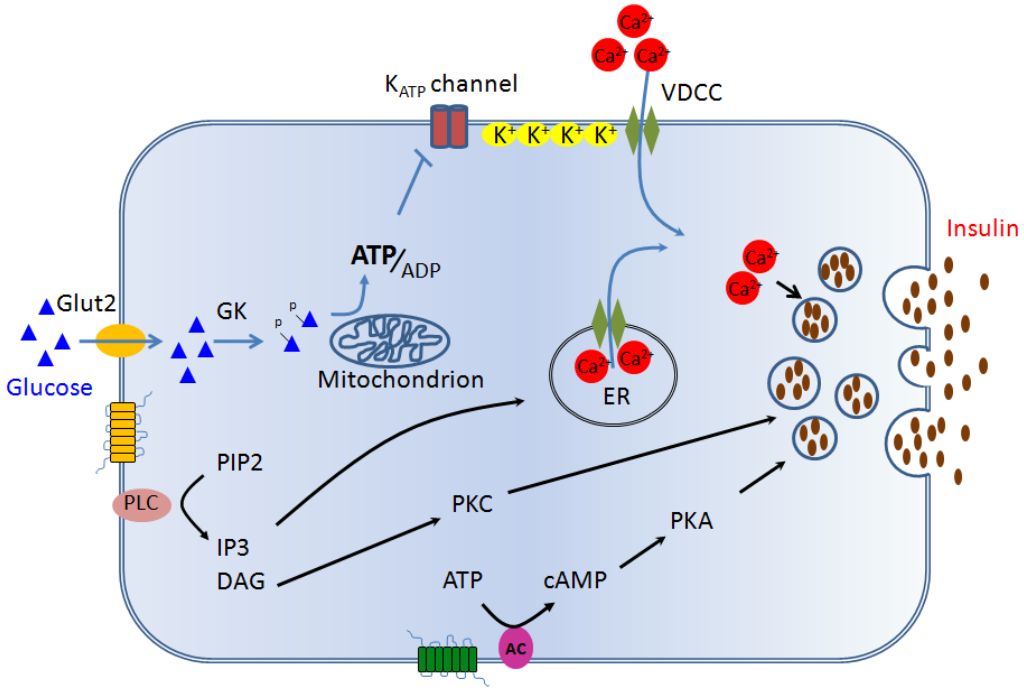

Fig. 1.2 Molecular mechanisms of insulin secretion from islet beta-cells.

Environmental cues that regulate endocrine pancreas

Being a master regulator of glucose homeostasis, the endocrine pancreas has to sense many environmental cues and respond properly. The major environmental cues that regulate islet function include hormones from other endocrine tissues, signals from the sympathetic/parasympathetic nervous system, and nutrient metabolites in the blood (Figure 1.3). Cells in islets are equipped with molecular sensor systems to receive these environmental signals, and these sensors are critical for islets' proper function. Many of the hormonal and neuronal factors bind to well characterized membrane receptors that lead to downstream signaling cascades to regulate gene transcription or insulin release. Nutrient metabolites are generally thought to act in an intracellular manner but with the

identification of nutrient regulated GPCRs, these signals can also be transmitted from the extracellular environment. The most well known nutritional factor to regulate islet function is glucose itself which was discussed earlier. In addition to glucose, many other nutrient intermediates are also known to regulate the function of islet cells. Several amino acids including arginine, alanine, and glutamate have also been shown to have effects on hormone secretion from islets (Fajans, Floyd et al. 1967). Recently, the importance of lipid molecules such as fatty acids and triglyceride on islet function has also been addressed (Jordan and Phillips 1978; Hjelte, Ahren et al. 1990; Yoshikawa, Tajiri et al. 2001). However, the molecular sensors for these lipid molecules in the islets cell are still poorly characterized.

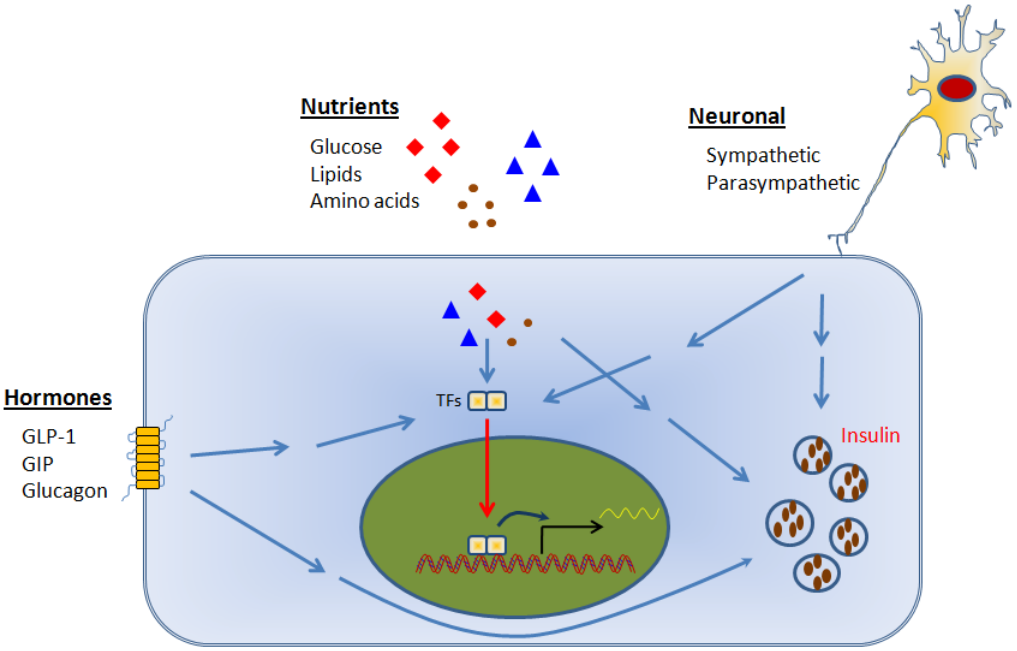

Fig. 1.3 Environmental cues that regulate beta-cell function.

Nuclear receptor superfamily as lipid sensors in the islet cells

Nuclear receptors are ligand-inducible transcription factors that directly link signaling molecules to transcriptional activities of target genes. The ligands for nuclear receptor are small, hydrophobic molecules including steroid hormones, vitamins, and metabolic intermediates. Targets genes of nuclear receptors participate in a wide range of physiological activities to affect development, proliferation, metabolism, reproduction, and immunity.

Nuclear receptor genes appear specific to multicellular organisms of the metazoan (animal) kingdom. Estrogen receptor (ER) was the first nuclear receptor identified by the use of tritiated-estradiol binding activity (Gorski, Toft et al. 1968; Jensen and DeSombre 1973; Jensen 2004). Shortly after, the glucocorticoid receptor was also cloned (Weinberger, Hollenberg et al. 1985), and based on the sequence similarities of these receptors, molecular techniques were used to identify a large number of nuclear receptor genes in several model organisms (Petkovich, Brand et al. 1987; Evans 1988; Laudet, Hanni et al. 1992; Mangelsdorf, Thummel et al. 1995). Unlike traditional endocrinology studies in which hormones and their biology were used to identify the receptors, these putative receptors were identified without knowledge of their physiological ligands. As a result, these receptors were called orphan nuclear receptors. The hunt for the endogenous ligands and characterization of the physiological functions for these orphan nuclear receptors has been the major goal of "reverse endocrinology" (Kliewer, Lehmann et al. 1999). After two decades of intensive research, physiological ligands for several of the orphan receptors have been found and these receptors are now referred to as 'adopted' orphan receptors (Allenby, Bocquel et al. 1993; Kliewer, Lenhard

et al. 1995; Janowski, Willy et al. 1996). Many of the newly identified ligands for the orphan receptors are hydrophobic metabolic intermediates including oxysterols, bile acids, and fatty acids. To date, there are 21 nuclear receptors in the genome of drosophila, 48 in human, 49 in mouse, and about 284 in *C.elegans*. Among them, many still remain orphans with their natural ligands awaiting identification.

Members of the nuclear receptor superfamily share a conserved structural organization. The variable N-terminal region (A/B domain) contains a ligand-independent transactivation region (AF-1). The DNA binding domain (DBD, C domain) is the most conserved region and contains two zinc finger motifs that allow the receptor to bind to specific sequences called hormone response elements (HREs) on genomic DNA. The hinge region (D domain) provides the structural flexibility for nuclear receptors to form various dimers and bind to DNA. The nuclear localization signal (NLS) of nuclear receptors is usually located in the junction of the DNA binding domain and hinge region. The ligand binding domain (LBD, E domain) is usually the largest protein region and is a multi-functional domain that participates in ligand binding, receptor dimerization, and ligand-dependent transactivation (AF-2). The LBD is very structurally conserved among nuclear receptors and is formed by the folding of 11-13 α-helixes. Some receptors have a C-terminal variable domain (F domain). The function of the F domain is not clear but some studies suggest that this domain may be responsible for co-factor recruitment and can fine-tune the molecular events associated with the transcriptional activity of the LBD domain. In some cases, the F domain has auto-repressive activity for receptors.

The fact that the ligands for many of the orphan nuclear receptors are small hydrophobic metabolic intermediates makes orphan nuclear receptors ideal lipid-molecule sensors for islet cells. Several nuclear receptors have indeed been reported to be able to regulate various aspects of islet function (Table 1.1).

Sex hormones such as estrogen and progesterone have been shown to modulate insulin secretion from islets (Costrini and Kalkhoff 1971; El Seifi, Green et al. 1981) and may contribute to the sexual dimorphism in diabetes (Bailey and Ahmed-Sorour 1980). Estrogen has been known to positively regulate insulin secretion and estrogen receptor alpha (ERα) has been proposed to provide protective effects in islets from toxicity of islet amyloid polypeptide (IAPP) (Geisler, Zawalich et al. 2002) and inflammatory cytokines (Eckhoff, Smyth et al. 2003). On the other hand, progesterone has been shown to inhibit insulin secretion (Howell, Tyhurst et al. 1977) and progesterone receptor (PR) null mice have improved insulin secretion and glucose homeostasis (Picard, Wanatabe et al. 2002).

Glucocorticoids have also been shown to inhibit insulin secretion (Barseghian and Levine 1980) and the glucocorticoid receptor (GR) has been shown to directly bind to the promoter of the insulin gene and repress the expression of insulin RNA (Goodman, Medina-Martinez et al. 1996).

In addition to steroid hormones, thyroid hormone also participates in regulating islet function. Hyperthyroidism has been known to a cause a decrease in insulin secretion and thyroid hormone receptor (TR) has been demonstrated to bind to the promoter of the insulin gene and repress insulin RNA expression (Clark, Wilson et al. 1995; Fukuchi, Shimabukuro et al. 2002). In addition, TR has also been shown to cause the activation of

the AKT pathway in β cells through a non genomic pathway (Verga Falzacappa, Petrucci et al. 2007).

Lipophilic vitamins such as Vitamin A (all-trans retinol) and Vitamin D (1, 25 dihydroxyvitamin D) are required for proper development of the endocrine pancreas (Clark, Stumpf et al. 1987; Matthews, Rhoten et al. 2004). Their receptors are the retinoic acid receptors (RARα, β, and γ) and Vitamin D receptor (VDR) respectively. In the adult islet, deficiency of these vitamins can cause impaired insulin secretion (Chertow, Blaner et al. 1987; Labriji-Mestaghanmi, Billaudel et al. 1988).

Recently, the role of PPARs in the islets has been the focus of many studies after they were discovered as the molecular targets of drugs widely used for the treatment of diabetes and hyperlipidemia. PPARα is the target of fibrates for treating lipid diseases and PPARγ is the target of Thiazolidinediones (TZD). Activation of PPARs has been shown to ameliorate insulin resistance in peripheral tissues and directly regulate insulin secretion as well. Endogenous fatty acids are low affinity ligands for PPARs and are known to regulate islet function at least partially through PPAR dependent mechanisms. More recently, the function of several other nuclear receptors including HNF4α, COUP-TF2, and SHP were also addressed.

Despite the accumulating data showing that members of the NR superfamily are important functional modulators of islet function, very little is known about the expression and function of the majority of nuclear receptor members in the islet. The goal of my studies is to establish a comprehensive understanding of the expression of these

receptors in cells of the pancreatic islet and to identify target genes and pathways by which these receptors impact islet function.

Advances in RNA technology have allowed me to quantitate receptors and their target genes in the mouse islets and representative α/β cell lines. The results of these studies will reveal novel therapeutic strategies to treat diabetes.

Table 1.1 Nuclear receptors that have been reported to regulate islet function.

Nuclear receptor	Ligands	Effect on islets	Species	Reference
ERα (NR3A1)	Estrogen	Suppress c-JNK; anti-inflammatory	Baboon, human, mouse	(Winborn, Sheridan et al. 1983; Heine, Taylor et al. 2000; Eckhoff, Smyth et al. 2003)
PR (NR3C3)	Progesterone	β cell growth; intracellular insulin degradation	Baboon, mouse	(Winborn, Sheridan et al. 1987; Sandberg and Borg 2007)
GR (NR3C1)	Glucocorticoid	Decrease insulin secretion/synthesis	Hamster	(Philippe and Missotten 1990),(Goodman, Medina-Martinez et al. 1996)
TRb (NR1A2)	Thyroid	Akt activation	Cell line (rRINm5f)	(Verga Falzacappa, Petrucci et al. 2007)
RAR	Retinoic acid	Required for fetal islet function	Rat	(Chertow, Blaner et al. 1987; Chertow, Goking et al. 1997; Driscoll, Adkins et al. 1997; Kadison, Kim et al. 2001)

still controversial in that some reports suggest that it is expressed in α-cells (Date, Nakazato et al. 2002), and some suggest that it is produced in unique, ε-cells (Wierup, Svensson et al. 2002). These hormones work together as important regulators for glucose homeostasis. By synthesizing and secreting these hormones, the endocrine pancreas is the master regulator of glucose metabolism. Islets can be separated from the exocrine compartment by carefully digesting the pancreas with collagenase (Figure 1.1C). Cultured islets maintain many of their *in vivo* characteristics such as glucose stimulated insulin secretion (GSIS) and thus provide an ideal culture model to investigate the complexity of islet physiology.

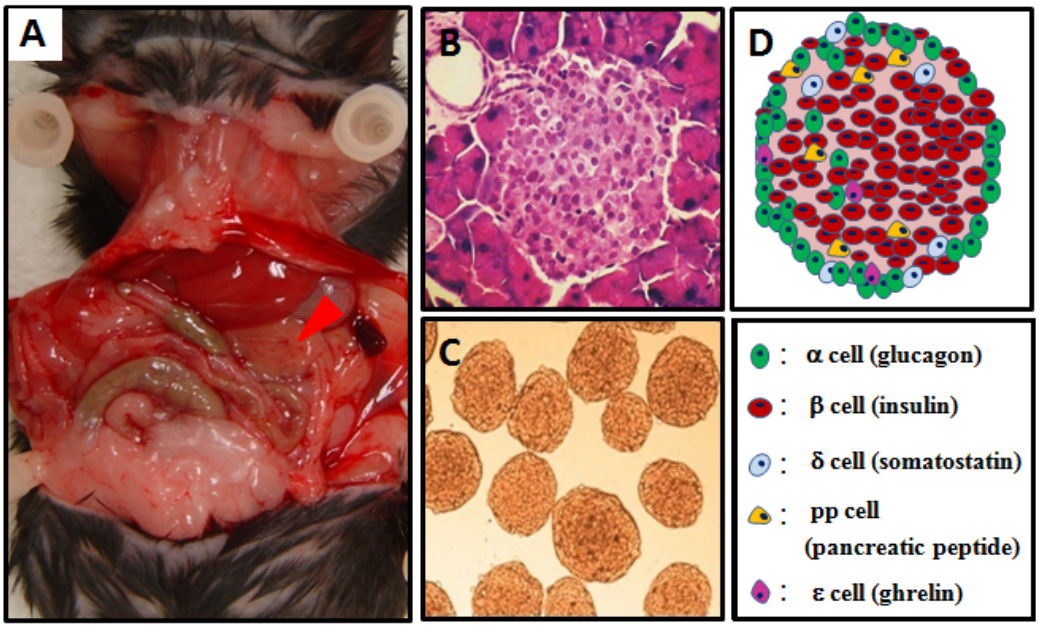

Fig. 1.1 Functional anatomy of the endocrine pancreas.
Pancreas (Red arrow head) is a glandular organ situated next to the intestine in the abdominal cavity (A). The endocrine pancreas (islet) is surrounded by exocrine tissue in the pancreas (B, H&E staining). Islets isolated from mouse can be maintained in culture for up to 2 weeks and used for a variety of ex-vivo studies (C). Specialized cells in the islet exhibit a distinctive distribution in the islet and are responsible for the production and secretion of a wide variety of peptide hormones (D).

RXR	*9-cis*-retinoic acid	Prevent islet degeneration	Mouse	(Lenhard, Lancaster et al. 1999)
VDR (NR1I1)	Vitamin D	Required for normal islet function	Human, rat	(Johnson, Grande et al. 1994; Lee, Clark et al. 1994; Chang, Lei et al. 2000)
PPARα (NR1C1)	Fatty acids/ fibrates	Required for TG homeostasis in islet	Rat	(Zhou, Shimabukuro et al. 1998; Yoshikawa, Tajiri et al. 2001)
PPARδ (NR1C2)	Fatty acids	Improve islet hyperplasia in *ob/ob* mice	Mouse	(Tanaka, Yamamoto et al. 2003)
PPARγ (NR1C3)	Fatty acids/ TZDs	Improve islet hyperplasia	Rat, mouse	(Buckingham, Al-Barazanji et al. 1998; Kameda, Okuya et al. 2000)
LXRβ (NR1H2)	Oxysterols	Increase GSIS	Mouse	(Efanov, Sewing et al. 2004; Gerin, Dolinsky et al. 2005), and current study
HNF4α (NR2A1)	Fatty acids	Mutations cause MODY1	Human, mouse	(Nakajima, Yoshiuchi et al. 1996; Odom, Zizlsperger et al. 2004)
COUP-TFII (NR2F2)	Orphan	Islet development	Mouse	(Zhang, Bennoun et al. 2002)
SHP (NR0B2)	Orphan	Positively regulate GSIS	Cell line (INS-1)	(Suh, Kim et al. 2004)

CHAPTER TWO

Expression of orphan nuclear receptors in the endocrine pancreas

Abstract

The endocrine pancreas is comprised of the islets of Langerhans, tiny clusters of cells that contribute only about 2% to the total pancreas mass. However, this little endocrine organ plays a critical role in maintaining glucose homeostasis by the regulated secretion of insulin (by beta-cells) and glucagon (by alpha-cells). The rapid increase in incidence of diabetes worldwide has spurred renewed interest in islet cell biology. Some of the most widely prescribed oral drugs for treating type 2 diabetes include agents that bind and activate the nuclear hormone receptor, PPARγ. As a first step in addressing potential roles of PPARγ and other nuclear hormone receptors (NHR) in the biology of the endocrine pancreas, we have used quantitative real-time PCR to profile the expression of all 49 members of the mouse NHR superfamily in primary islets, and cell lines that represent alpha-cells (αTC1) and beta-cells (βTC6 and MIN6). In summary, 19 NHR members were highly expressed in both alpha- and beta-cell lines, 13 receptors showed predominant expression (at least an 8-fold difference) in alpha- versus beta-cells, and 10 NHR were not expressed in the endocrine pancreas. In addition we evaluated the relative expression of these transcription factors during hyperglycemia and found that 16 NHR showed significantly altered mRNA levels in mouse islets. A similar survey was conducted in primary human islets to reveal several significant differences in the NHR expression between mouse and man. These data identify potential therapeutic targets in the endocrine pancreas for the treatment of diabetes mellitus.

Introduction

The incidence of diabetes mellitus is increasing at an alarming rate. The World Health Organization estimates that over 180 million people worldwide have diabetes. In the United States alone, the American Diabetes Association reports that roughly 7% of the population has diabetes. Some of the most widely prescribed oral drugs for treating type 2 diabetes include agents that bind and activate the peroxisome proliferator-activated receptor-γ (PPARγ) (Lehmann, Moore et al. 1995). PPARγ is one of the 48 members of the nuclear hormone receptor (NHR) superfamily of transcription factors (mice have FXRβ, thus have 49 members). In animal studies, additional nuclear hormone receptor ligands have been shown to have potent serum glucose-lowering effects. Synthetic agonists for the retinoid X receptor (RXR, (Mukherjee, Davies et al. 1997)), liver X receptor (LXR, (Cao, Liang et al. 2002; Laffitte, Chao et al. 2003)), PPARδ (Tanaka, Yamamoto et al. 2003), and farnesoid X receptor (FXR, (Zhang, Lee et al. 2006)) all have been reported to lower serum glucose levels in rodent models of diabetes.

While many of the positive effects of these NHR agonists have been attributed to improved insulin sensitivity and glucose clearance by peripheral tissues, there has been increased interest in their potential role in the endocrine pancreas: can they improve glucose responsiveness, insulin secretion or survival of beta-cells, or alter glucagon production and secretion by alpha-cells? As a first step in answering these questions, we have performed a comprehensive survey to identify the complement of NHR expressed in mouse primary islets and cell lines and in human islets of Langerhans.

Materials and methods

Animals

All tissues and islets were obtained from 3-month old, male A129/SvJ mice. Mice were maintained in a temperature-controlled room (23 ± 1°C) with 12 hours light (7 am – 7 pm)/dark cycle and ad libitum access to water and a standard rodent diet (Harlan Teklad Premier Laboratory Diet #7001). Tissues were harvested in early morning with mice in the fed-state.

Islet isolation and culture

The mouse pancreas was perfused and digested with liberase R1 (Roche). Islets were then isolated using Ficoll gradient centrifugation and hand-selection under a stereomicroscope for transfer to RPMI 1640 medium (11.1 mM glucose) supplemented with 10% (v/v) heat-inactivated fetal bovine serum, 100 IU/ml penicillin, and 100 μg/ml streptomycin (Invitrogen). These culture conditions are routinely used for murine islet studies to avoid apoptotic cell death and preserve optimal glucose-stimulated insulin secretion capacity. Islets were allowed to recover overnight (37°C, 5% CO_2) before further use. Typically 10-12 mice were used to isolate islets that would be pooled for each group then distributed evenly among multiple wells (200 islets/well) for each assay condition. To determine the effect of glucose, mouse islets and cell lines were incubated in 3 mM glucose for 8 hours, then shifted to 5 mM (low glucose) or 17.5 mM (high glucose) for 16 hours before RNA isolation. All experiments were performed a minimum of two times.

Human islet experiments

Human islets (obtained from cadaver pancreas of a nondiabetic individual) were procured at the University of Virginia (Kindly provided by Dr. Raghavendra G. Mirmira). Islets were maintained in 5.6 mM glucose in the presence of 10% fetal bovine serum prior to RNA isolation.

Cell culture

The insulinoma cell line Beta-TC-6 ([CRL-11506], (Poitout, Stout et al. 1995)) and the adenoma-derived glucagonoma cell line alphaTC1-clone 9 ([CRL-2350], (Powers, Efrat et al. 1990)) were obtained from American Type Tissue Culture. The MIN6 cell line (Miyazaki, Araki et al. 1990) was kindly provided by Dr. Melanie Cobb (UT Southwestern). Cells were maintained in their optimal culture conditions unless indicated otherwise. Beta-TC6 cells were routinely cultured in DMEM (4.5g/L glucose, 4 mM L-glutamine) with 15% heat-inactivated FBS. MIN6 cells were maintained in DMEM (4.5g/L glucose); 2 mM L-glutamine, 1 mM sodium pyruvate and 10% heat-inactivated FBS. Alpha-TC1 cells were cultured in DMEM with 4 mM L-glutamine adjusted to contain 1.5 g/L sodium bicarbonate and 3 g/L glucose with 10% heat-inactivated dialyzed FBS, further supplemented with 15 mM HEPES, 0.1 mM non-essential amino acids and 0.02% BSA.

RNA measurement

RNA was isolated from tissue samples or cultured cells using RNA STAT-60 (Tel-Test Inc.) and 2 μg of total RNA was treated with RNase-free DNase (Roche), then reverse-

transcribed with random hexamers using SuperScript II (Invitrogen)., as previously described in detail (Kurrasch, Huang et al. 2004).

Quantitative real-time PCR (qPCR) was performed using an Applied Biosystem Prism 7900HT sequence detection system and SYBR-green chemistry (Kurrasch, Huang et al. 2004; Valasek and Repa 2005). Gene-specific primers were designed using Primer Express Software (PerkinElmer Life Sciences) and validated by analysis of template titration and dissociation curves. Primer sequences are provided in Table 1 for mouse genes and primer sequences used for the measurement of human NHR are available at www.nursa.org/10/1621/datasets.04011. 10 μl qPCR reactions contained 25 ng of reverse-transcribed RNA, each primer (150 nM) and 5 μl of 2X SYBR Green PCR master mix (Applied Biosystems). Multiple housekeeping genes were evaluated in each assay to insure that their RNA levels were invariant under the experimental conditions of each study. Results of qPCR were evaluated by the comparative Ct method (user bulletin No.2, Perkin Elmer Life Sciences) using hypoxanthine-guanine phosphoribosyl transferase (HPRT) or cyclophilin as the invariant control gene.

Statistics

Values shown reflect the mean ± SEM, n=3 samples per tissue or cell line. Two-tailed Student's t-test was performed to compare low- and high-glucose treated samples (Fig 2.5), and significance was established at $p<0.05$.

Results

The expression of NHR in mouse islets and cell lines recognized as models for cells of the endocrine pancreas was determined by quantitative real-time PCR (qPCR). This technique is extremely sensitive, can utilize small amounts of RNA (thus allowing measurement with RNA from islets), provides a quantitative assessment of RNA species across a large linear range of values, and can analyze sufficient sample numbers to depict RNA levels as an average with biologic variance (Valasek and Repa 2005). In all qPCR analyses that were performed for our NHR survey, four tissues from young adult, male A129/SvJ mice were included as positive controls. NHR play a critical role in metabolism (adipose, liver), reproduction (testis) and nervous system (whole brain), and among these four tissues all 49 mouse nuclear hormone receptors are expressed at appreciable levels (Bookout, Jeong et al. 2006). Cyclophilin was selected as the housekeeping gene to use as the invariant control for each tissue, as previous northern analyses demonstrated that cyclophilin is expressed at equivalent levels in these four organs (Repa and Mangelsdorf 2000), and we determined that it was similarly expressed in mouse islets and cell lines relative to total RNA content (data not shown).

This survey of receptor expression is first presented by subfamily classification showing mRNA levels in islets and cell lines relative to various mouse tissues. This format is consistent with previous NHR surveys and provides a basis of comparison to tissues commonly associated with each receptor type.This receptor classification system is based on sequence similarity and phylogenetic tree construction and most often correlates with DNA-binding and dimerization characteristics (Figures 2. 1- 2.3 (Nuclear Receptors Nomenclature Committee 1999; Germain, Staels et al. 2006)). Additional

general information on any of the nuclear hormone receptors can be found in reviews (Germain, Staels et al. 2006; Benoit, Cooney et al. 2007) or at the website for the Nuclear Receptor Signaling Atlas (http://www.nursa.org/index.cfm). In addition, since this survey focused on expression in a select few cell types (islets, cell lines), we could analyze RNA levels for all receptors in a single assay for direct comparison of NHR levels within a given tissue. This rank order of expression is provided in Fig. 2.4. Finaly, we were able to obtain RNA from human islets to compare the relative expression of all 48 NHR in this tissue source (Fig. 2.4).

Nuclear hormone receptor subfamily 1 (Fig. 2.1)

The majority of these receptors function as RXR heterodimer partners (TRs, RARs, PPARs, LXRs, FXRs, VDR, PXR, and CAR) that respond to small lipophilic ligands of dietary origin to regulate gene expression (Chawla, Repa et al. 2001). Thyroid receptors are expressed in the endocrine pancreas at much lower levels than in other tissues, however among the receptors of the islet, TRα is found at appreciable levels and TRβ is expressed at moderate amounts (Fig. 2.4). RARγ is the most abundant of the RAR subtypes in the islet and beta-cell (Figure 2.1 and 2.4). PPARδ is highly expressed in mouse islets, alpha-cells and beta-cells, and is the most prominent of the PPARs. LXRβ is more highly expressed than LXRα in beta-cells and islets, in agreement with previous reports (Efanov, Sewing et al. 2004). FXRα mRNA is present in intact mouse islets, yet there is no evidence that this receptor is found in the alpha- or beta-cell lines examined in this study. This suggests that FXRα is present in one of the minor cell

types of the islet (δ–cells, ε–cells or PP-cells) or that these immortalized cell lines have lost expression of this receptor. Further confirmation that islets express FXRα was provided by the finding that islets exposed to synthetic FXR agonists alter the expression of several recognized FXR target genes (Kjallarsdottir & Repa, unpublished). FXRβ, a nuclear hormone receptor unique to mice (a pseudogene in humans (Robinson-Rechavi, Carpentier et al. 2001; Otte, Kranz et al. 2003)) is not expressed in the endocrine pancreas. The vitamin D receptor is highly expressed in islets, and represents the fourth most abundant nuclear hormone receptor, based on its level of RNA expression (Fig. 2.4).

The remaining members of subfamily 1 are thought to function as constitutive repressors (RevERBs) or activators (RORs) that play an important role in the regulation of circadian rhythm (Yang, Downes et al. 2006). RevERBβ and RevERBα are highly expressed in alpha-cells, and RevERBβ is also expressed in beta-cells and islets. All ROR members are expressed, again showing the highest expression in alpha-cells. In fact, the RORβ RNA level in alpha-cells is equivalent to that of brain, the mouse tissue exhibiting highest expression of this receptor (Bookout, Jeong et al. 2006).

In summary a large number of the lipid-activated receptors are present in cells of the endocrine pancreas, and several reports have appeared to suggest that ligands for some of these receptors affect insulin secretion, including the LXRs, (Efanov, Sewing et al. 2004; Gerin, Dolinsky et al. 2005), PPARα, (Tordjman, Standley et al. 2002; Bihan, Rouault et al. 2005; Ravnskjaer, Boergesen et al. 2005), PPARγ (Shimabukuro, Zhou et al. 1998), and VDR (Bourlon, Billaudel et al. 1999). In addition, receptors associated

HNF4α plays a fundamental role in the function of the mouse islet (Gupta, Vatamaniuk et al. 2005; Miura, Yamagata et al. 2006). Inactivating mutations in the human HNF4α gene are responsible for maturity onset diabetes of youth (MODY1, (Shih, Dansky et al. 2000)). HNF4α is expressed in beta-cells of the mouse islet at levels far below that seen in liver (Fig. 2.2), and represent the HNF4α7 and 8 isoforms, rather than the HNF4α1 and 2 isoforms of mature hepatocytes ((Briancon and Weiss 2006) and Fig. 4.1). The closely related receptor, HNF4γ, is highly expressed in islets, exclusively in beta-cells (Fig. 2.2 and 4.1). The common heterodimer partner, RXR, is expressed in islets, and the isoforms are found in the rank order RXRα >> RXRβ>>>RXRγ (Fig. 2.4). The testicular receptors, TR2 and TR4, which function as homodimers and heterodimers, are highly expressed in islets, in fact TR4 exhibits the highest relative RNA level of all the 49 mouse nuclear hormone receptors (Fig. 2.4). TLX is not expressed, and PNR is found at very low levels in the endocrine pancreas. The orphan monomeric receptors, COUP-TFs, are expressed with the following relative abundance: COUP-TFIII > COUP-TFII > COUP-TFI.

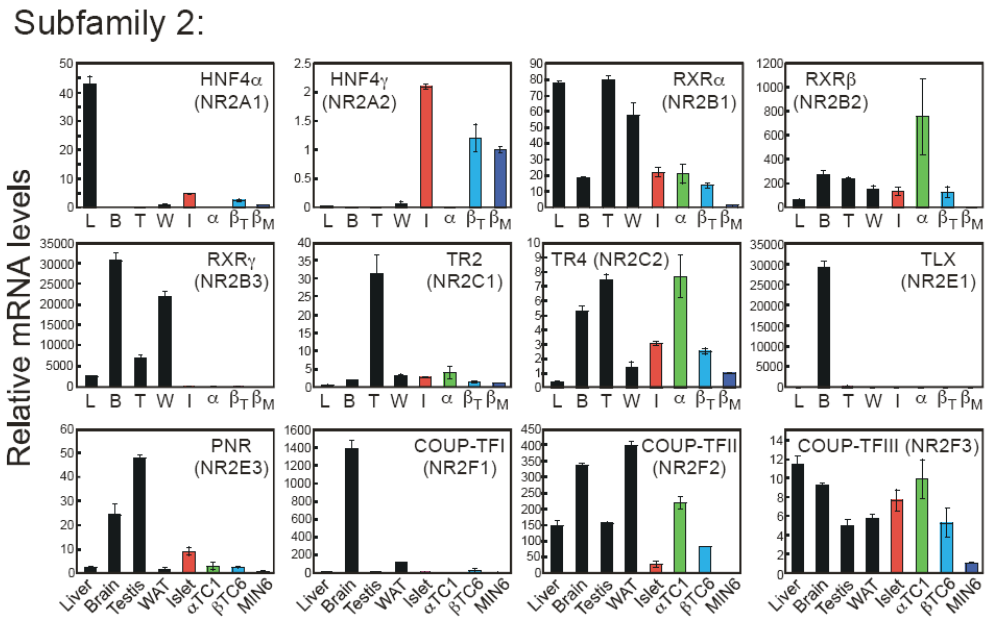

Fig. 2.2 Nuclear receptors expressed in the mouse endocrine pancreas: subfamily 2. Refer to the legend of Figure 1 for details.

Nuclear hormone receptor subfamilies 3 & 4 (Fig. 2.3)

Subfamily 3 contains the steroid receptors. The estrogen receptors are expressed in islets and cell lines at very low levels relative to other mouse tissues. GR is highly expressed in alpha-cells. The rank order of the steroid receptors in mouse islets is MR >> GR >> AR = PR = ERα > ERβ. Among the estrogen receptor-related receptors, ERRα and γ are highly expressed in islets, particularly in alpha-cells.

The NR4 members of the nuclear hormone receptor superfamily, are expressed in the following rank order: NGFIB >>> NURR1 = NOR1, and are found in intact islets as well as both beta- and alpha-cell lines.

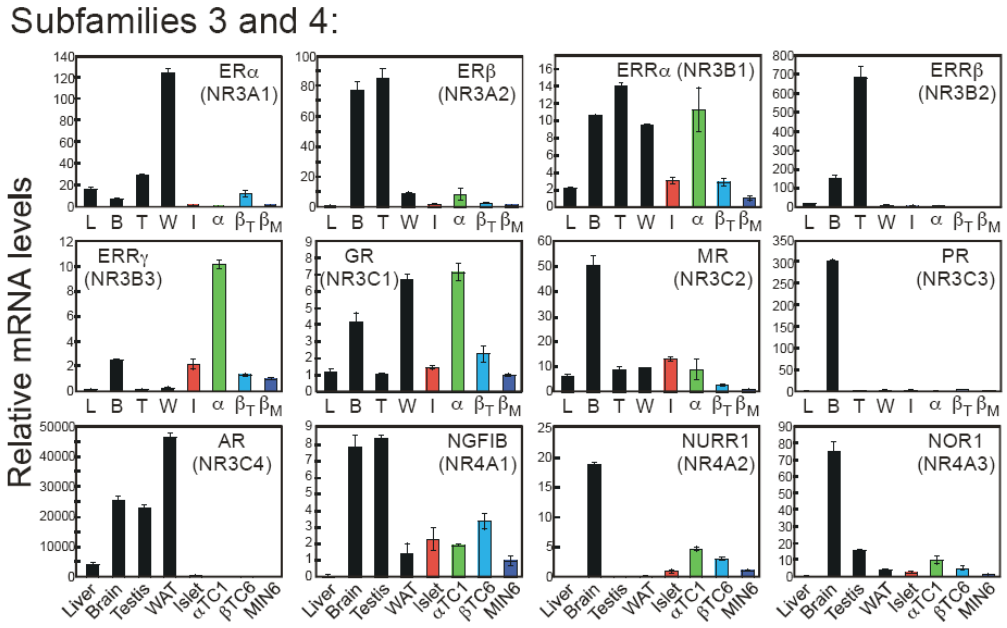

Fig. 2.3 Nuclear receptors expressed in the mouse endocrine pancreas: subfamilies 3 and 4. Refer to the legend of Figure 1 for details.

Nuclear hormone receptor subfamilies 5, 6, and 0 (Fig. 2.1)

There is no detectable RNA for the Steroidogenic Factor, SF1, in the mouse endocrine pancreas. The highly related protein, liver receptor homolog, LRH-1, was originally cloned from the pancreas (Becker-Andre, Andre et al. 1993), and its distribution has been evaluated by in situ hybridization to reveal that it is highly expressed in the exocrine pancreas (Fayard, Schoonjans et al. 2003). Our results confirm the lack of LRH-1 expression in beta-cells, but indicate that LRH-1 mRNA is present in an alpha-cell line at a level equivalent to that seen in liver tissue.

The Germ Cell Nuclear Factor, GCNF, is the sole member of subfamily 6, and plays critical roles in development and reproduction (Zhao, Li et al. 2007). There are detectable levels of GCNF mRNA in mouse islets, alpha- and beta-cells (Fig 2.1).

The receptors of subfamily 0 are unique in that they lack the conventional DNA-binding domain that defines the NHR family of transcription factors. DAX-1 is not expressed in the mouse endocrine pancreas, and SHP is found at very low levels in beta-cells (Fig 2.1).

Nuclear hormone receptor rank order of expression (Fig. 2.4) and comparison to mRNA levels in human islets.

The design of these studies allowed for a rank order determination of RNA levels for NHR within a given cell type. The PCR primers were designed to provide equivalent PCR amplification efficiency (Valasek and Repa 2005) and showed no evidence of product formation in the absence of template cDNA. Therefore, as all of these analyses were performed on the same triplicate samples for each tissue and cell type, we could compare the relative expression of all 49 NHR to one another within a given tissue (Fig. 2.4). In mouse islets the 6 most abundant receptors are TR4, RevERBβ, RORγ, VDR, RevERBα, and RXRα. Placing the NHR of the beta-cell line (MIN6) and the alpha-cell line in a similar arrangement, one can easily see the differences in relative expression of the receptors in these cells. MIN6 cells express relatively lower levels of RORγ, VDR, RevERBα, and RXRα than intact islets. The alpha cell line expresses no VDR, and higher levels of RORβ, LRH-1, PPARα, and TRα than islets or the beta-cell lines.

A similar survey of NHR transcripts in human islets was performed and revealed significant differences as compared to the receptor expression pattern observed in mouse (Fig. 2.4). The most abundant receptor is human islets is LRH-1, which is present at mRNA levels equivalent to the housekeeping gene cyclophilin (CT ~ 21.5). This increase may be partly attributable to the larger contribution of alpha-cells in the human islet (Cabrera, Berman et al. 2006), but also suggests that LRH-1 may play a more important role in the development and/or function of the endocrine pancreas in humans than rodents. The second most abundant NHR is COUP-TFIII, which falls into subtype rank order (COUP-TFIII > TFII > TFI) similar to that observed in mouse islets. ERα, HNF4α, and GR mRNA species are present at levels similar to the housekeeping gene HPRT1 (CT = 24), and receptors indicated by bars with heights greater than that shown for RARγ (CT = 26) would be declared “abundant” by the criteria used to rank receptor expression in the mouse islet.

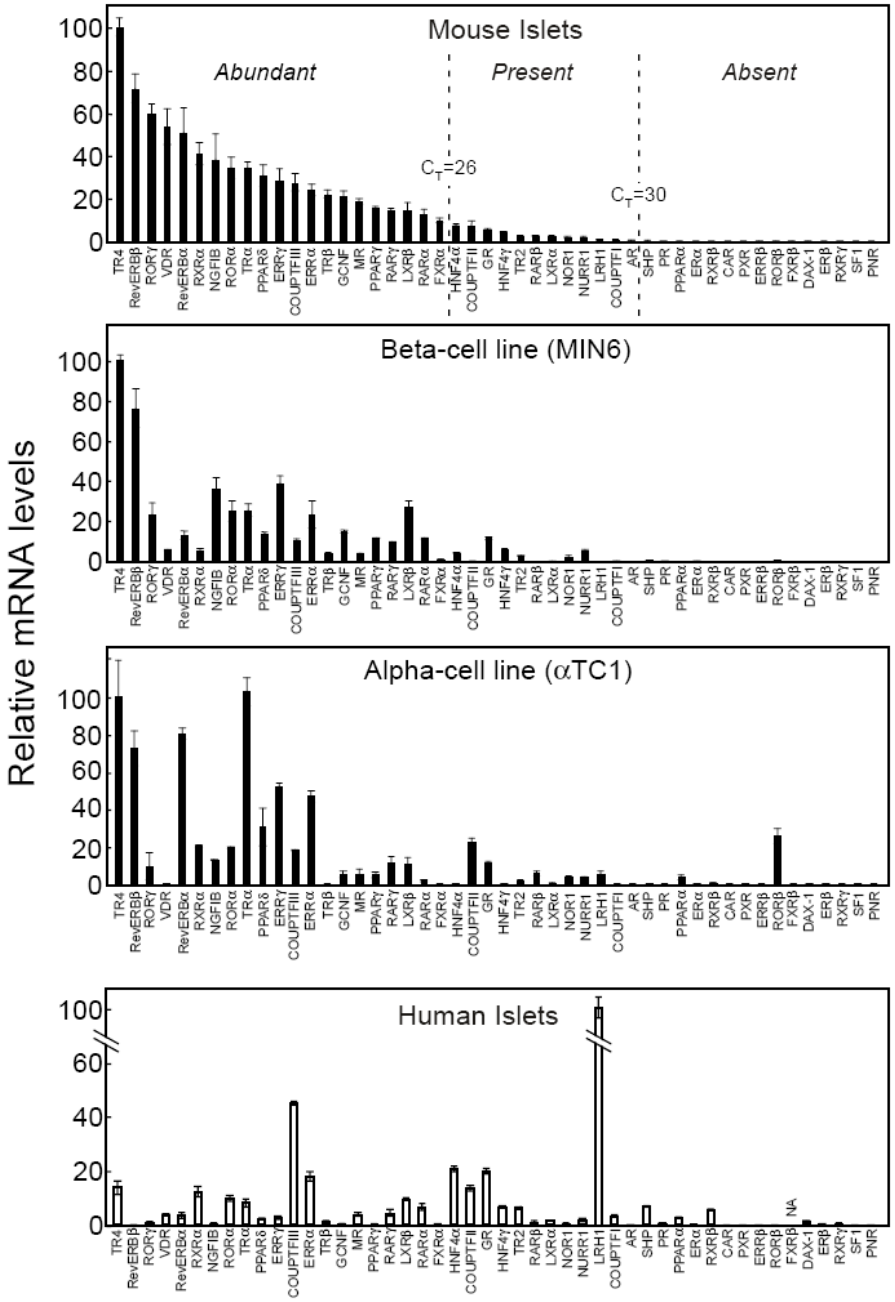

Fig. 2.4 Comparative expression levels of the 49 NHR for mouse islets, cell lines and human islets. The relative mRNA levels are depicted for mouse islets, beta-cells (MIN6 cell line) and alpha-cells (α−TC1), and human islets. All values are expressed relative to cyclophilin, and arithmetically adjusted to depict the highest-expressed NHR for each tissue/cell line as a unit of 100. Values represent the means and SEM of three

independent samples for each tissue or cell line. Note that comparisons can only be made between the NHRs within a tissue or cell type. Setting arbitrary cut-offs at $C_T < 26$ (abundant); $26 < C_T < 30$ (present); $C_T > 30$ (absent) as shown by broken lines in the mouse islet panel, reveals that 19 NHR are highly expressed in both alpha- and beta-cells; 5 NHR are predominant (greater than 8-fold difference in RNA level) only in beta-cell lines; 8 only in the alpha-cell line; and10 not expressed in the mouse endocrine pancreas or cell lines. For the analysis of human islets, these cutoffs correspond to bars of height greater or equal to RARγ (CT ~ 26, abundant) and less than PPARγ (CT = 30, absent).

Glucose regulation of nuclear hormone receptor expression in mouse islets and beta-cells (Fig. 2.5)

One of the most important functions of the endocrine pancreas is to respond to elevated circulating glucose by secreting insulin. Therefore, we also evaluated the expression of the 49 mouse NHR in islets to determine whether changes in RNA levels occur during hyperglycemia, thus suggesting they may play a role in the glucose-response of this organ. Islets were exposed to low-glucose (5 mM) or high-glucose (17.5 mM) conditions for 16 hours prior to RNA isolation. Although our aim was to evaluate the impact of elevated glucose on NHR gene expression, the 16h high-glucose exposure resulted in very high insulin levels in the culture media (insulin concentrations of 37 ng/ml for the low-glucose treated islets and 408 ng/ml, or approximately 70 nM, for the high-glucose treated islets). Therefore, genes upregulated under high-glucose conditions in islets could be either glucose-regulated or insulin-regulated. In the course of these studies, we also evaluated the mRNA levels of several common housekeeping genes in islets at various times after high-glucose administration and found that most (β-actin, HPRT, 36B4, RPL19) remained constant, however cyclophilin and GAPDH showed a gradual increase

with time, making them inappropriate for use as invariant calibrator genes in the studies shown in Fig. 2.5.

The efficacy of the high-glucose treatment was evident by the robust increase in the heterogenous, nuclear insulin II transcript (hnINSII), increases in mature insulins I and II, and the novel insulin splice variants NAT and SPV. In addition, established glucose-responsive genes were significantly induced (MafA and GLUT2) or repressed (Chop10) as expected. LXR has recently been identified as a glucose-responsive transcription factor (Mitro, Mak et al. 2007), therefore we also evaluated LXR target genes in islets exposed to high glucose. The bona fide LXR target genes ABCA1, ABCG1, and apoE were not induced by high glucose. SREBP-1c and SCD-1 were significantly elevated, although as these genes are also insulin-responsive, a role for LXR-mediated glucose regulation cannot be established. Overall, these results suggest that glucose does not regulate LXR target genes in the mouse endocrine pancreas.

Sixteen of the 49 mouse NHR exhibited significantly altered RNA levels in islets exposed to high glucose. Reduced RNA levels were observed for TRα, PPARα (as previously reported (Roduit, Morin et al. 2000)), PPARγ, RevERBs, RORα, TR2, ERβ, and MR. Significantly increased RNA levels were observed for RORβ, FXRα, VDR, and the early response genes NGFIB, NURR1, NOR1, and ERα. A similar increase of ERα mRNA was observed by microarray analysis of human islets exposed to high-glucose (data not shown).

A similar evaluation of glucose-mediated changes in gene expression in MIN6 cells demonstrates the limitations of insulinoma cell lines. Typically insulinoma cells lines have dampened glucose-responsiveness and insulin secretion capacity, and efforts

are underway to identify new cell lines or subclones with improved glucose-stimulated insulin secretion capacity (Hohmeier, Mulder et al. 2000; Hohmeier and Newgard 2004; Narushima, Kobayashi et al. 2005). High glucose exposure did not increase mature insulin RNA levels, although the primary INSII (hnINSII) transcript levels were modestly elevated and the Chop10 mRNA levels were altered. There were no changes in RNA levels for LXR target genes. Of the sixteen NHR that showed altered expression in mouse islets, only three exhibited significant changes in the MIN6 cells (VDR, ERα, and NGFIB, Fig 2.5).

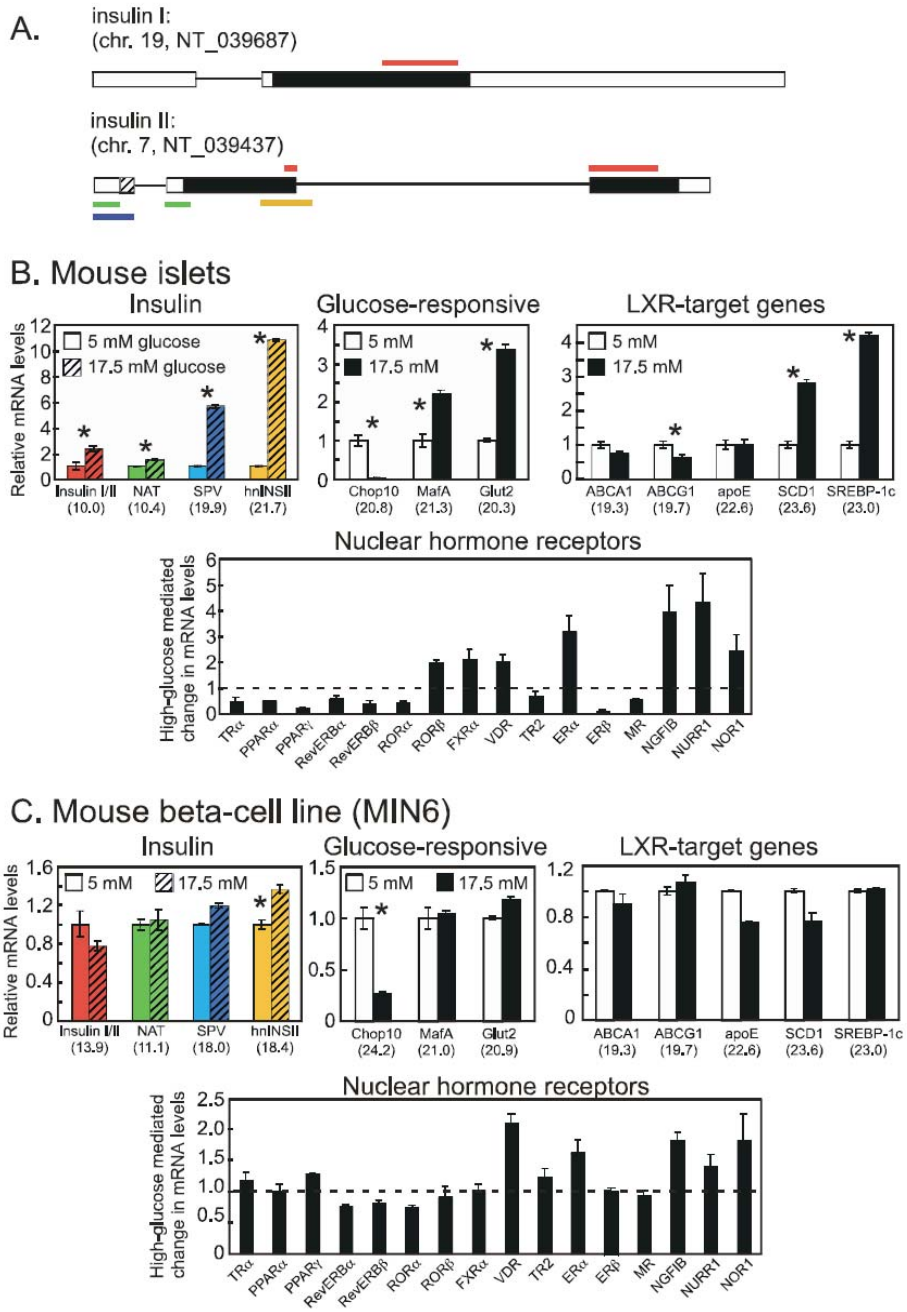

Fig. 2.5 The effect of elevated glucose on NHR expression in the mouse endocrine pancreas. Mouse islets and cell-lines were incubated in 3 mM glucose for 8 hours, then shifted to 5 mM (low glucose) or 17.5 mM glucose (high glucose) for 16 hours before RNA isolation. The efficacy of this treatment protocol is illustrated by the robust changes

in RNA levels for insulin and representative glucose-responsive genes. *A*, The gene structures for mouse insulin I and insulin II genes are provided, and the respective fragments amplified by qPCR are shown for total mature insulin (insulin I/II primer set, red), native insulin II (NAT, green), an insulin II splice variant (SPV, blue (51) and heterogenous nuclear insulin II, hnINSII, yellow). mRNA levels relative to the housekeeping gene HPRT are shown for mouse islets (*B*) and MIN6 cells (*C*). The three upper panels in *B* and *C* display the results of both low-glucose (open bars) and high-glucose (hatched or black bars) treatments for insulin, glucose-responsive genes, and LXR target genes. Values depict the means ± SEM of three independent samples. Below the results for each RNA species we have provided the qPCR cycle number (Ct) for the low-glucose group to allow for an appreciation of relative expression among various genes. In the lower panel the 16 nuclear hormone receptors, of the 49 tested, that showed significantly different mRNA levels by high-glucose treatment in islets are shown. Note that while all 16 were significantly different in mouse islets, only VDR, ERα, and NGFIB were significantly altered in the MIN6 cell line. Statistical significance was determined by Student's *t*-test, n=3, *P<0.05.

Discussion

Global gene expression profiling by microarray analysis is widely used to identify RNA species in a variety of mouse and human tissues (Su, Cooke et al. 2002; Zhang, Morris et al. 2004; Shyamsundar, Kim et al. 2005; Bono, Yagi et al. 2007). In these analyses pancreas was included among the many tissues examined. However, the islets of Langerhans comprise only about 2% by mass of the pancreas, so extrapolating the results from whole pancreas to endocrine pancreas is difficult. The comprehensive evaluation of transcription factor expression in fetal and adult human pancreas has identified potential regulators of pancreatic development (Kong, MacDonald et al. 2006), but again those factors expressed in the endocrine versus exocrine compartment are difficult to distinguish.

Nuclear hormone receptors are one of the largest transcription factor families in the mammalian genome. These receptors are clinically important, as many are bound and

activated by orally available lipophilic compounds, and represent about 3% of the druggable genome in humans (Hopkins and Groom 2002). The earliest surveys of nuclear hormone receptor expression relied on northern blot analysis (Repa, Makishima et al. 2001), thus requiring fairly large quantities of RNA. Subsequently, reverse-transcription PCR was utilized to identify NHRs in selected tissues, for example the mouse small intestine (Choi, Romer et al. 2006). Most recently the distribution of NHR RNA has been performed using qPCR. By this method the quantitative assessment of NHR RNA levels has been established for various mouse tissues (including the pancreas, (Bookout, Jeong et al. 2006)), mouse macrophages (Barish, Downes et al. 2005), mouse adipocytes (Fu, Sun et al. 2005), and during the circadian cycle in mouse liver, adipose, and muscle (Yang, Downes et al. 2006).

In this report, we provide the first survey of NHR expression in the adult mouse endocrine pancreas and commonly used mouse cell lines resembling beta-cells and alpha-cells. The mouse islet typically contains about 1500 cells, consisting of 75% beta-cells and 20% alpha-cells (Cabrera, Berman et al. 2006). Previous work by Gu and colleagues to elucidate gene expression changes in the mouse endocrine pancreas during development reported three findings relevant to NHRs: 1) LXRα and COUP-TFII are enriched in endoderm (versus mesoderm and ectoderm) in the E7.5 mouse; 2) LXRα is enriched in mature islets relative to early-stage pancreas; and 3) RXRα is down-regulated as the endocrine pancreas develops (Gu, Wells et al. 2004). Our current findings also suggest that the expression of various NHRs in the mouse islet can be affected by extracellular glucose levels. In addition, we provide a survey of nuclear hormone receptor expression in human islets obtained from a cadaveric pancreas of a nondiabetic adult. Of

the eighteen receptors that are abundantly expressed in human islet, 9 also fall into this category in mouse islet and 8 others are clearly present in mouse islet. The obvious exception is LRH-1 which is highly expressed in human islet, unlike the mouse islet where it is predicted to reside in the alpha-cell compartment, based on its expression in αTC1 cells.

In summary, our results identify NHR present in cells of the mouse and human endocrine pancreas, and suggest potential therapeutic targets to affect islet physiology. Future work that takes advantage of NHR ligands and genetically altered mouse strains should further reveal roles for these proteins in islet physiology, and ultimately these findings will need to be confirmed in human islets.

Table 2.1 qRT PCR primer sequences for mouse NRs

Gene Abbrev.	Gene Name	Accession Number	Sequence of Primers (5' to 3')	Amplicon position
NUCLEAR HORMONE RECEPTORS				
NR1A1	TRα	NM_178060	F: GGATGGAATTGAAGTGAATGGAA R: CCGTTCTTTCTTTTTCGCTTTC	414-522
NR1A2	TRβ	NM_009380	F: CTCTTCTCACGGTTCTCCTC R: AACCAGTGCCAGGAATGT	819-940
NR1B1	RARα	NM_009024	F: CCAGCTTCCAGTCAGTGGTTA R: TGCTCTGGGTCTCGATGGT	542-600
NR1B2	RARβ	NM_011243	F: ACAGATCTCCGCAGCATCAG R: GCATTGATCCAGGAATTTCCA	1319-1394
NR1B3	RARγ	NM_011244	F: CCATGCTTTGTATGCAATGACA R: TTCTGAATGCTGCGTCTGAAG	517-611
NR1C1	PPARα	NM_011144	F: CGTACGGCAATGGCTTTATC R: AACGGCTTCCTCAGGTTCTT	1444-1498
NR1C2	PPARδ	NM_011145	F: CCACGAGTTCTTGCGAAGTC R: AACTTGGGCTCAATGATGTCA	1211-1267
NR1C3	PPARγ	NM_011146	F: CCCACCAACTTCGGAATCA R: TGCGAGTGGTCTTCCATCAC	157-212
NR1D1	RevERBα	NM_145323	F: TCCAACAGAATATCCAGTACAAACG R: GCGATTGATGCGAACGAT	556-623

NR1D2	RevERBβ	NM_011584	F: CATCAGGATTCCACTATGGAGTTC R: ACTGGATGTTTTGCTGAATGCT	496-576
NR1F1	RORα	NM_013646	F: GGAATCCATTATGGTGTCATTACG R: GTGGCATTGCTCTGCTGACT	249-322
NR1F2	RORβ	NM_146095	F: GGCAGACCCACACCTACGA R: CAGAGCCTCCCTGGACTTG	873-931
NR1F3	RORγ	NM_011281	F: TCTACACGGCCCTGGTTCT R: ATGTTCCACTCTCCTCTTCTCTTG	1356-1423
NR1H2	LXRβ	NM_009473	F: CTCCCACCCACGCTTACAC R: GCCCTAACCTCTCTCCACTCA	1826-1889
NR1H3	LXRα	NM_013839	F: AGGAGTGTCGACTTCGCAAA R: CTCTTCTTGCCGCTTCAGTTT	635-735
NR1H4	FXRα	NM_009108	F: TGAGAACCCACAGCATTTCG R: GCGTGGTGATGGTTGAATGTC	1319-1390
NR1H5	FXRβ	NM_198658	F: GCGCAGAAAATGCCAAGA R: GAGCAAACATTCTGCCAACATC	615-684
NR1I1	VDR	NM_009504	F: GGCTTCCACTTCAACGCTATG R: ATGCTCCGCCTGAAGAAAC	238-296
NR1I2	PXR	NM_010936	F: CATCGTTCCTGATTCTTCAAGGT R: TCTAGGTTTACATCTGTGTGTCCTAG	240-334
NR1I3	CAR	NM_009803	F: GCTGCAAGGGCTTCTTCAG R: AACGGACAGATGGGACCAA	330-387
NR2A1	HNF4α	NM_008261	F: CCAACCTCAATTCATCCAACA R: CCCGGTCGCCACAGAT	254-316
NR2A2	HNF4γ	NM_013920	F: TCCCTGCCTTCTGTGAACTG R: CCAGCATGGGCTCTCAAGA	751-811
NR2B1	RXRα	NM_011305	F: TGCCCATCCCTCAGGAAA R: GCGGTCCCCACAGATAGC	607-670
NR2B2	RXRβ	NM_011306	F: TCCCCAAATCCCCTTTCTC R: CCCCATGGAAGAACTGATGA	396-530
NR2B3	RXRγ	NM_009107	F: GCCACCCTGGAGGCCTATA R: AGCAGAAGCTTGGCAAACCT	1567-1634
NR2C1	TR2	NM_011629	F: TGCACATCAAATTATCGACCAA R: GCTGTCACGATCTGCATTTTC	660-740
NR2C2	TR4	NM_011630	F: GTCATGAGTCTCTCCACCATCCT R: GCTTTATCCGGTCACCAGAAA	1375-1465
NR2E1	TLX	NM_152229	F: AGCCCGCCGGATCAA R: CAAGCGTAGACCCCGTAGTG	690-780
NR2E3	PNR	NM_013708	F: AGGTGATGCTAAGCCAGCATAG R: GAGGAGCAATTTCCCAAACC	1199-1269
NR2F1	COUP-TFI	NM_010151	F: TGGACCTTCCAGGATTTATTGTG R:AGTCCACTTCCATTGAGTAGTTTTCTG	1898-1971
NR2F2	COUP-TFII	NM_009697	F: TCAAGGCCATAGTCCTGTTCA R: TCCGGTGGTGCTGATCAA	1208-1285
NR2F6	EAR2	NM_010150	F: GAGGGCTGCAAGAGTTTCTTC R: TCCGGTGGTGCTGATCAA	336-432
NR3A1	ERα	NM_007956	F: GCAGATAGGGAGCTGGTTCA R: TGGAGATTCAAGTCCCCAAA	1242-1312

NR3A2	ERβ	NM_207707	F: GCCAACCTCCTGATGCTTCT R: TCGTACACCGGGACCACAT	1824-1924
NR3B1	ERRα	NM_007953	F: AGCAAGCCCCGATGGA R: GAGAAGCCTGGGATGCTCTT	808-912
NR3B2	ERRβ	NM_011934	F: CAGATCGGGAGCTTGTGTTC R: TGGTCCCCAAGTGTCAGACT	1177-1252
NR3B3	ERRγ	NM_011935	F: GTGCTTAGTGTGTGGCGACA R: TTCACATGATGCAAGCCCAT	519-576
NR3C1	GR	NM_008173	F: GCAAGTGGAAACCTGCTATGC R: CATACATGCAGGGTAGAGTCATTCTT	1980-2055
NR3C2	MR	XM_98332	F: AGCAGGCCTTTGAGGTCATT R: AAGGCCCCACCATTCATG	1378-1436
NR3C3	PR	NM_008829	F: GCTTGCATGATCTTGTGAAACA R: TGTCCGGGATTGGATGATT	2613-2677
NR3C4	AR	NM_13476	F: TGTCAACTCCAGGATGCTCTACT R: TGGCTGTACATCCGAGACTTG	2240-2320
NR4A1	NGFI-B	NM_010444	F: GTTGATGTTCCCGCCTTTG R: CCTGGAGCCCGTGTCG	1612-1678
NR4A2	NURR1	NM_013613	F: GCACTTCGGCGGAGTTG R: GGAATCCAGCCCGTCAGA	499-560
NR4A3	NOR1	NM_015743	F: AGTGTCGGGATGGTTAAGGAA R: ACGACCTCTCCTCCCTTTCA	1063-1122
NR5A1	SF1	NM_139051	F: CCCTTATCCGGCTGAGAATT R: CCAGGTCCTCGTCGTACGA	121-196
NR5A2	LRH1	NM_030676	F: TGGGAAGGAAGGGACAATCTT R: CGAGACTCAGGAGGTTGTTGAA	1406-1506
NR6A1	GCNF	NM_010264	F: CAGAGCTTGATCCAGGCACTAAT R: AGGTTCGTTGTTCAGCTCGAT	511-612
NR0B1	DAX-1	NM_007430	F: AAGGGACCGTGCTCTTTAACC R: TCTCCACTGAAGACCCTCAATGT	1178-1251
NR0B2	SHP	NM_011850	F:CAGCGCTGCCTGGAGTCT R: AGGATCGTGCCCTTCAGGTA	492-565
HOUSEKEEPING GENES				
36B4	36B4	NM_007475	F: CACTGGTCTAGGACCCGAGAAG R: GGTGCCTCTGAAGATTTTCG	455-527
β-ACTIN	β-Actin	NM_007393	F: CATCGTGGGCCGCTCTA R: CACCCACATAGGAGTCCTTCTG	179-246
CYCLO	Cyclophilin	NM_011149	F: TGGAGAGCACCAAGACAGACA R: TGCCGGAGTCGACAATGAT	642-707
GAPDH	GAPDH	NM_199472	F: CAAGGTCATCCATGACAACTTTG R: GGCCATCCACAGTCTTCTGG	602-690
HPRT1	HPRT1	NM_013556	F: GCCTAAGATGAGCGCAAGTTG R: TACTAGGCAGATGGCCACAGG	739-839
RPL19	RPL19	NM_013556	F: GACGGAAGGGCAGGCATATG R: TGTGGATGTGCTCCATGAGG	209-430
GLUCOSE- AND LXR-RESPONSIVE GENES				
ABCA1	ABCA1	NM_013454	F: CGTTTCCGGGAAGTGTCCTA R: GCTAGAGATGACAAGGAGGATGGA	6805-6883

ABCG1	ABCG1	NM_009593	F: GCTGTGCGTTTTGTGCTGTT R: TGCAGCTCCAATCAGTAGTCCTAA	1676-1759
APOE	apoE	NM_009696	F: GCAGGCGGAGATCTTCCA R: CCACTGGCGATGCATGTC	965-1037
CHOP10	CHOP10	NM_007837	F: CACCACACCTGAAAGCAGAAC R: GGTGAAAGGCAGGGACTCA	125-189
GLUT2	SLC2A2	NM_031197	F: CAACTGGGTCTGCAATTTTGTC R: GAACACGTAAGGCCCAAGGA	1386-1458
hnINSII	Heterogenous nuclear INSII	NT_039437 X04724	F: GGGGAGCGTGGCTTCTTCTA R: GGGGACAGAATTCAGTGGCA	1262-1347
InsulinI/II	InsulinI/II	NM_008386 NM_008387	F: TGAAGTGGAGGACCCACAAGT R: AGATGCTGGTGCAGCACTGAT	351-475 241-371
MafA	MafA	NM_194350	F: TTCAGCAAGGAGGAGGTCATC R: GCGTAGCCGCGGTTCT	757-821
NAT	NAT	NM_008387	F: AGCCCTAAGTGATCCGCTACAA R: ATCCACAGGGCCATGTTGAA	2-88
SCD1	SCD1	NM_009127	F: CCGGAGACCCCTTAGATCGA R: TAGCCTGTAAAAGATTTCTGCAAACC	3778-3866
SPV	SPV	NT_039437 DQ250569.1	F: AGCCCTAAGTGATCCGCTACAA R: TCAAGTCCCTGAGGTCTTAGCTG	7-103
SREBP1C	SREBP-1c	NM_011480 NT_096135 (Genomic seq.)	F: GGAGCCATGGATTGCACATT R: GGCCCGGGAAGTCACTGT	10438-10419 7291-7308

CHAPTER THREE

The roles of LXR and ChREBP in the mouse islet

Abstract

LXRs have been characterized as oxysterol sensors to regulate the expression of genes critical for cholesterol homeostasis and bile acid metabolism. Recently, the roles of LXRs in regulating lipid metabolism and glucose homeostasis have also been addressed. In diabetic rodent models, an oral administration of LXR agonists has been reported to reduce serum glucose levels. It is proposed that this glucose lowing occurs by LXR-mediated repression of hepatic gluconeogenesis and an increase in glucose uptake by adipose. In my studies, I also addressed a potential role for LXR signaling in beta-cells to enhance insulin secretion and hence improve glucose clearance. LXRβ is abundant in beta-cells of the islet. Exposure of isolated mouse islets to various LXR agonist increases glucose-stimulated insulin secretion (GSIS). Using both a candidate approach and an unbiased microarray analysis, we identified LXR target genes in the mouse and human islets. We identified ChREBP as a novel target gene of LXR in the beta-cells, and demonstrated that ChREBP plays an important role in regulating insulin secretion.

Introduction

The liver X receptors, LXRα (NR1H3) and LXRβ (NR1H2), were considered orphan members of the nuclear receptor superfamily until oxysterols, were identified as endogenous ligands (Willy, Umesono et al. 1995; Repa, Liang et al. 2000). LXRs function as obligate heterodiners with RXR and bind to LXREs (AGGTCAn4AGGTCA)

in the promoters of target genes. LXRα is expressed in metabolically active tissues including liver, white adipose tissue, intestine, macrophages, and kidney while LXRβ is ubiqutously expressed. Oxysterols including 22(*R*)-hydroxycholesterol, 24(*S*)-hydroxycholesterol, 27-hydroxycholesterol, and 24,25 epoxycholesterol have been identified as endogenous ligands for LXRs. In the absence of ligand, the LXR/RXR heterodimer binds to an LXRE and interacts with co-repressors to mediate target gene silencing (Ahuja 2003, (Wagner, Valledor et al. 2003)). Ligand binding elicits a receptor conformation change resulting in the release of co-repressors and recruitment of co-activators to promote transcription of target genes.

Studies using synthetic LXR agonists and *Lxr*-null mice led to the identification of numerous target genes of LXR. Many of these genes are enzymes and transporters that participate in cholesterol metabolism such as *Cyp7a1*, *ABCA1*, *ABCG5*, *ABCG8*, and *APOE*. LXRs are also involved in fatty acid and lipid metabolism by regulating key genes in the lipogenesis pathway such as *FAS*, *SCD-1*, and *SREBP-1c*.

More recently, LXRs have also been shown to participate in the regulation of glucose homeostasis. Administration of an LXR synthetic agonist improved glucose clearance and insulin sensitivity in both genetic and diet-induced diabetic murine models (Cao, Liang et al. 2003; Laffitte, Chao et al. 2003). Underlying mechanisms have been proposed to account for these observations, and include a decrease of hepatic gluconeogenesis and an increase in glucose uptake by adipocytes (Dalen, Ulven et al. 2003).

In our mouse islet nuclear receptor profiling study, we found that LXRβ is expressed abundantly in the beta cells of the islet. Based on this observation, we aimed to

reveal the functional significance of LXRβ in the beta cell of islet. Using a combination of cell-based and whole animal studies we found that LXR activation improves beta-cell insulin secretion. We also identified novel target genes that may contribute to this beta-cell function.

Materials and methods

Mouse islet isolation and culture

The mouse pancreas was perfused and digested with liberase R1 (Roche). Islets were then isolated using Ficoll gradient centrifugation and hand-selection under a stereomicroscope for transfer to RPMI 1640 medium (11.1 mM glucose) supplemented with 10% (v/v) heat-inactivated fetal bovine serum, 100 IU/ml penicillin, and 100 μg/ml streptomycin (Invitrogen). Islets were allowed to recover overnight (37°C, 5% CO_2) before further use. Typically 10-12 mice were used to isolate islets that would be pooled for each group then distributed evenly among multiple wells (200 islets/well) for each assay condition. All experiments were performed a minimum of two times.

Human islet experiments

Human islets (obtained from cadaver pancreas of a nondiabetic individual) were procured at the University of Virginia (kindly provided by Dr. Raghavendra G. Mirmira). Islets were maintained in 5.6 mM glucose in the presence of 10% fetal bovine serum prior to RNA isolation.

In vivo study of LXR agonist T1317 effects on glucose homeostasis

Female wild-type and *Lxr*-null mice on a mixed strain (A129/C57BI6) background and maintained on a standard mouse chow (Teklad 7001) were treated daily with T1317 by oral gavage (50 mg/kg body weight) for five days. After 3 days of treatment, mice were fasted 15 hours and given a single oral dose of glucose (15% glucose solution, 10 ml/g mouse). Blood was collected and glucose measurements were performed using a PGO Enzyme assay. After blood was collected, mice were given two more treatments of T1317 and were sacrificed after five days of treatment.

Cell culture

The insulinoma cell line Beta-TC-6 ([CRL-11506], (Poitout, Stout et al. 1995)) and the adenoma-derived glucagonoma cell line alphaTC1-clone 9 ([CRL-2350], (Powers, Efrat et al. 1990)) were obtained from American Type Tissue Culture. The MIN6 cell line (Miyazaki, Araki et al. 1990) was kindly provided by Dr. Melanie Cobb (UT Southwestern). Cells were maintained in their optimal culture conditions unless indicated otherwise. Beta-TC6 cells were routinely cultured in DMEM (4.5g/L glucose, 4 mM L-glutamine) with 15% heat-inactivated FBS. MIN6 cells were maintained in DMEM (4.5g/L glucose); 2 mM L-glutamine, 1 mM sodium pyruvate and 10% heat-inactivated FBS. Alpha-TC1 cells were cultured in DMEM with 4 mM L-glutamine adjusted to contain 1.5 g/L sodium bicarbonate and 3 g/L glucose with 10% heat-inactivated dialyzed FBS, further supplemented with 15 mM HEPES, 0.1 mM non-essential amino acids and 0.02% BSA.

RNA measurements

RNA was isolated from tissue samples or cultured cells using RNA STAT-60 (Tel-Test Inc.) and 2 μg of total RNA was treated with RNase-free DNase (Roche), then reverse-transcribed with random hexamers using SuperScript II (Invitrogen)., as previously described (Kurrasch, Huang et al. 2004).

Quantitative real-time PCR (qPCR) was performed using an Applied Biosystem Prism 7900HT sequence detection system and SYBR-green chemistry (Kurrasch, Huang et al. 2004; Valasek and Repa 2005). Gene-specific primers were designed using Primer Express Software (PerkinElmer Life Sciences) and validated by analysis of template titration and dissociation curves. Primer sequences are provided in Table 1. 10 μl qPCR reactions contained 25 ng of reverse-transcribed RNA, each primer (150 nM) and 5 μl of 2X SYBR Green PCR master mix (Applied Biosystems). Multiple housekeeping genes were evaluated in each assay to insure that their RNA levels were invariant under the experimental conditions of each study. Results of qPCR were evaluated by the comparative Ct method (user bulletin No.2, Perkin Elmer Life Sciences) using hypoxanthine-guanine phosphoribosyl transferase (HPRT) or cyclophilin as the invariant control gene.

Western analysis

Tissues, islets, and cultured cells were lysed in cold lysis buffer (Cell Signaling Technology, MA) containing 1 mM PMSF and were centrifuged at 10,000x g for 10 min at 4 ^{0}C. Protein concentrations were measured using the BCA protein assay kit (Pierce). Proteins were size-fractioned on an 8% denaturing SDS-polyacrylamide gel and were transferred to nitrocellulose membrane. Rabbit anti-ChREBP antibody (Novus Biology,

1:1000) and mouse anti-gamma tubulin antibody (Sigma Aldrich, 1:5000) were used with the species-appropriate HRP-conjugated secondary antibodies and the Supersignal West pico-chemiluminescent substrate (Pierce) to generate a signal by autoradiograph. Signal density of bands was determined by analyzing scanned images with OptiQuant v3.1 software (Packard Bioscience).

Glucose-stimulated insulin secretion-static measurement

Mouse islets (5-10/well of 24-well culture plate, each condition represented in 4 independent wells) were incubated in Secretion Assay Buffer (SAB, containing 0.114 M NaCl, 4.7 mM KCl, 1.2 mM KH_2PO_4, 1.16 mM $MgSO_4$, 12.75 mM $NaHCO_3$, 25 mM $CaCl_2$, 20 mM HEPES and 0,2% BSA, pH 7.4) without glucose for 1 hour then were stimulated with 5 or 17.5 mM glucose for 1 hour . Secreted insulin was measured using radioimmunoassay (RIA, Linco Diagnosis). Islets were collected and lysed by sonication, and total insulin (by RIA) and/or DNA (using Hoechst 33528, Sigma Aldrich) was quantified.

Glucose-stimulated insulin secretion-perifusion

Islets were incubated for 1 hour in SAB without glucose, then were transferred onto a nitrocellulose filter (Millipore) in a plastic perifusion chamber (Millipore) with 100 islets/chamber performed in duplicate. Culture media contains varying glucose concentrations, warmed to 37^0C was then applied to the chamber by peristaltic pump at a flow of 0.5 ml/min, and effluent fractions were collected for insulin measurement by RIA.

ATP measurement

Islets were incubated in SAB containing 2.7 mM glucose for 1 hour. Following the pre-incubation, islets were transferred to wells (15 islets each well x 5 for each condition) of 24-well culture plate containing 0.5 ml SAB with either 2.7 mM or 17.5 mM glucose and incubated for 1 hour. Islets were then transferred into 1.5ml tube, snap-frozen in liquid nitrogen, and stored at -80^{0}C before assay. ATP content of islets was measured using an ATP bioluminescence assay kit HS II (Roche) following the manufacturer's instructions.

Glucose and insulin measurement in mice

To measure postprandial plasma analytes, food was removed 3 hours before blood sampling at 9 am. To obtain plasma samples in the fasted-state, food was removed from the mouse cages at 7 pm (for 14-15 hours fasting). For glucose tolerance tests, mice were fasted overnight, then received an intraperitoneal glucose injection (1 g/kg body weight) and plasma samples were collected at 0, 2, 5, 15, 30, 60, and 120 min after glucose administration. Plasma glucose levels were measured using PGO kit (Sigma) and insulin measurements were performed using Ultrasensitive rat insulin ELISA kit (Crystal Chemical).

Immunohistochemistry and beta cell mass determination

Dorsal pancreata dissected from adult mice were fixed overnight in 10% Formalin Solution (Sigma), dehydrated, and paraffin-embedded in Paraplast Plus tissue Embedding Medium (McCormick). 10 μm sections spanning from distal to proximal regions of the pancreas were mounted in Superfrost/Plus slides (Fisher). For immunofluorescence,

sections were de-waxed; rehydrated using decreasing concentrations of ethanol; washed several times in PBS; blocked for 1 hr at RT with 5%NDS, 5%NGS (Sigma); and incubated with primary antibody diluted in blocking solution overnight at 4°C. The primary antibodies used were: rabbit anti-Glucagon (LINCO Research, 1:300) and guinea pig anti-Insulin (DakoCytomation, 1:300). Signal was detected the following day by incubating the slides at RT for 1 hr with fluorophore-conjugated antibodies and mounted using Vectashield with DAPI (Vector Laboratories). The secondary antibodies used were: TRITC-conjugated goat anti-Guinea pig (Jackson ImmunoResearch) and FITC-conjugated donkey anti-Rabbit (Jackson ImmunoResearch). Images were acquired on a LSM510META confocal microscope. For pancreas area determination, sections were de-waxed, rehydrated using a graded series of ethanol concentrations; sections were stained with Harris Hematoxylin (Fisher) and counterstained with Eosin-Y (Fisher); dehydrated and mounted with permount solution (Fisher). Pancreatic sections and β-cell areas were analyzed using AxioVersion 4.5 software.

Whole pancreas insulin measurement

Three wild type and three *ChREBP* -/- female mice aged 10 months were fasted overnight and the pancreases were carefully dissected and wet weights were obtained. Pancreatic insulin was extracted in acid ethanol (180mM HCl in 70% ethanol). Whole pancreas was homogenized in 3 ml acid ethanol and the homogenate was left overnight at 4^{o}C. The homogenate was then centrifuged at 2000g for 3min and the supernatant was collected. The extraction was repeated three times and the supernatants from each time were pooled and used for determination of insulin content by RIA kit.

Oligonucleotide array

Human islets was treated with vehicle (DMSO, final conc. of 0.1%) or T1317 (1 μM) for 24 hours (n=2 per group) under both low (2.5 mM) and high (25 mM) glucose culture conditions and RNA were extracted. RNA samples were hybridized to the Illumina Human Ref-8.2 v2 Beadchip. Expression of genes was analyzed and compared using Genesifter software (http://www.genesifter.net/web/). Genes up- or down-regulated by T1317 under low glucose condition are shown in Supplemental Table 3.2 and Supplemental Table 3.3, respectively.

Statistics

Data are reported as the mean ± SEM or Std. Dev. (as stated in each figure legend) for the specified number of conditions or animals. GraphPad Prism software (GraphPad, San Diego CA) was used to perform all statistical analyses. The assumption of equal variance was tested by Bartlett's test, and log transformation was performed if necessary prior to statistical evaluation.

Results

Expression of LXRs/ RXRs in the endocrine pancreas

We used qPCR to determine the expression of LXRα, LXRβ, and their heterodimer partner, RXRs, in isolated mouse islet and representative cell lines (βTC6, MIN6, αTC1). LXRβ is the predominant isoform of LXR in islet cells, and RXRα is the most abundant among all three RXR isoforms (Figure 3.1 A). This relative distribution was also observed in hamster, rat, and human islets (data not shown). mRNA levels of LXRs and

RXRs did not change in mouse islets cultured in low glucose (5 mM) or high glucose (17.5 mM) medium (data not shown).

To test the functional integrity of the LXR/RXR pathway in the islet, a synthetic ligand (T1317) of LXR was used to treat isolated islets. Many known target genes of LXR including *ABCA1*, *SREBP-1c*, *SCD-1*, and *FAS* are expressed in islets and were activated when islets were exposed to T1317 for 16 hours (Figure 3.1 B). These results demonstrate that the LXR/RXR pathway is present and functional in cells of the islet.

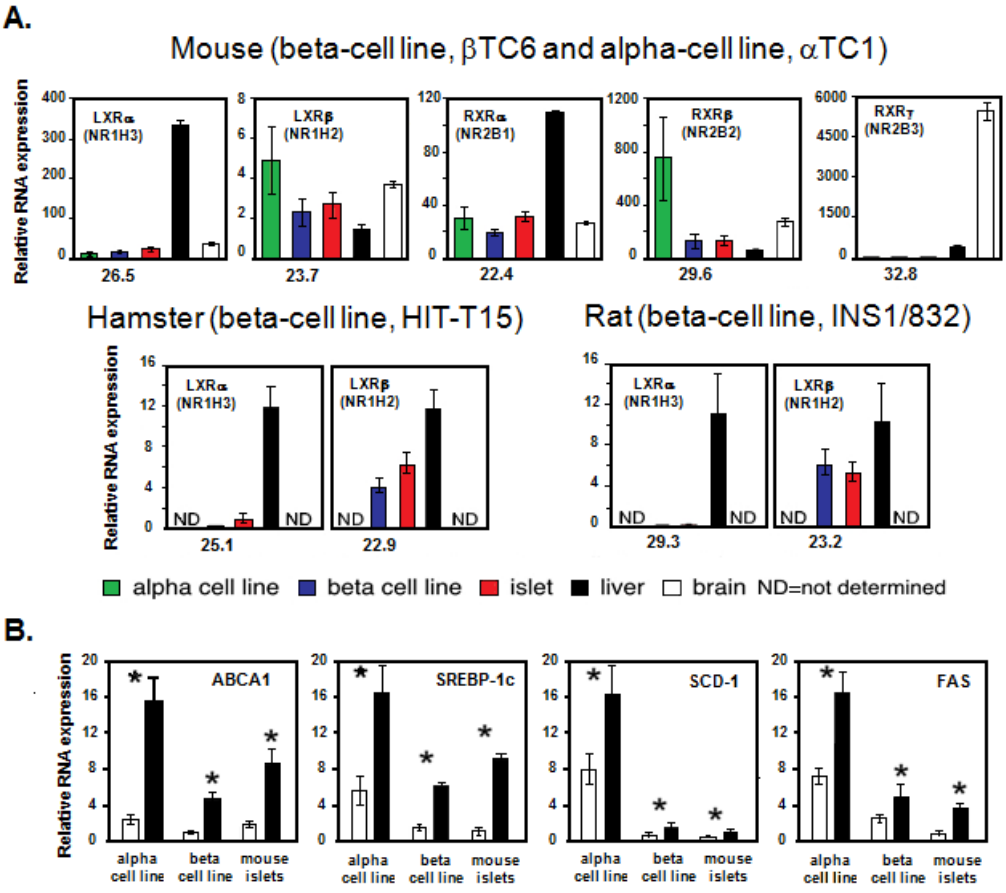

Figure 3.1. LXRs and RXRs are expressed in islets and beta-cell lines.
(**A**) Distribution of mRNA encoding LXRα, LXRβ and their heterodimerization partner, RXRs, in tissues, a mouse alpha-cell line (αTC-1), and beta-cell lines of mouse (βTC-6), hamster (HIT-T15), and rat (INS-1/832). RNA was measured by quantitative real-time PCR, using cyclophilin as

the invariant calibrator gene. Values depict the mean and standard error of three independent samples. The numbers provided under the islet values are the PCR cycle numbers.
(**B**) Activation of known LXR target genes in mouse islets and cell lines by the synthetic ligand T1317. Isolated mouse islets and βTC-6 cell line were treated with either vehicle (DMSO, white bars) or T1317 (10μM, black bars) for 16 hours and the activation of previously identified target genes of LXR were measures by qPCR. (* $p<0.05$, as compared to vehicle).

Administration of LXR agonist in mice leads to better glucose control

To evaluate the effects of LXR activation on glucose metabolism, wild type and *Lxr* α-/-/β-/- knockout mice were treated with the LXR synthetic ligand T1317 daily (50 mg/kg body weight). After 3 days of treatment, oral glucose tolerance tests were performed. The results demostrate that T1317-treated wild type mice exhibit improved glucose clearance compared to vehicle-treated wild-type mice. This effect is not observed in *Lxr* α-/-/β-/- knockout mice suggesting that the glucose lowing effects of this drug are indeed LXR-dependent (Fig 3.2).

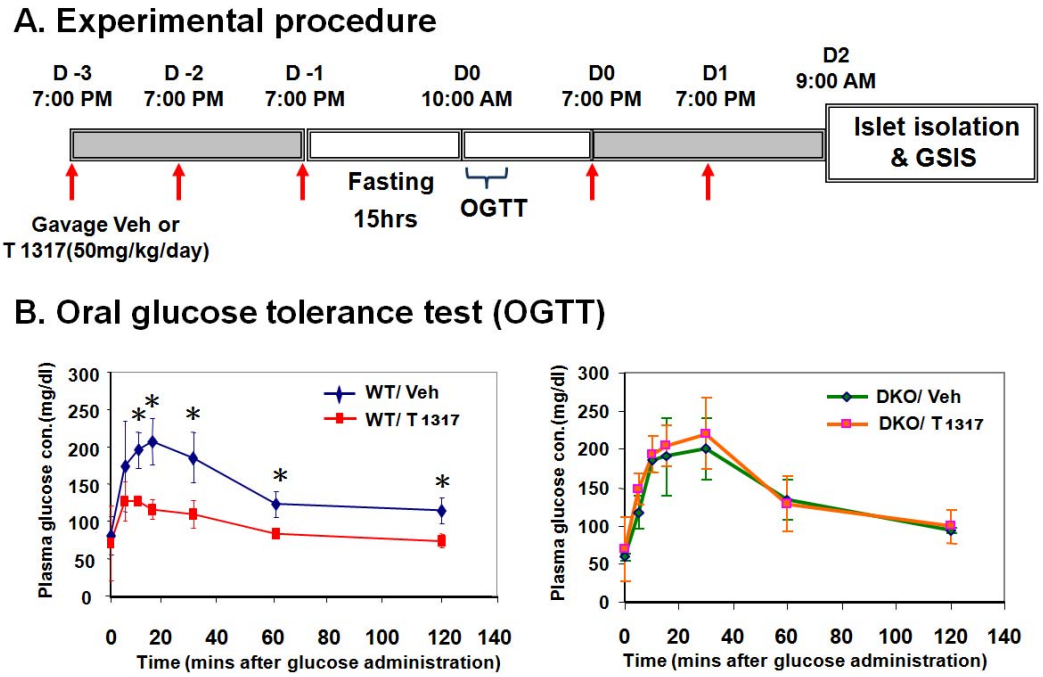

Figure 3.2. *In vivo* study of LXR agonist T1317 effects on glucose homeostasis. (A) Female wild-type and LXR-DKO mice (3 monthes of age, A129/C57BI6 mix strain) maintained on a standard mouse chow (Teklad 7001) were treated daily with T1317 by oral gavage (50 mg/kg body weight). After three days of treatment, mice were fasted for 15 hours and then received a single oral dose of glucose (15% glucose solution, 10 ml/g mouse). Blood was collected and glucose measurements were performed using a PGO Enzyme assay (B). Values depict the mean and Std. Dev., n=3. Asterisks denote statistically significant ($p<0.05$).

Activation of LXR by synthetic ligand leads to increased GSIS from islets

To test our hypothesis that activation of LXR in the islet cells also contributes to the observed glucose-lowering effects of LXR ligands, we performed glucose-stimulated insulin secretion (GSIS) experiments on isolated mouse islets. Islets that were treated with LXR agonist for 16 hours after isolation showed enhanced insulin secretion upon glucose challenge compared to vehicle-treated islets (Fig 3.3A). This effect was not observed in islets isolated from *Lxr*- null mice (Fig 3.3 B), which confirms that this effect is specifically mediated by LXR. Enhanced GSIS was observed in both static

experiments (1 hour glucose exposure, Fig 3.3 A, B, C, E, F) and a perfusion study (Fig 3.3 D). In fact, a glucose dose response experiment revealed a pronounced left-shift (Fig 3.3 C) indicative of increased glucose sensitivity and/or improved insulin secretion capacity in islets treated with T1317. Finally, in addition to glucose, we also tested other secretagogues including KCl, Tolbutamide, and arginine. Like glucose, all of these stimuli induced more insulin secretion from T1317-treated islets (Fig 3.3 E). To test if T01317 can also affect islet function *in vivo*, we isolated islets from animals that were given T1317 by daily oral gavage for 5 days and measured GSIS immediately. Similar results were observed from these islets that were exposed to T1317 *in vivo* (Fig 3.3 F). These data suggest that activation of LXR in islets can potentiate insulin secretion and thus contributes to the glucose-lowering effects of T1317 in mice.

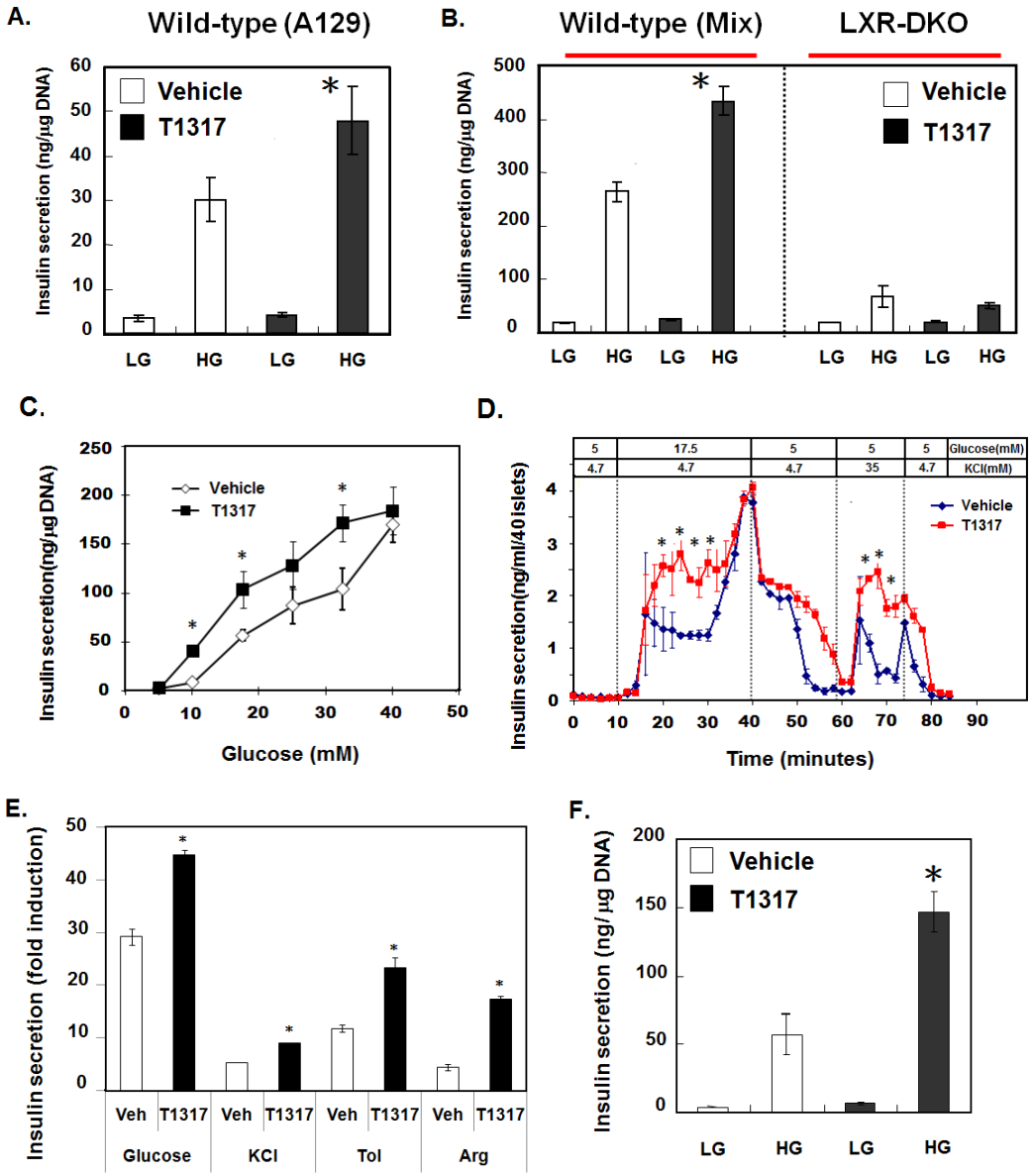

Figure 3.3. LXR activation enhances GSIS. (A) Islets from A129 wild type mice were treated with vehicle (DMSO) or 10 µM T1317 for 16 hours. For static insulin secretion assay, islets were incubated in secretion assay buffer (SAB) without glucose for one hour and then groups of 10 islets were placed into wells containing SAB with 5 mM glucose (LG) or 17.5 mM glucose (HG) for another hour. Media were collected and insulin content was measured using the Sensitive Rat Insulin RIA kit (Linco Res. Inc., St.Charles, MO). (B) LXR is required for GSIS enhancing effect of T1317 since islets from LXRα-/-β-/- knockout (LXR-DKO) mice failed to respond to T1317 treatment. (C) T1317 treated islets are more sensitive to glucose concentration. (D) GSIS enhancing effect of T1317 can also be detected in a perifusion GSIS experiment. (E) In addition to glucose, T1317 can enhance insulin secretion from several other secretagogus including KCl (30

mM), Tolbutamide (Tol, 100 μM), and arginine (Arg, 10 mM). (F) Islets isolated from mice that were orally treated with T1317 (5 days, 50 mg/kg body weight) also show GSIS enhancing effect. Asterisks denote significant differences ($p<0.05$, as compared to vehicle treatment).

Genes regulated by LXR in the islet

As shown in Fig 3.1 and Fig 3.4, many previously identified LXR target genes were up-regulated when mouse islets were treated with T1317. To test if these target genes are required for the insulin potentiating effect of LXR, we examined islets isolated from *Abca1-/-*, *Scd1-/-*, *PPARα-/-*, and *Srebp-1c-/-* knockout mice. In all cases, T1317 treatment still regulated GSIS suggesting that other target gene(s) of LXR affect this pathway (data not shown).

Insulin itself does not appear to be a direct target gene in the mouse since the mRNA levels for insulin (mouse insulin I + II) and alernative splice variants (*SPV* and *NAT*) were not changed by LXR activation (Fig 3.4). In agreement with these RNA data, insulin protein content in mouse islets was not changed by LXR ligand either (data not shown).

In addition to the well characterized LXR target genes, we also detected several genes that may be important for regulating insulin secretion and were also up-regulated by LXR in the islet, these genes included the glucose-sensing transcription factor ; *ChREBP*, calcium channel components (*Cav1.2* and *Cav2.1*), and *SNAP25,* a protein involved in vesicle trafficing (Fig 3.4).

Combined, these data imply that after LXR activation in the beta cells of islet, a group of target genes are altered and coordinately regulate insulin secretion.

In order to identify novel targets of LXR in the human islet, we had the unique opportunity to evaluate RNA from human islets treated with vehicle or T1317 by microarray analysis. The fidelity of this approach was clear by the detected increase of known target genes of LXR such as *ABCA1*, *SCD1*, *SREBP-1c*. Numerous novel genes were also up regulated by activation of LXR in the human islets (Table 3.2 and Table 3.3). These data provide us several interesting candidates such as *Ghrelin*, islet amyloid polypeptide (*IAPP*), and sulfatase 1 (*Sulf1*) for further investigation.

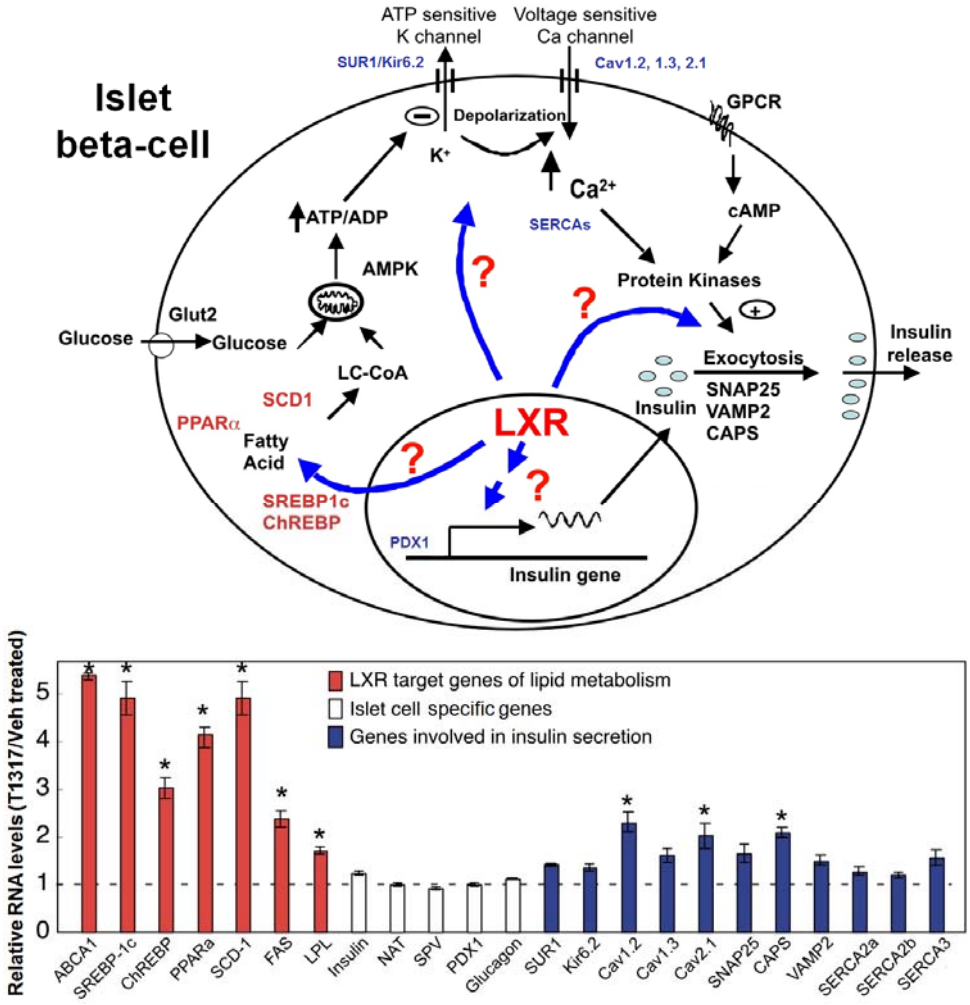

Figure 3.4. The effects of LXR activation on the expression of genes involved in the glucose-insulin secretion axis of the beta-cell. Mouse islets were treated with 10μM T1317 for 16 hours and RNA levels were measured by qPCR using cyclophiline as the invariant housekeeping gene. The values depicted reveal the fold change observed with T1317 treatment. Asterisks denote significant differences ($p<0.05$).

ChREBP is a direct target gene of LXR and is critical for insulin secretion.

One of the novel LXR targets that we identified in islets was the carbohydrate response element binding protein (ChREBP). Previous studies from our group defined the molecular mechanism by which LXR directly regulates ChREBP in mouse liver (Cha and

Repa 2007). Since ChREBP is a carbohydrate sensing transcriptional factor, we decided to evaluate the functional importance of the LXR-ChREBP axis in mouse islets.

We first examined the expression level for this transcription factor and its dimerization partner, Mlx (Stoeckman, Ma et al. 2004) in the islet relative to other mouse tissues. ChREBP mRNA levels were measured by qRT-PCR (Figure 3.5.A), and in close agreement with earlier reports of tissue distribution by northern analysis, this transcription factor is expressed in liver, adipose, intestine, kidney, heart and muscle (Iizuka, Bruick et al. 2004). Our qRT-PCR results demonstrated that ChREBP mRNA is also abundant in the mouse islet, at a level comparable to the common housekeeping gene cyclophilin and to an equal or greater level than seen in liver. In addition, based on analysis of representative cell lines, ChREBP mRNA is present only in beta-cells (βTC-6, MIN6), not alpha-cells (αTC-1) of the endocrine pancreas. Mlx mRNA is ubiquitous and highly expressed in alpha-cells, as is MondoA, a mammalian paralog of ChREBP was recently reported to sense Glucose-6-phosphate to regulate gene transcription (target genes include *Txnip* and *ARDCC4*, (Stoltzman, Peterson et al. 2008)) (data not shown).

To confirm whether the levels of ChREBP protein in selected tissues and cells (Figure 3.5.B) correlates with RNA levels we performed an immunoblot analysis. The specificity of the antibody was demonstrated by detection of a protein only in tissue extracts of wild-type, and not *Chrebp*$^{-/-}$ mice. Overall, ChREBP protein levels in mouse beta-cells and islets were higher than in liver. In addition, there was no detectable protein in a representative alpha-cell line. Therefore, protein levels correlated well with the RNA levels in these tissues. The molecular mass (~103 kDa) of ChREBP protein was slightly

higher than predicted by the mouse cDNA sequence, but is likely due to the highly phosphorylated nature of this transcription factor (Kawaguchi, Takenoshita et al. 2001).

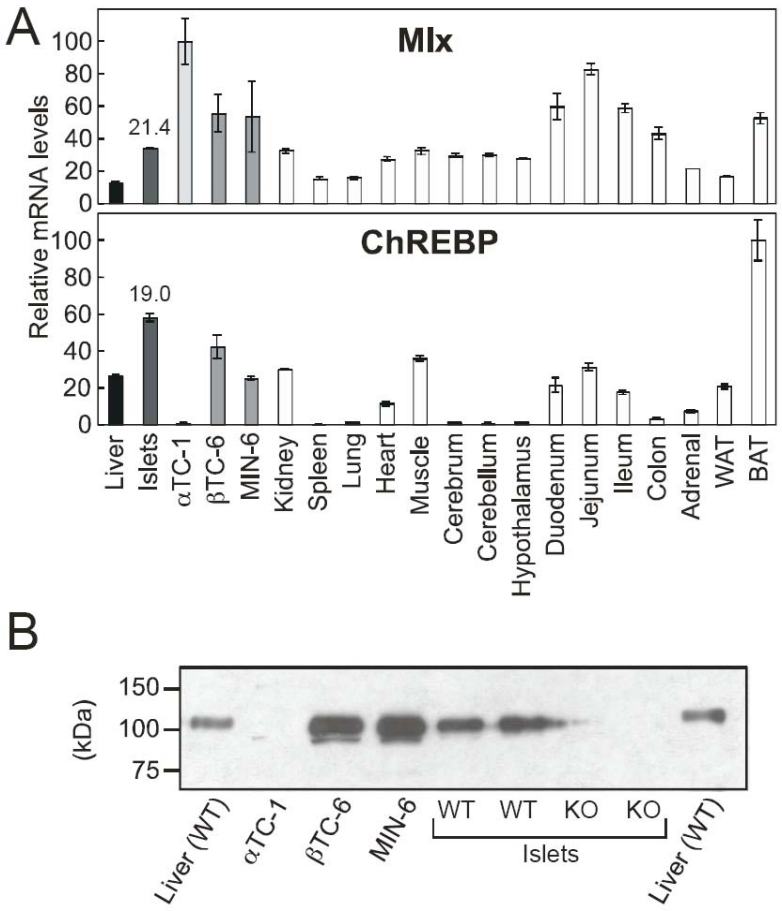

Figure 3.5. ChREBP is highly expressed in mouse islets and beta-cell lines.
(**A**) Distribution of mRNA encoding ChREBP and its dimerization partner, Mlx, in mouse tissues, an alpha-cell line (αTC-1), and beta-cell lines (βTC-6 and MIN6). RNA was measured by quantitative real-time PCR, using cyclophilin as the invariant calibrator gene. Values depict the mean and standard error of three independent samples. The numbers provided above the islet values are the PCR cycle numbers, and compared to cyclophilin (Ct = 19.7) further demonstrate the abundance of ChREBP mRNA in the mouse islet.
(**B**) Distribution of ChREBP protein as revealed by western analysis of whole-cell protein lysates from cell lines and tissues of wild-type (WT) and *Chrebp*-/- (KO) mice. 10 μg of total protein was loaded per lane.

To determine if ChREBP plays a role in GSIS, pancreatic islets were obtained from wildtype and *Chrebp*$^{-/-}$ mice by standard methods involving collagenase digestion of the pancreas followed by separation on a Ficoll gradient and hand-selection of similarly sized islets. Recovered islets were placed in glucose-free medium for 1 hour then were subjected to low-glucose- (2.7 mM) or high-glucose- (12.5 mM)-containing medium for 1 hour and secreted insulin was measured (Figure 3.6.A). Under low-glucose conditions, there was no difference between wildtype and *Chrebp*-null islets in the amount of insulin secreted into the culture medium. However, upon exposure to high-glucose, wildtype islets exhibited a 10-fold increase in insulin secretion whereas *Chrebp*$^{-/-}$ islets only showed a 3.3-fold change, a reduction in response of 67%. Similarly, when islets were evaluated in a perifusion system that allows for continuous monitoring of insulin secretion (Figure 3.6.B), introducing high-glucose (17.5 mM) into the perfusate resulted in robust insulin secretion in wildtype islets, a response that was severely blunted (greater than 50% reduction) in islets from *Chrebp*$^{-/-}$ mice. These results demonstrate that ChREBP plays an important role in glucose-stimulated insulin secretion by the mouse endocrine pancreas.

To further evaluate the deficit in insulin secretion capacity of islets lacking ChREBP, we tested islet response to a variety of insulin secretagogues (Figure 3.6.C). Again, a 1 hr exposure to high-glucose (17.5 mM) resulted in an approximately 10-fold increase in insulin secretion in control islets and only a 3.5-fold increase in the *Chrebp*$^{-/-}$ islets. Exposure to high extracellular potassium chloride (30 mM), which elicits membrane depolarization independent of glucose, resulted in equivalent insulin secretion by islets of either genotype suggesting that intracellular insulin stores were similar. This

was confirmed by the finding that total insulin contents of wildtype and *Chrebp*$^{-/-}$ islets were identical when measured prior to glucose exposure (Figure 3.6.D).

Other nonglucose insulin secretagogues also caused modest but significant (1.5- to 2-fold) increases in insulin secretion (Figure 3.6.C) regardless of the presence or absence of ChREBP in beta-cells. Tolbutamide works by blocking the SUR1/Kir6.2 channel, forskolin acts by elevating cAMP levels and high-dose arginine promotes calcium inflow by voltage-insensitive channels (Herchuelz, Lebrun et al. 1984; Liang and Matschinsky 1994; Liang and Matschinsky 1994). Methyl pyruvate, at low concentrations (5 mM), initiates membrane depolarization and insulin release by factors other than ATP, and was equally effective in wildtype and *Chrebp*$^{-/-}$ islets, however, at high concentrations (20 mM) methyl pyruvate serves as a cell-permeant mitochondrial energy substrate and failed to induce robust GSIS in the knockout islets (Dukes, Sreenan et al. 1998; Lembert, Joos et al. 2001). In summary those secretagogues that did not require ATP generation worked equally well in wild-type and *Chrebp-/-*islets, while glucose and high-dose methylpyruvate were less effective in stimulating insulin secretion from the knockout islets. We therefore measured the rise in intracellular ATP in wildtype and *ChREBP*$^{-/-}$ islets following glucose exposure (Figure 3.6.E) and we found that it was significantly decreased in the knockout islets (0% to 9.5% increase compared to 39% to 64% increase in wildtype islets). These findings suggest that *Chrebp*-null beta-cells exhibit a defect in insulin secretion, rather than failure of insulin production or storage, and this defect is the result of a disruption in glucose uptake and/or metabolism.

Finally, through the course of all of these experiments using isolated islets, insulin secretion changes were similar whether measurements were carried out as insulin

secretion per islet (such as in Figures 3.6.A&B), per islet total DNA content (such as in Figure 3.6.C) or as a percent of total insulin secreted (not shown). This suggests that altered insulin secretion is not secondary to changes in islet size or cell composition, or to a fundamental lack of insulin production.

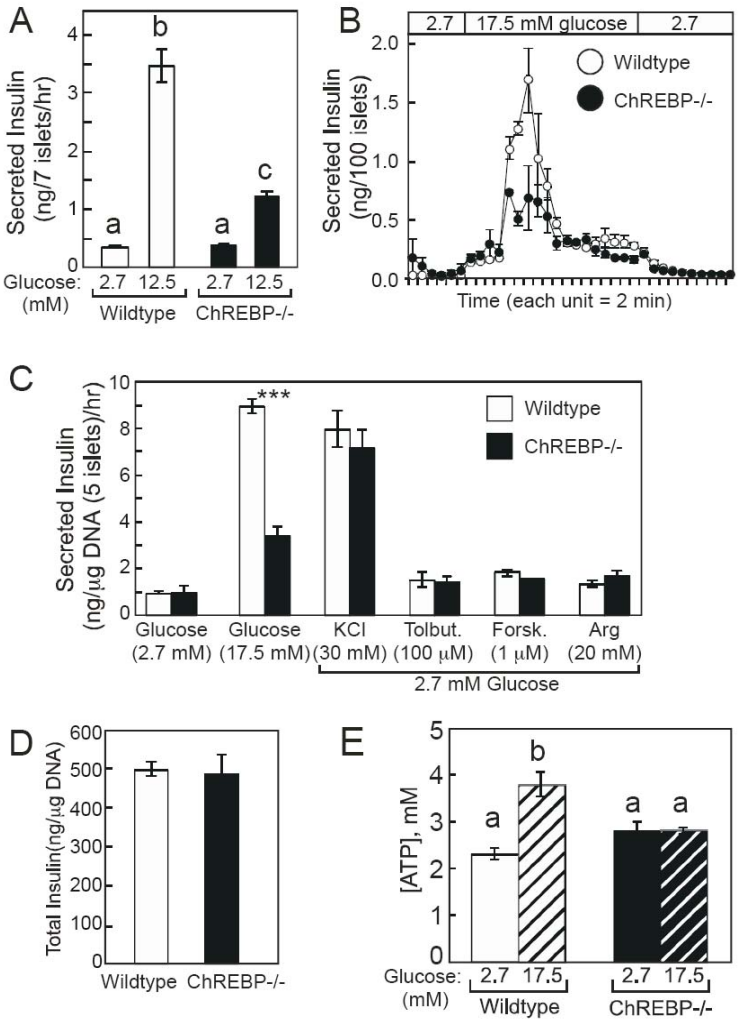

Figure 3.6. Glucose-stimulated insulin secretion is diminished in islets of *Chrebp-/-* mice. (**A**) Insulin secretion during a 1 hr exposure to low (2.7 mM) or high (12.5 mM) glucose was determined for islets isolated from wildtype (open bars) and *Chrebp-/-* (black bars) mice. Values

depict the mean and SEM of 4 wells for each condition. These results are representative of 4 independent experiments.
(**B**) GSIS measured by perifusion was performed using 100 islets/chamber in duplicate for wildtype (open circles) and *Chrebp*-/- mice (black circles). The glucose concentration of the perfusate was increased from 2.7 mM to 17.5 mM at 14 min. The insulin concentrations of each 2-min fraction are provided as the mean and SEM, and the results are representative of 4 independent experiments.
(**C**) Insulin secretion was determined for wildtype and *Chrebp-/-* islets (5 islets/well in triplicate) during a 1 hr exposure to various secretagogues. These data are expressed relative to islet DNA content to further confirm that these changes are not due to altered islet size or composition. Non-standard abbreviations: Tolbut, Tolbutamide; Forsk, forskolin; Arg, arginine; and Me-Pyr, methyl pyruvate.
(**D**) Total insulin content of freshly isolated islets was not different between wildtype and *Chrebp*-null mice.
(**E**) 1 hr exposure to high glucose (17.5 mM) resulted in a significant increase in intracellular ATP concentration in islets from wildtype, but not *Chrebp*-knockout mice. Statistical significance was evaluated by Student's *t* test ((C), ***$P<0.001$) or 2-Way ANOVA using glucose and genotype as factors ((A&E) different letters denote significant difference, $P<0.05$).

To further elucidate the molecular basis of impaired GSIS in *Chrebp*$^{-/-}$ islets, we exposed wildtype and knockout islets to either low-glucose (5 mM) or high-glucose (17.5 mM) conditions for 16 hours and measured mRNA levels of genes implicated in islet development and function by qRT-PCR (Figure 3.7). While we recognize that the insulin secretion deficit is evident within minutes after exposure to high-glucose (Figure 3.6.B), our goal was to identify glucose-regulated ChREBP target genes in islets and a longer glucose exposure time would be necessary to produce measurable changes in mRNA levels. In addition, although our aim was to evaluate the impact of elevated glucose on ChREBP-regulated gene expression, the 16 h high-glucose exposure resulted in very high insulin levels in the culture media (wildtype islets averaged 37 ng/ml for the low-glucose group and 408 ng/ml, or approximately 70 nM, for the high-glucose treated islets). Therefore, genes upregulated under high-glucose conditions could be either glucose-

regulated or insulin-regulated, but importantly our experimental design revealed whether ChREBP was involved in their transcriptional control.

The genotype of islets used in the gene expression analysis was confirmed by the absence of ChREBP mRNA in the islets from knockout mice (Figure 3.7). There was no significant change in ChREBP mRNA level by high-glucose treatment in the wildtype islets. This finding contrasts with a previous report using rat beta-cell sources and may be attributable to species differences or the longer glucose-exposure time used in our study (Wang and Wollheim 2002). We confirmed that the high-glucose treatment regimen was effective as evidenced by the altered expression of two well-documented glucose-responsive genes, Chop10 (also called GADD153, Ddit3 (Shalev, Pise-Masison et al. 2002)) and TXNIP (thioredoxin interacting protein, (Minn, Hafele et al. 2005)). Glucose-mediated regulation of Chop10 and TXNIP expression was unaffected by deletion of *Chrebp*.

We then measured the expression of various transcription factors relevant to ChREBP activity and/or GSIS in the mouse islet. The mRNA levels of Mlx were unaffected by glucose treatment or the absence of ChREBP. High-glucose treatment of islets of either genotype resulted in a dramatic increase in SREBP-1c mRNA levels. The precise inducer, glucose or insulin, is still a matter of debate for beta-cell regulation of SREBP-1c (Sandberg, Fridriksson et al. 2005). It is interesting to note that SREBP-1c target genes such as fatty acid synthase (FAS) are similarly upregulated in both genotypes, yet ChREBP mRNA levels are unchanged by glucose in the wildtype islets even though ChREBP has recently been identified as a direct target gene of SREBP-1 in the rat (Satoh, Masatoshi et al. 2007). Liver X receptor (LXR) agonists have been shown

to increase GSIS (Efanov, Sewing et al. 2004), and LXR itself has been implicated as a glucose-sensor (Mitro, Mak et al. 2007), however neither glucose nor ChREBP status had any effect on the expression of LXRα or LXRβ (data not shown) nor on the expression of *bona fide* LXR-target genes, such as ABCA1 or ABCG1 (data not shown), suggesting that altered LXR activity could not account for the decrease in GSIS of these islets. The RNA levels of other nutrient/hormone-regulated transcription factors, including PPARα, PPARδ and FOXO1 were unaltered by glucose treatment or ChREBP status of islets (data not shown). Of particular importance, the transcriptional coactivator PGC-1α was elevated in the *Chrebp*$^{-/-}$ islets, a situation previously associated with diminished GSIS (Yoon, Xu et al. 2003).

Glucose treatment of islets resulted in significant increases in the mRNA levels of NeuroD1 (Beta2), PDX-1, and MafA (data not shown) as previously reported (Webb, Akbar et al. 2000). Notably the expression of these genes was not affected by the loss of ChREBP. The RNA levels of HNF1α, HNF3β and HNF4α were not changed by high-glucose exposure or *Chrebp* deletion. Therefore our data suggest that ChREBP does not appear to play a role in regulating the expression of transcription factors integral to proper islet development and previously reported to affect beta-cell GSIS (Dukes, Sreenan et al. 1998; Wang, Maechler et al. 2000; Shih, Heimesaat et al. 2002; Wang, Coffinier et al. 2004; Gupta, Vatamaniuk et al. 2005; Holland, Gonez et al. 2005; Zhang, Moriguchi et al. 2005; Miura, Yamagata et al. 2006)

Next we examined the mRNA levels of proteins important in glucose uptake and insulin secretion. Expression of the glucose transporter, GLUT2, was significantly

reduced in *Chrebp*$^{-/-}$ islets at low glucose (45% decrease), medium glucose (11 mM, 51% decrease, data not shown), and high glucose (32% decrease), which would suggest that glucose uptake in *Chrebp*$^{-/-}$ beta-cells is likely impaired. No significant changes were observed by glucose treatment or ChREBP-genotype for glucokinase, the components of the ATP-sensitive potassium channel (SUR1 and Kir6.2) or the insulin-degrading enzyme (IDE). qRT-PCR measurement of insulin (both mouse insulin I and II) and proinsulin (primers detect only insulin II) mRNA levels revealed a significant glucose-mediated increase independent of genotype. IRS-2 mRNA levels were enhanced by high-glucose treatment of islets, as previously reported (Amacker-Francoys, Mohanty et al. 2005), and this increase was greater in *Chrebp*$^{-/-}$ islets. Glucagon mRNA levels were significantly elevated in the *ChREBP*-null islets, most likely by an indirect mechanism relating to the diminished release of insulin into the culture medium of null islets thereby reducing the insulin-mediated repression of this gene in neighboring alpha-cells. Recent reports have implicated the novel hormone, fibroblast growth factor-21 (FGF21), in the function and survival of beta-cells (Wente, Efanov et al. 2006). We found that this metabolic regulator is expressed in cells of the mouse islet, and that high-glucose treatment of islets results in decreased FGF21 mRNA levels, consistent with reports of nutritional regulation of hepatic FGF21 (Inagaki, Dutchak et al. 2007).

Finally, we measured the expression of genes involved in glycolysis. Aldolase B (Aldo2), which can cleave both fructose 1-phosphate and fructose 1,6-bisphosphate to form glyceraldehyde and dihydroxyacetone-phosphate, was dramatically induced by glucose in a ChREBP-dependent manner. There was a significant reduction in aldolase C (Aldo3) mRNA levels in islets exposed to high-glucose conditions, as has been reported

previously (Dvorak, Hardstedt et al. 2007), but neither Aldo1 nor Aldo3 mRNA expression appeared to be affected by the absence of ChREBP. Liver-type pyruvate kinase (L-PK) mRNA levels were reduced in islets lacking ChREBP (16% reduction under 5 mM glucose conditions, 36% reduction in 17.5 mM glucose), as previously described in the liver of *Chrebp-/-* mice (Iizuka, Miller et al. 2006). However, L-PK, a *bona fide* ChREBP target gene (Ishii, Iizuka et al. 2004; da Silva Xavier, Rutter et al. 2006; Satoh, Masatoshi et al. 2007) failed to show any increase in islets upon glucose exposure. This was somewhat surprising, although likely attributed to a concomitant insulin-mediated repression of this gene (Ishii, Iizuka et al. 2004; Dentin, Benhamed et al. 2005). Our studies using intact mouse islets capable of robust insulin secretion would therefore differ from other reports of glucose-stimulated L-PK levels using insulinoma cell lines that secrete far less insulin (Wang and Wollheim 2002; Wang, Kouri et al. 2005; da Silva Xavier, Rutter et al. 2006). This observation is also supported by the failure to identify L-PK among glucose-regulated genes in a microarray study of human islets (Shalev, Pise-Masison et al. 2002). The impact of these changes in islet L-PK expression on glycolytic flux may be minimal, as the muscle-type pyruvate kinase (M-PK) appears to be far more abundant.

All pyruvate dehydrogenase kinase (PDK) isoforms were present in mouse islets, and PDK4 exhibited a glucose (insulin)-mediated repression in wild-type islets as previously reported (Huang, Wu et al. 2002; Xu, Han et al. 2006). PDK4 mRNA levels were elevated in *Chrebp*$^{-/-}$ islets and unaffected by high glucose exposure, which would suggest a metabolic shift from glucose to other substrates for energy homeostasis (Kwon and Harris 2004). The similarity in expression profile of PDK4 to glucagon, an insulin-

repressed gene, supports the assertion that insulin, not glucose, is responsible for PDK4 repression and that the diminished GSIS capacity of the *Chrebp*$^{-/-}$ islets would result in enhanced PDK4 mRNA levels. A possible molecular mechanism for this effect is provided by reports that glucose-mediated insulin via paracrine action in the beta-cell promotes nuclear exclusion of FoxO1, a positive transcriptional regulator of PDK4 (Furuyama, Kitayama et al. 2003; Martinez, Cras-Meneur et al. 2006).

In summary these gene expression changes support the hypothesis that *Chrebp*$^{-/-}$ islets secrete less insulin when exposed to glucose than their wildtype counterparts. We observed a change in the expression of genes that play a role in the cellular uptake and utilization of glucose (GLUT2, L-PK, Aldo2, PDK4, PGC-1α) in islets that lack the glucose-sensitive transcription factor, ChREBP. Diminished insulin secretion by *Chrebp*$^{-/-}$ islets was evident as known insulin-regulated genes (glucagon, PDK4) exhibited little or no change in mRNA levels in the knockout islets exposed to high glucose when compared to wildtype islets under the same conditions.

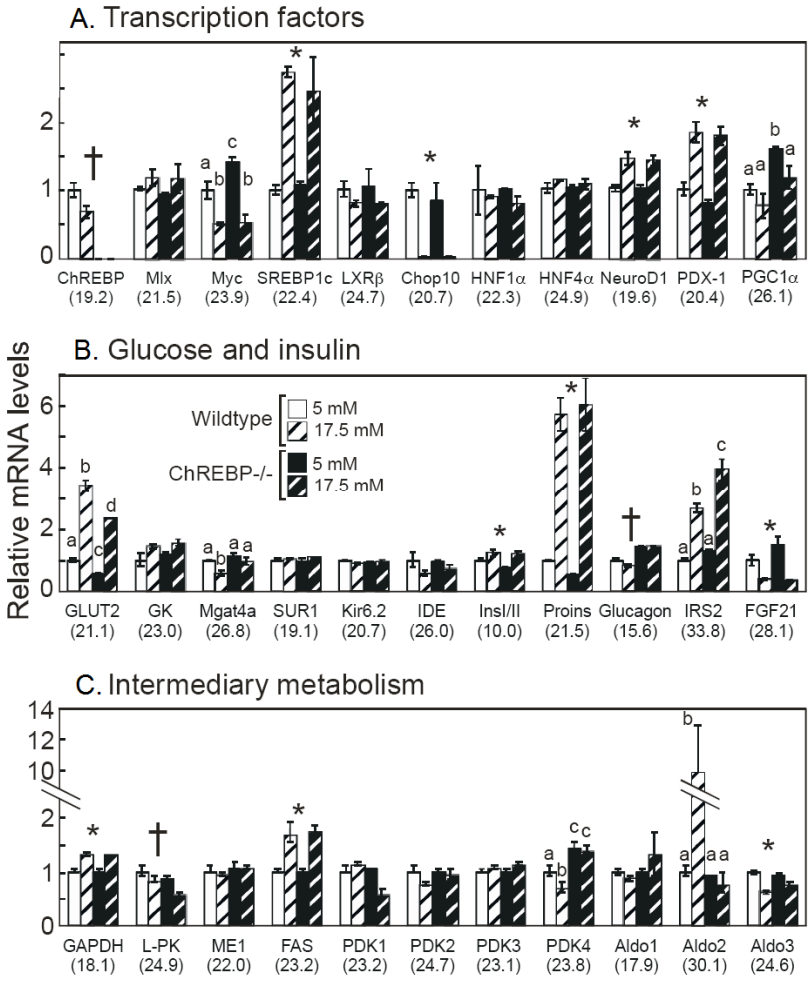

Figure 3.7. The effect of extracellular glucose concentration on gene expression in wildtype and *Chrebp*-/- mouse islets. 200 islets/well in duplicate for each condition were incubated in 3 mM glucose for 8 hours, then switched to low (5 mM, solid) or high (17.5 mM, hatched) glucose for 16 hours before RNA was harvested. mRNA levels were measured by qRT-PCR using HPRT as the invariant housekeeping gene. Values reflect the means and Std. Dev. of multiple islet samples. 2-way ANOVA was used to establish statistical significance, with glucose and genotype as factors. If only glucose (*) or genotype (†) effects were significant a symbol denotes $P<0.05$. If a significant interaction of factors was evident, different letters denote groups that are significantly different ($P<0.05$). The cycle number at threshold for each gene is indicated in parentheses to provide a relative sense of RNA abundance (a smaller Ct value reflects a larger RNA quantity, with each Ct unit roughly equivalent to a 2-fold RNA difference). The full name of each gene is available in Supplementary Table 3.1.

The effects of *Chrebp* deletion on insulin dynamics and glucose homeostasis were then evaluated in the *Chrebp*-knockout mice. Plasma glucose levels were statistically greater in *Chrebp*$^{-/-}$ mice in the postprandial state, but no difference was observed upon fasting (Figure 3.8A). In both nutritional states, however plasma insulin levels were significantly reduced in the knockout mice compared to wildtype mice (Figure 3.8B). Glucose clearance from the bloodstream following an intraperitoneal injection of glucose was impaired in *Chrebp*-null mice and this was accompanied by lower plasma insulin levels and a delay in the typical glucose-initiated insulin rise (Figure 3.8C). These observations were evident in both male and female mice (data not shown) further confirming our previous results that *Chrebp*$^{-/-}$ mice have impaired insulin secretion. Although *in vitro* assessment of islet GSIS suggested that very little insulin secretion occurs in the absence of ChREBP (Figure 3.6), there were still substantial circulating insulin levels in the null animals. To test the possibility that insulin stability was enhanced in the knockout mice, we determined the hepatic expression levels of the insulin-degrading enzyme (IDE) and found that there was a compensatory decrease in mRNA and protein levels for IDE, which would be predicted to preserve the integrity of insulin secreted by the *Chrebp*-knockout mice.

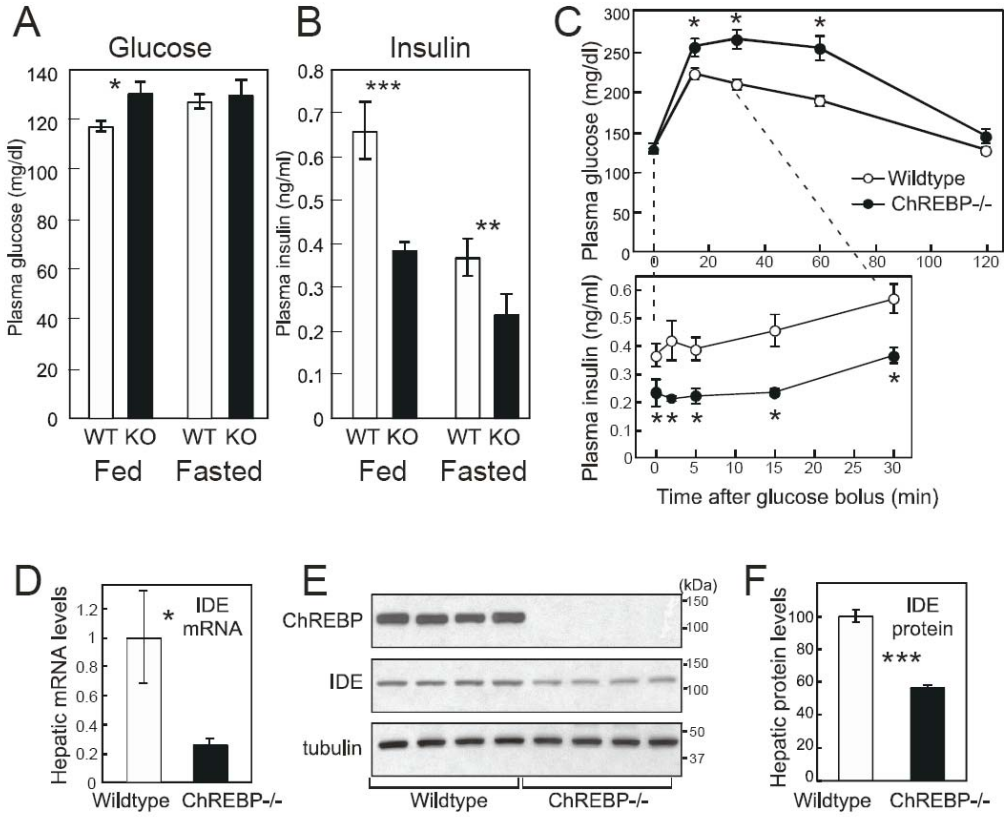

Figure 3.8. ***Chrebp*-/- mice exhibit lower insulin levels and impaired glucose clearance.**
(**A**) Plasma glucose and (**B**) plasma insulin levels were measured for 3-4 month-old wildtype (open bars, n=8-14) and *Chrebp-/-* (closed bars, n=8-16) mice in the fed-state, or following an overnight fast. Values denote the means and SEM, and Student's *t* test revealed statistical significance at **P*<0.05, ***P*<0.01, ****P*<0.001.
(**C**) After an overnight fast, 3.5 month-old male wildtype (open circles) or *Chrebp-/-* (closed circles) mice received a glucose bolus (1g/kg body wt) by intraperitoneal injection. Blood was collected at the various time points and plasma glucose (upper panel) and insulin (lower panel) were measured. Means and SEM are provided, n=8 per group, and* *P*<0.05 by Student's *t* test. (**D**) Hepatic mRNA expression of the insulin-degrading enzyme (IDE) in wildtype (open bars) and *Chrebp-/-* (closed bars) mice was determined by qRT-PCR using cyclophilin as the housekeeping gene. Comparable changes were observed at the protein level by western analysis (**E**) with quantitation by densitometry provided in (**F**). Values in (D-F) are means and STD. Dev. for n=4, and Student's *t* test revealed differences at **P*<0.05, ****P*<0.001.

To test whether the altered insulin dynamics observed in the *Chrebp*$^{-/-}$ mice could also occur due to a change in islet architecture, size or number, we performed

immunohistochemical analyses of the dorsal lobe of the pancreas in these mice to more accurately assess islet morphology. Although we found the predicted change in islet size along the proximal-distal axes of the dorsal pancreata, there was no apparent difference in islet size between the *Chrebp*$^{-/-}$ and wildtype mice (Figure 3.9. A). We found no change in islet architecture in the *Chrebp*-null mice as they exhibited the typical spherical structure with beta-cells in the core and alpha-cells on the mantle (Cabrera, Berman et al. 2006). Beta-cell mass was defined by insulin immunofluorescence and found to be unaltered in the dorsal pancreata of mice lacking ChREBP (% pancreas area, mean ± Std. Dev.: wildtype = 0.69 ± 0.14, *Chrebp*$^{-/-}$ = 0.68 ± 0.09**)**. In support of these histological analyses, we never observed a discernable difference in the quantity, size or shape of islets obtained from either *Chrebp*$^{-/-}$ or wildtype mice in the many islet isolations we performed. In addition, pancreases from *Chrebp*$^{-/-}$ mice have similar weights (Figure 3.9.B) and total pancreatic insulin contents (Figure 3.9.C) when compared to pancreases form wild type mice. In summary there appears to be no alteration in islet development in the *Chrebp*$^{-/-}$ mice, an observation consistent with the equivalent expression of key transcriptional regulators (HNF1α, HNF3β, HNF4α, MafA, Pdx1, see Figure 3.7) and unaltered insulin content and RNA levels (Figures 3.6 and 3.7).

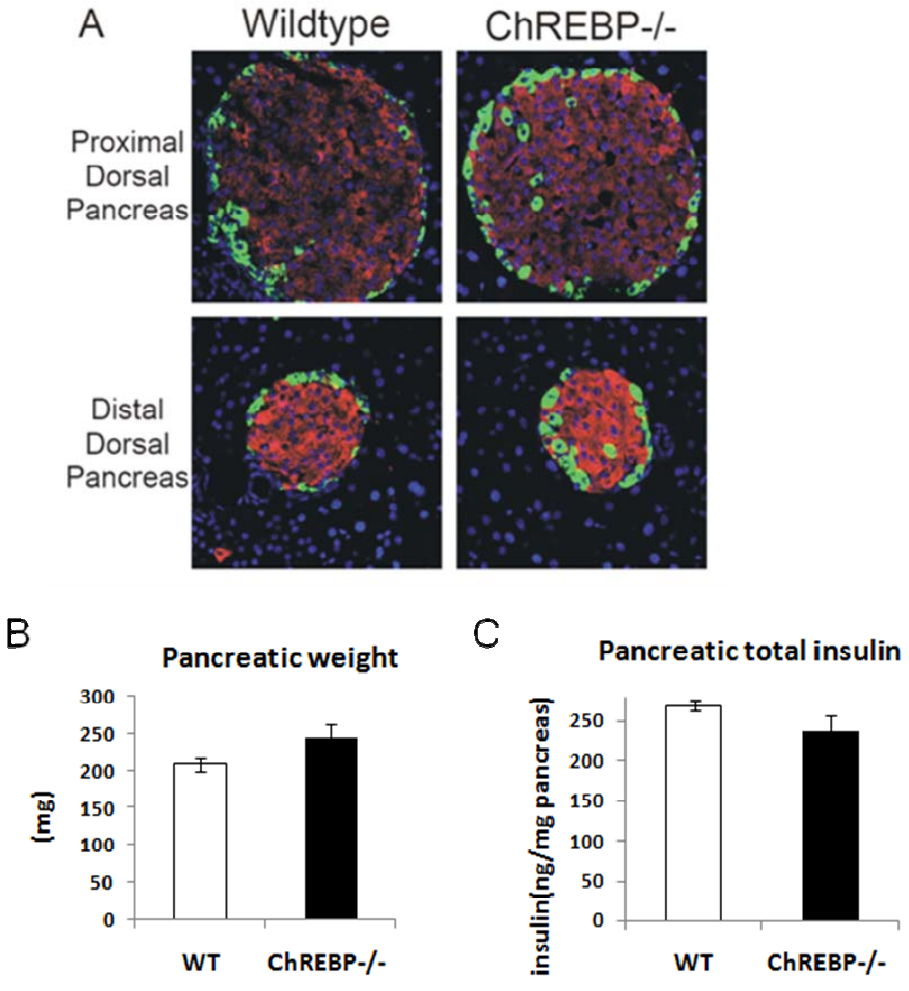

Figure 3.9. Pancreatic weight, islet size, islet architecture, and total pancreatic insulin are unaltered in *Chrebp*-null mice. (A) Beta-cells (red) and alpha-cells (green) were visualized in adult mouse dorsal pancreas by immunostaining for insulin and glucagon, respectively. DAPI-counterstain (blue) reveals cell nuclei. Fluorescent images were captured by confocal microscopy at a magnification of 40X. (B) Wet pancreatic weights were obtained after the pancreases were carefully dissected from wild type (WT) and *ChREBP-/-* mice. (C) Pancreatic insulin was extracted in acid ethanol from whole pancreas and was measured using RIA. There is no significant difference in pancreatic weight and total pancreatic insulin between genotypes (n=3).

Discussion

In this study, we addressed the effects of LXR activation in the mouse pancreatic islet and evaluated the contribution of islet function changes due to LXR in ameliorating the diabetic phenotype when mice are treated with an LXR agonist.

We established that LXRβ is the predominant receptor subtype expressed in beta-cells of islet and that the LXR/RXR pathway is functional in isolated mouse islet. This pathway can be activated by T1317, a synthetic LXR ligand, and results in regulation of recognized LXR target genes such as SCD1, FAS, ABCA1, and SREBP-1c (Fig 3.1).

We also demonstrated that a short term (16 hour) pretreatment of isolated mouse islets with T1317 is sufficient to enhance GSIS (Fig 3.3). This effect is LXR-dependent since T1317 failed to enhance GSIS in islets of *Lxr* -/- mice. The enhanced GSIS of islets is not due to an increase of insulin synthesis since the mRNA and protein of insulin was not altered after T1317 treatment. We hypothesized that the activation of LXR regulates genes that are involved in glucose processing and/or proteins that are components in the insulin secretion pathway.

Using a candidate approach, we examined several groups of genes that are involved in the signaling cascade linking glucose entrance and insulin release by the beta-cell. Genes of the first group are glucose transporters, processing enzymes, and glucose sensing proteins. Glucokinase and ChREBP are the two genes that belong to this category that are induced by LXR in the islet. The second group of genes include membrane channels that regulate the flux of intracellular calcium that initiates vesicle trafficking. Our qPCR data revealed that Cav1.2 and Cav1.3 are likely to be regulated by LXR in the mouse islet. The final group of genes includes vesicle proteins involved in the

translocation of vesicles necessary for insulin release. SNAP25 and CAPS are candidates that appeared to be regulated by LXR.

We ruled out the possibility that many of the well known target genes of LXR such as *SREBP1c*, *SCD1*, *ABCA1*, or *PPARα* are the exclusive mediators of the observed GSIS enhancing effects of LXR by testing T1317 on islets from mice that harber deletions in each of these genes.

Among the several candidate targets identified, we chose to further characterize ChREBP because of its important role in sensing glucose (Uyeda and Repa 2006). We determined that it is a direct target gene of LXR and is abundantly expressed in the beta-cells of the islets (Fig 3.5) and demonstrated that ChREBP plays a vital role in linking glucose exposure to insulin secretion in the beta-cell. Islets from *ChREBP* -/- mice do not exhibit the typical rise in ATP following high glucose treatment, and fail to secrete insulin at levels seen in wild-type mice. However, *ChREBP* -/- islets contain similar quantities of insulin and respond appropriately to non-glucose secretagogues.

Although our data clearly established that LXR affects ChREBP in islet and that ChREBP is critical for proper GSIS responses, islets from *Chrebp*-/- mice still exhibit enhanced insulin secretion after T1317 treatment. This implies that ChREBP is not the only mediator for the GSIS enhancing effect of LXR activation and that other LXR targets are involved in this response.

With these results, we believe that the GSIS enhancing effect of LXR agonists in mouse islets is the consequence of the activation of several pathways that facilitate glucose processing and insulin shuttling inside the beta-cells.

Using a microarray assay, we also identified several novel candidate genes that show altered expression in islets by LXR activation. Among these candidates, *Ghrelin, Sulf1*, and *IAPP* are the most attractive genes for us to pursue further because of their potential roles in regulating insulin secretion and amyloid formation in the islet (Haataja, Gurlo et al. 2008; Yada, Dezaki et al. 2008). Whether these genes are direct targets of LXR or not is still under investigation.

Results from our studies and from others provide evidence that the activation of LXR in mouse islets enhances GSIS (current study and (Efanov, Sewing et al. 2004; Gerin, Dolinsky et al. 2005)). Recently, in collaborative studies with Dr. Raghu Mirmira (IUPUI), we have extended these observations to human islets. Exposing human islets to LXR agonists T1317 or GW3965 leads to enhanced GSIS (data not shown). These observations demonstrate that the role of LXR in regulating GSIS is conserved between mouse and human and suggests that these findings may contribute to novel therapies for the treatment of type II diabetes.

Our studies took a pharmacological approach to the questions by utilizing high affinity, synthetic ligands/drugs. However, the endogenous LXR ligands and physiological importance of this pathway will be a future area of study and will be facilitated by advances in technology that allow for the measurement of low abundance sterols in small tissues. The recent report that mice harboring a beta-cell deletion of ABCA1 (that results in cholesterol accumulation) exhibit impaired insulin secretion (Brunham, Kruit et al. 2008) suggests a role for sterols in beta-cell function.

Our qPCR results revealed that the abundance of LXR mRNA is not altered in islets by varing the glucose concentration in the culture medium (Fig 2.4). However, the

protein level and activity of LXR in islet cells has not yet been examined. A recent report suggests that the glucose may regulate the cytoplasmic to nuclear translocation of LXRα in a rat beta-cell line (Helleboid-Chapman, Helleboid et al. 2006). This suggests that while the synthesis of LXR might not be regulated by glucose, the activity of the protein may be subject to post-translational modifications. The functional relevance of this observation will also require further study since LXRα appears to be less abundant than LXRβ.

In summary, in this study we demostrated a novel function of LXR-ChREBP axis in regulating GSIS in mouse islets by the use of synthetic ligand and islets of mouse with global deletion of LXRs. Future studies that utilize beta-cell specific knockout of LXRs and beta-cell specific expression of a constitutively active LXR will further advance our understanding of the role(s) of islet LXR in glucose homeostasis. Results of these studies may reveal novel therapies for treatment of type II diabetes.

Table 3.1 qRT PCR primer sequences for LXR study

Gene Abbrev.	Gene Name	Accession Number	Sequence of Primers (5' to 3')
Aldo1	Aldolase 1	NM_007438	F: CCCTTCCCCCAAGTTATCAA R: GGGCACCACACCCTTATCTAC
Aldo2	Aldolase 2	NM_144903	F: AATGGGCTGGTCCCTATTGTT R: GGCAGTGCTCCAGGTCATG
Aldo3	Aldolase 3	NM_009657	F: GAGAAGGTCCTGGCTGCTGTATA R: CATGTTGGGCTTGAGCAGAGT
Chop10	C/EBP-homologous Protein (GADD153, Ddit3)	NM_007837	F: CACCACACCTGAAAGCAGAAC R: GGTGAAAGGCAGGGACTCA
ChREBP	Carbohydrate Response Element Binding Protein	NM_021455	F: AGAACCGACGTATCACACACATCT R: CAGGGTGTCGAATCCTAGCTTAA
Cyclo	Cyclophilin	NM_011149	F: TGGAGAGCACCAAGACAGACA R: TGCCGGAGTCGACAATGAT

FAS	Fatty Acid Synthase	NM_007988	F: GCTGCGGAAACTTCAGGAAAT R: AGAGACGTGTCACTCCTGGACTT
FGF21	Fibroblast Growth Factor 21	NM_020013	F: CCTCTAGGTTTCTTTGCCAACAG R: AAGCTGCAGGCCTCAGGAT
FOXO1	Forkhead Box O1	NM_019739	F: TCATGGATGGAGATACCTTGGA R: CTTGACACTGTGTGGGAAGCTT
GAPDH	Glyceraldehyde-3-phosphate Dehydrogenase	NM_199472	F: CAAGGTCATCCATGACAACTTTG R: GGCCATCCACAGTCTTCTGG
GCK	Glucokinase (HK4)	NM_010292	F: GGCCACCAAGAAGGAAAAGG R: TCTGCATCCGGCTCATCAC3
Glucagon	Glucagon	XM_130336	F: ATTCACCAGCGACTACAGCAA R: TCATCAACCACTGCACAAAATC
GLUT2	Glucose Transporter Type II (SLC2A2)	XM_124017	F: CAACTGGGTCTGCAATTTTGTC R: GAACACGTAAGGCCCAAGGA
HNF1α	Hepatocyte Nuclear Factor 1α	NM_009327	F: CTGACCGAGTTGCCTAATGG R: CCATCGTCATCCGTGTCATC
HNF3β	Hepatocyte Nuclear Factor 3β (Foxa2)	NM_010446	F: AGAGCCCCAACAAGATGCTGA R: AGAGAGTGGCGGATGGAGTTCT
HNF4α	Hepatocyte Nuclear Factor 4α (NR2A1)	NM_008261	F: CCAACCTCAATTCATCCAACA R: CCCGGTCGCCACAGAT
IDE	Insulin Degrading Enzyme	NM_031156	F: TGATAGACATGGTTCTTGATAAACTCA R: TTTTCCCTTCAAATGATTTGGA
InsI/II	Insulin I/II	NM_008386 NM_008387	F: TGAAGTGGAGGACCCACAAGT R: AGATGCTGGTGCAGCACTGAT
IRS2	Insulin Receptor Substrate 2	XM_976196	F: GGAGAACCCAGACCCTAAGCTACT R: GATGCCTTTGAGGCCTTCAC
Kir6.2	ATP-sensitive K^+ Channel Subunit Kir6.2	NM_010602	F: GCAGAGCCCAGGTACCGTACT R: CGTTGCAGTTGCCTTTCTTG
L-PK	Liver-type Pyruvate Kinase	NM_013631	F: GGGCCGCATCTACATTGAC R: GTCCCTCTGGGCCAATTTT
LXRα	Liver X Receptor α (NR1H3)	NM_013839	F: AGGAGTGTCGACTTCGCAAA R: CTCTTCTTGCCGCTTCAGTTT
LXRβ	Liver X Receptor β (NR1H2)	NM_009473	F: CTCCCACCCACGCTTACAC R: GCCCTAACCTCTCTCCACTCA
MafA	MafA	NM_194350	F: TTCAGCAAGGAGGAGGTCATC R: GCGTAGCCGCGGTTCT
Mlx	Max-like Protein X	NM_011550	F: GGAGCTCTCAGCTTGTGTCTTCA R: CACCGATCACAATCTCTCGTAGAGT
M-PK	Muscle-type Pyruvate Kinase	NM_011099	F: CCTCGACAACGCTTACATGGA R: CCACCACCTTGCAGATGTTCT
NeuroD1	NeuroD1	NM_010894	F: TCCAGGGTTATGAGATCGTCACTA R: CCCGCTCTCGCTGTATGATT
PDK1	Pyruvate Dehydrogenase Kinase1	NM_172665	F: GTGTTTGCTGAAGCTCCTAAAGG R: TGTTCAAAACCACGCCCAAT

PDK2	Pyruvate Dehydrogenase Kinase 2	NM_133667	F: TCTTTGATGGCAGCACCAA R: AGGAGCTTAGCCATGTCATAGG
PDK3	Pyruvate Dehydrogenase Kinase 3	NM_145630	F: CCAGAGACGCGTATTTCTACCA R: GCCATTATAAAGAAAGCAACTAAGCA
PDK4	Pyruvate Dehydrogenase Kinase 4	NM_013743	F: CAAAGACGGGAAACCCAAGC R: CGCAGAGCATCTTTGCACAC
PDX1	Pancreatic and Duodenal Homeobox Factor-1	XM_124700	F: AGTGGGCAGGAGGTGCTTA R: GCCCGGGTGTAGGCAGTC
PGC1α	PPARγ Coactivator 1α	NM_008904	F: AACCACACCCACAGGATCAGA R: TCTTCGCTTTATTGCTCCATGA
Proinsulin	Proinsulin	NM_008387	F: GGGGAGCGTGGCTTCTTCTA R: GGGGACAGAATTCAGTGGCA
SREBP-1c	Sterol Response Element Binding Protein 1c	NM_011480	F: GGAGCCATGGATTGCACATT R: GGCCCGGGAAGTCACTGT
SUR1	Sulfonylurea Receptor 1 (ABCC8)	NM_011510	F: TCTCGCCTTTTTCCGAATG R: TGTCGATGCCATCAATGATA
TXNIP	Thioredoxin-interacting Protein	NM_023719	F: TATGTACGCCCCTGAGTTCCA R: GTTAAGGACGCACGGATCCA

Table 3.2. List of genes up-regulated in human islets by LXR agonist (T1317, 24 hours, 2.5mM glucose).

Ratio	Gene Identifier	Gene Name	Gene ID
10.59	NM_005502	ATP-binding cassette, sub-family A (ABC1), member 1	ABCA1
7.92	NM_004915	ATP-binding cassette, sub-family G (WHITE), member 1	ABCG1
3.38	NM_004176	Sterol regulatory element binding transcription factor 1	SREBF1
2.59	NM_005629	Solute carrier family 6 (neurotransmitter transporter, creatine), member 8	SLC6A8
2.54	NM_001124	Adrenomedullin	ADM
2.52	NM_005623	Chemokine (C-C motif) ligand 8	CCL8
2.49	NM_198857	solute carrier family 6 (neurotransmitter transporter, creatine), member 10 (pseudogene)	-
2.47	NM_002155	Heat shock 70kDa protein 6 (HSP70B)	HSPA6
2.44	NM_013262	Myosin regulatory light chain interacting protein	MYLIP
2.18	NM_004104	Fatty acid synthase	FASN
2.17	NM_014495	Angiopoietin-like 3	ANGPTL3
2.08	NM_000096	Ceruloplasmin (ferroxidase)	CP

2.08	NM_001063	Transferrin	TF
2.06	NM_005063	Stearoyl-CoA desaturase (delta-9-desaturase)	SCD
2.04	NM_198452	pregnancy upregulated non-ubiquitously expressed CaM kinase	-
2	NM_015714	G0/G1switch 2	G0S2
1.98	NM_016362	Ghrelin/obestatin preprohormone	GHRL
1.91	NM_021242	MID1 interacting protein 1 (gastrulation specific G12 homolog (zebrafish))	MID1IP1
1.89	NM_005768	Membrane bound O-acyltransferase domain containing 5	MBOAT5
1.86	NM_021870	Fibrinogen gamma chain	FGG
1.83	NM_000509	Fibrinogen gamma chain	FGG
1.81	NM_000041	Apolipoprotein E	APOE
1.79	NM_000033	ATP-binding cassette, sub-family D (ALD), member 1	ABCD1
1.79	NM_003247	Thrombospondin 2	THBS2
1.79	NM_003632	Contactin associated protein 1	CNTNAP1
1.79	NM_003043	Solute carrier family 6 (neurotransmitter transporter, taurine), member 6	SLC6A6
1.78	NM_173803	MPV17 mitochondrial membrane protein-like	MPV17L
1.77	NM_006516	Solute carrier family 2 (facilitated glucose transporter), member 1	SLC2A1
1.75	NM_005952	Metallothionein 1X	MT1X
1.72	NM_020351	Collagen, type VIII, alpha 1	COL8A1
1.71	NM_006472	Thioredoxin interacting protein	TXNIP
1.71	NM_000095	Cartilage oligomeric matrix protein	COMP
1.7	NM_000917	Procollagen-proline, 2-oxoglutarate 4-dioxygenase (proline 4-hydroxylase), alpha polypeptide I	P4HA1
1.69	NM_145693	Lipin 1	LPIN1
1.67	NM_153322	Peripheral myelin protein 22	PMP22
1.67	NM_000664	acetyl-Coenzyme A carboxylase alpha	-
1.64	NM_001002921	adenylate kinase 3-like 2 (AK3L2), mRNA.	-
1.64	NM_003517	Histone cluster 2, H2ac	HIST2H2AC
1.62	NM_000576	Interleukin 1, beta	IL1B
1.62	NM_013402	Fatty acid desaturase 1	FADS1
1.61	NM_004331	BCL2/adenovirus E1B 19kDa interacting protein 3-like	BNIP3L
1.61	NM_144726	Ring finger protein 145	RNF145
1.59	NM_022918	Transmembrane protein 135	TMEM135
1.58	NM_002521	Natriuretic peptide precursor B	NPPB
1.58	NM_000591	CD14 molecule	CD14
1.56	NM_005953	Metallothionein 2A	MT2A
1.55	NM_021871	Fibrinogen alpha chain	FGA
1.54	NM_014470	Rho family GTPase 1	RND1
1.54	NM_004750	Cytokine receptor-like factor 1	CRLF1
1.54	NM_012261	Chromosome 20 open reading frame 103	C20orf103
1.54	NM_012215	Meningioma expressed antigen 5 (hyaluronidase)	MGEA5
1.53	NM_005110	Glutamine-fructose-6-phosphate transaminase 2	GFPT2
1.53	NM_001995	Acyl-CoA synthetase long-chain family member 1	ACSL1

1.53	NM_018719	Cell division cycle associated 7-like	CDCA7L
1.52	NM_001964	Early growth response 1	EGR1
1.51	NM_002133	Heme oxygenase (decycling) 1	HMOX1
1.5	NM_002145	Homeobox B2	HOXB2

Table 3.3. List of genes down-regulated in human islets by LXR agonist (T1317, 24 hours, 2.5mM glucose).

Ratio	Gene Identifier	Gene Name	Gene ID
2.44	NM_006890	Carcinoembryonic antigen-related cell adhesion molecule 7	CEACAM7
2.26	NM_002281	Keratin 81	KRT81
2.23	NM_000669	Alcohol dehydrogenase 1C (class I), gamma polypeptide	ADH1C
2.2	NM_000667	Alcohol dehydrogenase 1A (class I), alpha polypeptide	ADH1A
2.13	NM_181339	Interleukin 24	IL24
2.09	NM_000477	Albumin	ALB
2.09	NM_001740	Calbindin 2, 29kDa (calretinin)	CALB2
2.04	NM_001073	UDP glucuronosyltransferase 2 family, polypeptide B11	UGT2B11
2.01	NM_006498	Lectin, galactoside-binding, soluble, 2	LGALS2
2	NM_001077	UDP glucuronosyltransferase 2 family, polypeptide B17	UGT2B17
2	NM_000771	Cytochrome P450, family 2, subfamily C, polypeptide 9	CYP2C9
1.98	NM_138786	Transmembrane 4 L six family member 18	TM4SF18
1.98	NM_018414	ST6 (alpha-N-acetyl-neuraminyl-2,3-beta-galactosyl-1,3)-N-acetylgalactosaminide alpha-2,6-sialyltransferase 1	ST6GALNAC1
1.94	NM_000239	Lysozyme (renal amyloidosis)	LYZ
1.92	NM_001074	UDP glucuronosyltransferase 2 family, polypeptide B7	UGT2B7
1.89	NM_005555	Keratin 6A	KRT6A
1.87	NM_007193	Annexin A10	ANXA10
1.87	NM_020665	Transmembrane protein 27	TMEM27
1.81	NM_175056	Zona pellucida-like domain containing 1	ZPLD1
1.77	NM_015515	Keratin 23 (histone deacetylase inducible)	KRT23
1.76	NM_001031692	Leucine rich repeat containing 17	LRRC17
1.74	NM_138768	Myeloma overexpressed gene (in a subset of t(11;14) positive multiple myelomas)	MYEOV
1.7	NM_002785	Pregnancy specific beta-1-glycoprotein 11	PSG11
1.69	NM_003561	Phospholipase A2, group X	PLA2G10
1.68	NM_020384	Claudin 2	CLDN2
1.65	NM_000065	Complement component 6	C6
1.65	NM_015170	Sulfatase 1	SULF1
1.64	NM_002989	Chemokine (C-C motif) ligand 21	CCL21
1.62	NM_000691	Aldehyde dehydrogenase 3 family, memberA1	ALDH3A1
1.6	NM_176813	Anterior gradient homolog 3 (Xenopus laevis)	AGR3
1.58	NM_000415	Islet amyloid polypeptide	IAPP

1.58	NM_006418	Olfactomedin 4	OLFM4
1.57	NM_004086	Coagulation factor C homolog, cochlin (Limulus polyphemus)	COCH
1.57	NM_002960	S100 calcium binding protein A3	S100A3
1.56	NM_002242	Potassium inwardly-rectifying channel, subfamily J, member 13	KCNJ13
1.56	NM_152321	Endoplasmic reticulum protein 27 kDa	ERP27
1.56	NM_002658	Plasminogen activator, urokinase	PLAU
1.56	NM_178125	Tripartite motif-containing 50	TRIM50
1.55	NM_015964	Tubulin polymerization-promoting protein family member 3	TPPP3
1.55	NM_007127	Villin 1	VIL1
1.54	NM_000562	Complement component 8, alpha polypeptide	C8A
1.54	NM_005769	Carbohydrate (N-acetylglucosamine 6-O) sulfotransferase 4	CHST4
1.53	NM_002044	Galactokinase 2	GALK2
1.52	NM_173213	keratin 23 (histone deacetylase inducible)	-
1.51	NM_002993	Chemokine (C-X-C motif) ligand 6 (granulocyte chemotactic protein 2)	CXCL6
1.51	NM_025047	ADP-ribosylation factor-like 14	ARL14
1.51	NM_001001548	CD36 molecule (thrombospondin receptor)	CD36
1.5	NM_012449	Six transmembrane epithelial antigen of the prostate 1	STEAP1

CHAPTER FOUR

Identification of novel interaction between HNF4α and HNF4γ in the beta cells of islets

Abstract

Hepatocyte nuclear factor 4α (HNF4α) and hepatocyte nuclear factor 4γ (HNF4γ) are closely related members of the nuclear receptor superfamily. HNF4α was first discovered as a liver enriched transcriptional factor that is important for both liver development and function. In addition to liver, HNF4α is also expressed in intestine, kidney, and endocrine pancreas. Mutations of HNF4α in human are responsible for MODY1, one of the monogenic forms of type II diabetes mellitus. Using quantitative RT-PCR, we confirmed the expression of HNF4α in the beta-cells of the mouse islet and also found that its closely related family member, HNF4γ, is abundantly expressed in these cells. The high level of primary sequence similarity and the coexpression of these two nuclear receptors in this cell type lead us to hypothesize that there may be a novel interaction between HNF4α and HNF4γ. Using a variety of biochemical and cell-based approaches, we demonstrate that HNF4α and HNF4γ can form a functional heterodimer. More importantly, this endogenous heterodimer can be identified by co-immunoprecipitation from nuclear lysates of mouse islets and beta-cell lines. Cell reporter assays revealed the differential interaction of coactivators and corepressors with these two HNF4 receptor subtypes. Thus, the formation of various dimer combinations coupled with the

differential coregulator interactions suggest that novel mechanisms may exist for HNF4α and HNF4γ to regulate gene expression in the islets.

Introduction

HNF4α is a liver-enriched transcription factor that was first identified in rat liver nuclear extracts (Sladek, Zhong et al. 1990). HNF4α regulates many genes that are important for fetal liver development and adult liver function. In addition to liver, HNF4α is present in kidney, intestine, and beta cells of the pancreatic islets. Mutations in HNF4α are responsible for maturity-onset diabetes of the young (MODY1), a monogenic form of diabetes. (Yamagata, Furuta et al. 1996). Mice harboring a beta-cell specific HNF4α deletion exhibit impaired insulin secretion (Miura, Yamagata et al. 2006). These findings confirm that HNF4α is important in islet function and diabetes pathology. Multiple transcript variants of HNF4α, generated by differential promoter usage and alternative splicing, were subsequently characterized and appear to show a tissue-specific distribution with HNF4α1 and α2 present predominantly in liver while HNF4α7 and α8 are highly expressed in beta-cells (Taraviras, Monaghan et al. 1994; Nakhei, Lingott et al. 1998; Thomas, Jaschkowitz et al. 2001).

HNF4γ was originally cloned from a mouse gut cDNA library and found to share a high degree of similarity in amino acid sequence with HNF4α (94% in the DNA-binding domain and 80% in the ligand-binding domain (LBD)). However, unlike HNF4α, HNF4γ is not present in liver, but is similarly expressed in intestine, kidney, and beta-cells of the islets (Drewes, Senkel et al. 1996; Taraviras, Mantamadiotis et al. 2000).

Very little is known about the function of HNF4γ. In the intestine, HNF4γ levels have been linked to the regulation of *apoAIV* expression and recent reports have found an association between SNPs in the HNF4γ gene and the occurrence of inflammatory bowel disease (Franke, Hampe et al. 2007; Wu, Dassopoulos et al. 2007).

HNF4s have been classified as constitutively active nuclear receptors, since their overexpression in nearly any cell type appears to confer enhanced transcription of target genes. The structural analysis of these receptors by crystallography revealed a fatty acid within the ligand-binding pockets for both HNF4α (Δηε–Παγανον, Δυδα ετ αλ. 2002) and HNF4γ (Ωισελψ, Μιλλερ ετ αλ. 2002), which did not appear to be exchangeable as required for traditional ligands (Petrescu, Hertz et al. 2002). Other reports suggest that fatty acyl-CoA thioesters may function as HNF4α ligands. Further studies will be required to determine whether these nuclear receptors may serve as tractable drug targets.

The majority of nuclear hormone receptors function as dimers, and the most important dimer interface is located within their ligand-binding domain (Kurokawa, Yu et al. 1993). A subset of receptors function as obligate heterodimers with the retinoid X receptor (RXR), and this interaction appears to rely on critical amino acid residues within the LBD (Jiang and Sladek 1997). HNF4α contains a unique amino acid sequence signature ($K(X)_{26}E$) in this region that prohibits its interaction with RXR, and allows formation of an HNF4α homodimer. Interestingly, HNF4γ shares this unique dimerization signature with HNF4α, which suggests that HNF4α and HNF4γ may form a heterodimer in cells that express both receptor subtypes.

In this study, we first establish by an electrophoretic gel shift assay that recombinant HNF4α and HNF4γ can form a heterodimer that binds DNA. We then confirm, using both a mammalian two hybrid system and subcellular localization of GFP-tagged HNF4 protein variants, that HNF4α/HNF4γ heterodimers can be formed in cultured cells. Finally, using subtype-specific antibodies, we demonstrate by coimmunoprecipaitation that an endogenous HNF4 heterodimer exists in cells and tissues that express both of these receptor subtypes. To address the functional significance of heterodimer formation, we used a cell reporter assay and titrated varing amounts of each subtype in the presence and absence of coregulators to identify differential effects of transcriptional activity by HNF4 homodimer and heterodimers.

Materials and Methods

Cell culture

The insulinoma cell line Beta-TC-6 ([CRL-11506], (Poitout, Stout et al. 1995)) and the adenoma-derived glucagonoma cell line alphaTC1-clone 9 ([CRL-2350], (Powers, Efrat et al. 1990)) were obtained from American Type Tissue Culture. The MIN6 cell line (Miyazaki, Araki et al. 1990) was kindly provided by Dr. Melanie Cobb (UT Southwestern). Cells were maintained in their optimal culture conditions unless indicated otherwise. Beta-TC6 cells were routinely cultured in DMEM (4.5 g/L glucose, 4mM L-glutamine) with 15% heat-inactivated FBS. MIN6 cells were maintained in DMEM (4.5 g/L glucose); 2 mM L-glutamine, 1 mM sodium pyruvate and 10% heat-inactivated FBS. Alpha-TC1 cells were cultured in DMEM with 4 mM L-glutamine adjusted to contain 1.5 g/L sodium bicarbonate and 3 g/L glucose with 10% heat-inactivated dialyzed FBS,

further supplemented with 15 mM HEPES, 0.1 mM non-essential amino acids and 0.02% BSA. HEK293 and HeLa cells were cultured in DMEM (25 mM glucose) with 10% FBS, 100 IU penicillin, and 100 μg/ml streptomycin.

Plasmid construct generation

The coding region of mouse liver HNF4α transcripts (HNF4α1/2: NM_008261), islet HNF4α variants (HNF4α7/8: AF015275), and HNF4γ (NM_013920) were PCR-amplified from mouse liver cDNA and islet cDNA respectively using the following primers, which were designed to incorporate a Kpn1site (italics) or BamH1 site (underlined):

HNF4α1/2-F: 5'-TA*GGTACC*ATGCGACTCTCTAAAACCCTTGC-3',

HNF4α1/2-R: 5'-GCGGATCCAGCTTGCTAGATGGCTTCTTG-3';

HNF4α7/8-F: 5'-TA*GGTACC*GTCATGGTCAGTGTGAACGCG-3',

HNF4α7/8-R: 5'-GCGGATCCAGCTTGCTAGATGGCTTCTTG-3';

HNF4γ-F: 5'-CTA*GGTACC*AGCTCCATTGCCGCTGGCATG-3',

HNF4γ-R: 5'-CGCGGATCCCAGAAGGAAGCCCCATCTCA-3'.

PCR products were digested with *Kpn1* and *BamH1* and cloned into the pCMX expression vector (Umesono, Murakami et al. 1991). The fidelity of all PCR-generated constructs was confirmed by DNA sequencing.

Truncated variants lacking the carboxyterminal F-domain were generated by PCR amplification using the forward primers described above, and the following reverse primers:

HNF4α ΔF-R: 5'-GCGGATCCCTAAGACCCTCCGAGAACTGC-3';

HNF4γ ΔF-R: 5'-GCGGATCCCTAAGCACCACCCAGCAGCATTTC-3'.

Truncated variants lacking the DNA binding domain were generated by PCR amplification using the reverse primers listed initially and the following forward primers:

HNF4α ΔABC F: 5'- CAT*GGTACC*ATGAAGGAAGCTGTCCAAAAT-3',

HNF4γ ΔABC F: 5'-CAT*GGTACC*ATGGAGGGCAGCAACATCCCC-3'.

HNF4 variants were also subcloned in-frame into pCMX expression vectors harboring the herpes simplex virus activation domain (VP16), the yeast GAL4 DNA-binding domain, or a GFP coding sequence (see Fig 4.2). The fidelity of these constructs was confirmed by sequencing, and further demonstrated by functional assay detecting transcriptional activity (Fig 4.4), DNA-binding (Fig 4.3), cellular localization (Fig 4.5), and detection of proteins of appropriate size (Fig 4.6).

Reporter constructs were generated to contain previously described HNF4 response elements (Sladek, Zhong et al. 1990). The following oligonucleotides were annealed, and cloned to the upstream of the minimal thymidine kinase promoter in a luciferase reportor vector (de Wet, Wood et al. 1987; Luckow and Schutz 1987):

HNF4 consensus-F: 5'-AGCTTGGGCCAAAGGTCATC-3',

HNF4 consensus-R: 5'-AGCTGATGACCTTTGGCCCA-3';

HNF4 ApoAIV-F: 5'-AGCTTTGAACAAGGTCCATC-3',

HNF4 ApoAIV-R: 5'-AGCTGATGGACCTTGTTCAA-3';

HNF4 ApoCIII-F: 5'-AGCTTTGGGCAAAGGTCATC-3',

HNF4 ApoCIII-R: 5'-AGCTGATGACCTTTGCCCAA-3'.

Reporter constructs with 3 response elements each were selected for use in cell transfection experiments.

Antibodies

SC-6556 (polyclonal, goat anti-human HNF4α) and SC-6558 (polyclonal, goat anti-human HNF4γ) were purchased from Santa Cruz Biotechnology. The monoclonal antibodies were supplied by Drs. Juro Sakai and Toshiya Tanaka (University of Tokyo) and are now available through Perseus Proteomics Incorporated (http://www.ppmx.com/en/products/antibody/NuclearReceptor/index.html) and include H1415 (monoclonal, mouse anti-human HNF4α), B6502A (monoclonal, mouse anti-human HNF4γ). Anti-VP16 polyclonal antibody (3844-1, rabbit anti-VP16) was obtained from BD Bioscience.

Animals

Male agouti 129/SvJ mice at 3 months of age were used to provide tissue samples for all experiments. Mice were maintained in a temperature-controlled room (23±1 °C) with a 12-h light/dark cycle and provided water and food (Teklad diet 7001) ad libitum. All experiments were performed with the approval of the Institutional Animal Care and Use Committee of the University of Texas Southwestern Medical Center.

Islet isolation and culture

Liberase RI (Roche) was used to perfuse and digest mouse pancreas. Mouse islets were then separated from the exocrine pancreas by Ficoll gradient centrifugation and hand-

picked under a stereomicroscope. RPMI 1640 medium (11.1 mM glucose) supplemented with 10% FBS, 100 IU penicillin, 100 μg/ml streptomycin (Invitrogen) was used for islet culture. All islets were allowed to recover overnight (37 °C, 5% CO_2) before use.

Quantitative Real-Time PCR analysis

Quantitative real-time PCR (qPCR) was performed using an Applied Biosystems Prism 7900HT sequence detection system and SYBR-green chemistry as previously described (Kurrasch, Huang et al. 2004). In brief, total RNA was isolated from tissue samples or cultured cells using RNA STAT-60 (Tel-Test Inc.) and 2 μg of total RNA was treated with RNase-free DNase (Roche), then reverse transcribed with random hexamers using SuperScript II (Invitrogen). Gene specific primers were designed using Primer Express Software (PerlinElmer Life Sciences) and validated by analysis of template titration and dissociation curves. Primer sequences are provided in Table1. 10 μl qPCR reactions contained 25 ng of reversed-transcribed RNA, 150 nM of each primer and 5 μl of 2 SYBR Green PCR master mix (Applied Biosystem). Results of qPCR were evaluated by the comparative Ct method (user bulletin No.2, Perkin Elmer Life Sciences) using cyclophilin as the invariant control gene.

Electrophoretic mobility shift assay

Recombinant mouse HNF4 receptors were produced by *in vitro* transcription and translation (IVTT) using T7-directed expression from the pCMX plasmids (TNT Quick Coupled Transcription/Translation System, Promega, Madison, WI). Annealed oligonucleotide probes were labeled with Klenow enzyme (Roche) in the presence of

[^{32}P] dCTP. Binding reactions were performed in a total volume of 20 μl consisting of 75 mM KCl, 20 mM HEPES (pH7.4), 2 mM dithiothreitol, 7.5% (v/v) glycerol, 0.1% Nonidet P-40, 2 μg of poly (dI-dC) (Amersham Bioscience), 2 μl of IVTT nuclear receptor lysates or unprogrammed lysates, and 1μl of radiolabeled HNF4RE probe. 1 μg of anti-HNF4α (SC-6556) or anti-HNF4γ (SC-6558) polyclonal antibody was added to the binding reaction to supershift the protein-DNA complex. Protein- DNA complexs were resolved by electrophoresis on a 6% nondenaturing polyacrylamide gel and visualized by autoradiography.

Mammalian two-hybrid assay

HEK293 cells at 40-60% confluence in 96-well plates were transfected with 50ng of the bait (Gal4 (DBD)-conjugated HNF4) plasmid, 50 ng of prey (VP16-tagged HNF4) expression plasmid, and 10 ng of to β-galactosidase expression vector using FuGENE6 transfection reagent (Roche Applied Science). The cells were cultured for 48 hours after transfection and luciferase and β-galactosidase activities were measured using a Torcon Instruments, Inc. AML-34 luminometer and a Dynatech model MR5000 spectrophotometer, respectively. Luciferase data was normalized to an internal β-galactosidase control and represents the mean (± standard deviation) of triplicate assays. The assay results were normalized to β-galactosidase activity to compensate for variation in transfection efficiency.

Transfection and immunocytochemistry.

HeLa cells were transfected with HNF4 expression plasmids using Fugene HD (Roche). Three days after transfection, the cells were fixed in 3.7% formaldehyde for 1 hour, washed with PBS, and permeabilized for 1 hour in blocking buffer (0.25% Triton X-100, 1% FCS, in PBS). Primary antibody (Rabbit anti-VP16, BD bioscience) was used at dilution of 1:200 for 1 hour incubation at room temperature. Rhodamine- conjugated Goat anti rabbit antibody (Jackson ImmunoResearch) was used as secondary antibody at 1:200 dilution. Images were collected using a Zeiss Axioplan 2 epifluorescence microscope and Open Lab 5 imaging software.

Preparation of nuclear extracts and coimmunoprecipitation

For liver and intestine samples, 1 ml of homogenizing buffer (20 mM Tris [pH 7.4], 2 mM $MgCl_2$, 0.25 mM sucrose, 10 mM EDTA, 10 mM EGTA) was used for every 100 mg of frozen tissue. Protease inhibitor (1%, Calbiochem) and DTT (5 mM) were added to the homogenizing buffer immediately before use. Samples were homogenized gently by polytron and were centrifuged at 3800 rpm (~3000xg) for 5 min at 4^0C (Sorvall RT7 Plus). Supernatants (cytoplasmic fractions) were discarded and the pellets (nuclei) were washed once with 1 ml of homogenizing buffer and then were resuspended with 400µl of nuclear extraction buffer (20 mM HEPES [pH 6.8], 2.5% Glycerol, 0.42 M NaCl, 1.5 mM $MgCl_2$, 1 mM EDTA, 1 mM EGTA) and were incubated while rocking for 45 minutes at 4°C. After incubation, samples were centrifuged at 100,000xg for 30 minutes at 4°C. Supernatants (nuclear extracts) were transferred to fresh tubes and protein concentrations were determined by BCA kit (Pierce).

For cell lines, cells from one 10 cm plate were harvested and washed twice with cold PBS. The cell pellets were then suspended with 400 µl of hypotonic buffer (10 mM HEPES, 10 mM KCl, 0.1 mM EDTA, 0.1 mM EGTA, 1 mM DTT, 1 mM PMSF, 1% protease inhibitor) and kept on ice for 15 minutes. 25 µl of 10% (w/v) NP-40 was added and the samples were vortexed vigorously for 10 seconds. The samples were then centrifuged at 4°C for 2 minutes, supernatants were discarded and pellets (nuclei) were resuspended with 50 µl of hypertonic buffer (20 mM HEPES, 400 mM NaCl, 1 mM EDTA, 1 mM EGTA, 1 mM DTT, 1 mM PMSF, 1% protease inhibitor). Samples were then incubated while rocking at 4° C for 45 minutes and further processed as described above for tissues.

Nuclear extracts from cell lines or tissue samples (100 µg total protein) or IVTT-generated recombinant mouse HNF4 proteins (5 µl of 50 µl reaction) were incubated with 2 µg HNF4α antibody (Santa Cruz, sc-6556) in 200 µl of CoIP buffer (20 mM Tris [pH 7.4], 140 mM NaCl, 10% glycerol, 0.2% Triton, 1 mM PMSF, 1 mM EDTA, 1 mM EGTA). Samples were incubated at 4°C overnight. On the following day, agarose beads coupled to protein A/G (Santa Cruz) were pre-washed five times with CoIP buffer and resuspended 1:1 (vol/vol) with the same buffer. 30 µl of beads were added to each immunoprecipitation reaction and incubated while rocking for 2 hours at 4°C. After incubation, the tubes were centrifuged (3000xg, 30 seconds) and the pellets were washed 5 times with CoIP buffer (supplemented with 1 mg/ml BSA). After the final wash, the pellets were resuspended with 30 µl denaturing SDS-PAGE sample buffer and boiled 5 minutes. Following a final quick spin, 10 µl were loaded onto the gel.

Results

Tissue distribution of HNF4α isoforms and HNF4γ in the mouse

The relative expression of HNF4α and HNF4γ RNA in mouse tissues, isolated pancreatic islets, beta cell lines (βTC6 and MIN6), and an alpha cell line (αTC1) were determined by quantitative real-time PCR (Fig. 4.1). In agreement with previous reports, HNF4α is very highly expressed in liver, kidney and different sections of intestine with isoforms 1 and 2 (transcribed from promoter 1A) being the predominant isoforms. HNF4α is also expressed in the beta-cells of the islet with HNF4α 7 and 8 (transcribed from promoter 1D) being the major species.

Unlike HNF4α, HNF4γ is not expressed in liver but is abundantly expressed in the intestine, colon, and pancreatic islet. Data from the cell lines suggest that within islets, HNF4α and HNF4γ are expressed by beta-cells but not alpha-cells. In addition, our results demonstrate that HNF4α and HNF4γ are expressed at comparable levels in beta-cells of the islet (Ct: 24.3 for 4α7/8 and Ct: 25.0 for 4γ in islets).

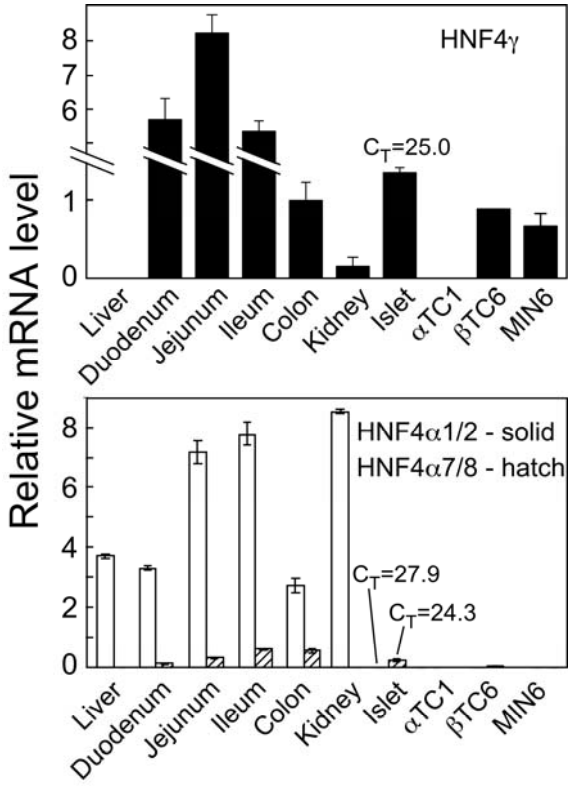

Figure 4.1. Relative mRNA expression levels of HNF4α isoforms and HNF4γ in selected mouse tissues and cell lines. Alpha-cells are represented by the αTC1 cell line, and beta-cells by the βTC6 and MIN6 cell lines. RNA levels were measured by qPCR and are expressed relative to the housekeeping gene, cyclophilin. Values depict mean±SEM, n=3.

Since HNF4α and HNF4γ are expressed in the beta-cells of islets with comparable abundance, and the dimerization motifs of the two are very well conserved, we hypothesized that HNF4α/HNF4γ heterodimers may exist in islets.

Acquiring the tools necessary to detect and characterize HNF4 dimers

To enable us to detect and characterize HNF4 dimers, a variety of HNF4 expression vectors and reporter constructs were prepared as shown in Figure 4.2. qPCR primers were

also designed and validated to use on measuring RNA expression of HNF4α isoforms and HNF4γ. Oligonucleotides containing HNF4RE sequences previously identified for HNF4α homodimers were purchased and cloned into reporter constructs. Receptor specific antibodies were also acquired to perform immunoblotting and immunoprecipitation experiments.

Figure 4.2. Tools developed to study HNF4s.

Expression plasmid constructs

Applications

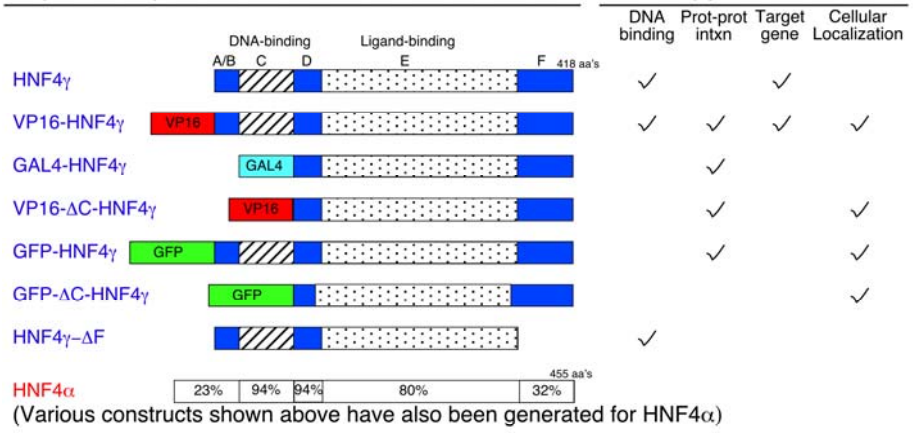

	DNA binding	Prot-prot intxn	Target gene	Cellular Localization
HNF4γ	✓		✓	
VP16-HNF4γ	✓	✓	✓	✓
GAL4-HNF4γ		✓		
VP16-ΔC-HNF4γ		✓		✓
GFP-HNF4γ		✓		✓
GFP-ΔC-HNF4γ				✓
HNF4γ–ΔF	✓			

(Various constructs shown above have also been generated for HNF4α)

Oligonucleotides:

HNF4 response elements (probes in gel shifts, enhancers in reporter plasmids):

Consensus: GGGCCA a AGGTCA

ApoCIII: TGGGCA a AGGTCA

ApoCIV: TGAACA a GGTCCA

Quantitative real-time PCR primers for measuring RNA:

Mouse HNF4α (NM_008261)	F: 5'-CCAACCTCAATTCATCCAACA	R: 5'-CCCGGTCGCCACAGAT
Mouse HNF4γ (NM_0013920)	F: 5'-TCCCTGCCTTCTGTGAACTG	R: 5'-CCAGCATGGGCTCTCAAGA
Human HNF4α (NM_000457)	F: 5'-TGCAGGCTCAAGAAATGCTT	R: 5'-TCATTCTGGACGGCTTCCTT
Human HNF4γ (NM_004133)	F: 5-TGGGTGCAAGGGTTTCTTC	R: 5-CCGACTGAACCTGCAAGAATA
Mouse HNF4α isoforms 1/2	F: 5'-CCCTGGACCCAGCCTACA	R: 5'-GCTCGAGGCTCCGTAGTGT
Mouse HNF4α isoforms 7/8	F: 5'-TCCATGCCCCCCAGTGTC	R: 5'-GCTCGAGGCTCCGTAGTGT

Antibodies:

Applications

	Immunoblot: Recomb. prot.	Immunoblot: Tissue	Gel Supershift	Immuno-Precptn.	Immuno-Histochem.
N3224 (mAb, anti-HNF4γ, IgG2a: epitope aa 96-408 of hHNF4γ)	✓	✓	✓	No	?
B6502A (mAb, anti-HNF4γ, IgG1: epitope aa 91-202 of hHNF4γ)	✓	✓	✓	?	?
SC-6558 (pAb, anti-HNF4γ, epitope C-terminus of hHNF4γ)	✓	No	✓	?	✓
K9218 (mAb, anti-HNF4α1, IgG2a: epitope aa 3-49 of hHNF4α1)	✓	✓	?	?	?
H1415 (mAb, anti-HNF4α-all, IgG2a: epitope aa 393-461 hHNF4α2)	✓	✓	?	?	?
H6939 (mAb, anti-HNF4α7/8, IgG1: epitope aa 1-16 of hHNF4α7/8)	✓	?	?	?	?
SC-6556 (pAb, anti-HNF4α, epitope C-terminus of hHNF4α)	✓	No	✓	✓	✓
3844-1 (pAb, anti-VP16, from BD Bioscience)	✓	—	✓	?	✓

Detection of an HNF4α/ HNF4γ heterodimer by EMSA

Our first test of heterodimer formation by electrophoretic mobility assay (EMSA) utilized recombinant mouse receptors generated by in vitro transcription and translation (IVTT). Since the molecular size difference between HNF4α (~53 Kda) and HNF4γ (~46 Kda) is not sufficient to distinguish different dimer complexes on the gel, a VP16 tag was added to HNF4α to increase its molecular mass to ~64 Kda. In agreement with others' observations, HNF4α and HNF4γ can each form a homodimer and bind to P^{32}-labeled oligonucleotides that contain an HNF4RE (Fig 4.3, panel A, lanes 2 and 7 for 4α dimers and lanes 5 and 10 for 4γ dimers). When VP16-HNF4α and HNF4γ were synthesized in the same IVTT reaction and assessed by EMSA, a band of intermediate size was observed (Fig 4.3, panel A, lanes 3, 4, 8, and 9) suggesting the formation of a heterodimer. To further identify the components within this protein complex, antibodies specific to HNF4α and HNF4γ were used to super-shift this band. Addition of both HNF4α- and HNF4γ- antibodies caused the formation of a larger (supershifted) complex confirming the presence of these receptor subtypes (Fig 4.3, panel B, lanes 5 and 6). Interestingly, when HNF4α and HNF4γ proteins were synthesized in separate IVTT reactions and then mixed together, heterodimers of HNF4α and HNF4γ were not detected (Fig 4.3, panel B, lane 10). This behavior is distinct from that of RXR heterodimers, which readily form dimers upon mixing recombinant proteins prior to EMSA (Cha and Repa 2007), and suggests unique protein association kinetics for HNF4 heterodimers.

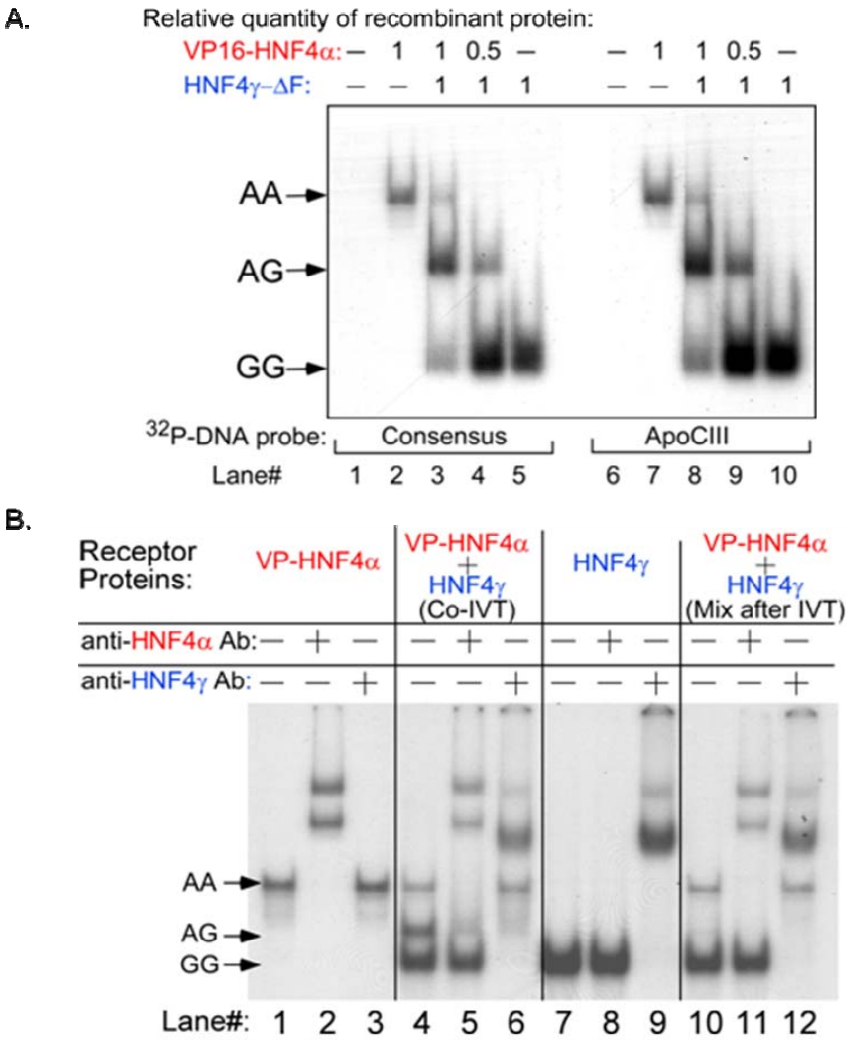

Figure 4.3. Formation of an HNF4α/HNF4γ heterodimer as revealed by EMSA. ^{32}P-labeled double-stranded oligonucleotide probes previously identified as HNF4α binding motifs (consensus, apoCIII, [160], see Figure 4.2) were incubated with recombinant HNF4 proteins produced by *in vitro* transcription/translation (IVTT) and ran on a non-denaturing polyacrylamide gel. **A. Identification of an HNF4 heterodimer**. The migration/location for homodimers of VP16-tagged HNF4α (AA, lanes 2 and 7) and HNF4γ, shortened by deletion of its F domain, HNF4γ-ΔF (GG, lanes 5 and 10) were significantly different. When these variants of HNF4α and HNF4γ were produced in the same IVTT reaction and analyzed by EMSA, a band of intermediate sized was evident (AG, lanes 3,4,8, and 9). Maximal formation of this intermediate was observed when using IVTT reactions containing equal quantities of each receptor subtype (lanes 3 and

8). **B. Both HNF4 subtypes are present in this intermediate-sized complex**. HNF4 subtype-specific antibodies (anti-HNF4α= SC-6556, anti-HNF4γ=SC-6558, see Fig.4.2) were incubated with VP16-HNF4α, full-length HNF4γ, and the ^{32}P-apoCIII probe for the EMSA. The specificity of each antibody is demonstrated by the selective supershift of the HNF4α homodimer (AA, lane 2) and not the HNF4γ homodimer (GG, lane 8) by SC-6556. Similar antibody selectively is observed for the HNF4γ antibody SC-6558 (compare lanes 9 and 3). The intermediate band (AG) is supershifted by both antibodies (lanes 5 and 6). Note that the heterodimer is found only when both receptor subtypes are produced in the same IVTT reaction (lane 4, Co-IVTT) and not when the proteins are mixed following IVTT (lane 10, Mix after IVTT).

Formation of the HNF4α/ HNF4γ heterodimer in transfected mammalian cells

To test if the HNF4α/HNF4γ heterodimer can be formed in living cells, we performed mammalian two-hybrid experiments. We generated expression vectors that produce chimeric proteins (see Fig. 4.1): the bait vectors contain the GAL4 yeast DNA-binding domain fused to the mouse HNF4 receptor sequences containing the ligand-binding domain through the carboxyterminus; the prey vectors contained the mouse HNF4 ligand-binding domain through the carboxyterminus fused to the VP16 herpes simplex virus activation domain (AD). The reporter vector contained 4 copies of the GAL4 binding sequence upstream of a minimal thymidine kinase promoter to drive expression of luciferase. When HEK293 cells were transfected with reporter, a beta-galactosidase expression plasmid to standardize for transfection efficiency, and HNF4α bait and prey vectors, HNF4α homodimerization resulted in a 2-fold increase in luciferase activity (Fig. 4.4, lane 5). Likewise, when both bait and prey vectors contained HNF4γ, luciferase activity was increased by the formation of this homodimer (3.5-fold, Fig. 4.4, lane 9). Most importantly, using the combination of HNF4α and HNF4γ as bait and prey vectors resulted in enhanced expression of the luciferase reporter (3 to 3.5-fold, lanes 6

and 8). These data demonstrate that HNF4 heterodimers can be formed in transfected cells.

To further confirm this interaction between HNF4α and HNF4γ in cultured cells, a microscopy-based experiment was performed using HeLa cells (Fig. 4.5). HeLa cells were chosen for this experiment as there is no endogenous HNF4α or HNF4γ detectable by qPCR in this cell type (data not shown). When full length HNF4α or HNF4γ are transfected into HeLa cells these receptor proteins localize to the nucleus as revealed by their respective tags (GFP-HNF4α, Fig. 4.5 panel A; VP16-HNF4γ, Fig. 4.5 panel L). If the nuclear localization sequence is deleted in HNF4α (GFP-ΔHNF4α) the receptor accumulates in the cytosolic compartment (Fig. 4.5 panel B). However, if this "cytosolic" GFP-HNF4α variant is cotransfected with full-length VP16-HNF4α (homodimer formation, Fig. 4.5 panels C, G, K) or VP16-HNF4γ (heterodimer formation, Fig. 4.5 panels D, H, and L), the GFP signal translocates to the nucleus.

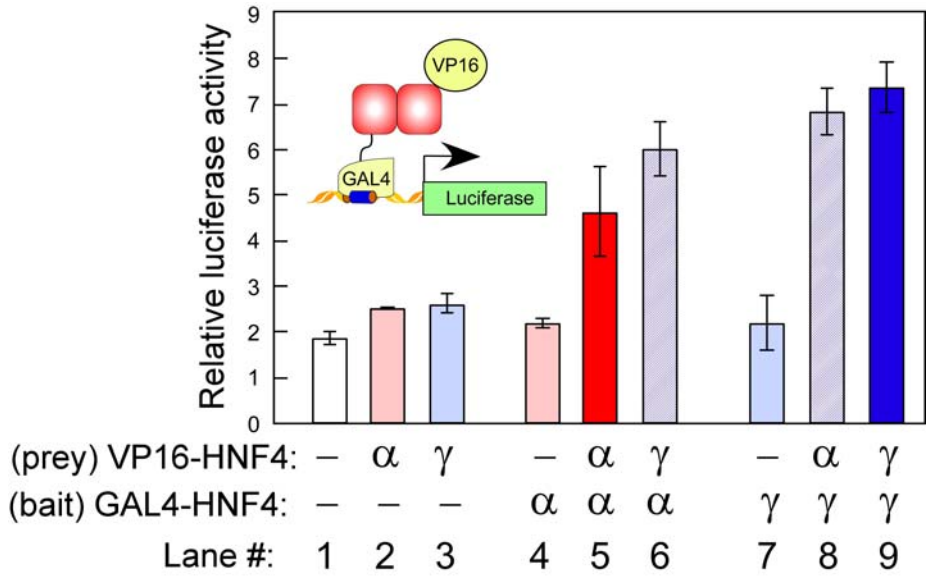

Figure 4.4. Formation of an HNF4α/HNF4γ heterodimer demonstrated by mammalian two-hybrid experiment. HEK293 cells were transiently transfected with expression plasmids for GAL4-, and/or VP-16-tagged variants of HNF4α and γ along with a luciferase reporter plasmid containing the GAL4 binding motif. The formation of HNF4α homodimer is shown in lane 5 which gives a ~2 fold induction over basal activity. The formation of HNF4γ homodimer is shown in lane 9 which gives a ~3.5-fold induction. The formation of HNF4α/HNF4γ heterodimer is shown in lanes 6 and 8, which show ~3-3.5-fold induction of activity.

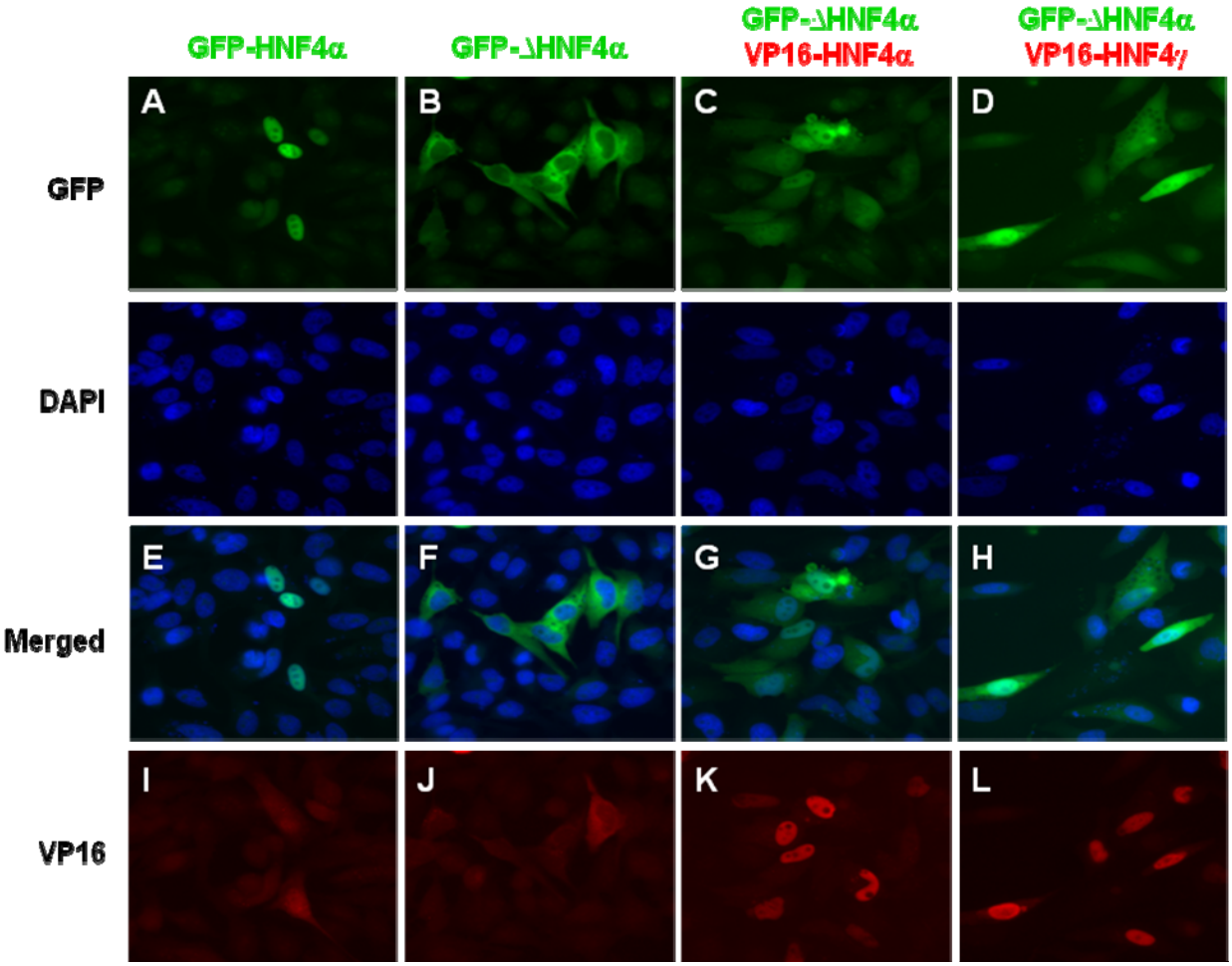

Figure 4.5. HNF4α/4γ heterodimer can be observed in transfected Hela cells. Hela cells were transiently transfected with pCMX expression plasmids listed at top. 48 hours later, cells were fixed and stained with anti-VP16 antibody and DAPI. Panel A reveals that full length HNF4α localizes to the cell nucleus. Deletion of the DNA binding domain results in a truncated HNF4α that resides in the cytosol (panel B). VP-16-tagged full length HNF4α or HNF4γ localizes to the nucleus as revealed by the VP-16 staining (panels K and L), and supplying this full length HNF4α or HNF4γ promotes the nuclear localization of the truncated GFP-ΔHNF4α (formly cytosolic) presumably by formation of homo- or heterodimers, respectively (panels C and D). Note, Hela cells express no detectable endogenous HNF4 isoforms (data not shown).

Detection of endogenous HNF4α/ HNF4γ heterodimer in islet beta-cells

Our qPCR data revealed that mouse islets, intestine, and beta-cell lines are the only cell sources that express HNF4α and HNF4γ with comparable abundance. Therefore we used these tissue sources in conjunction with receptor-specific antibodies to detect endogenous heterodimers by co-immunoprecipitation. Nuclear extracts were prepared and protein complexes that contain HNF4α were immunoprecipitated with an antibody (SC-6556) specific to HNF4α. The immunoprecipitated proteins were then size fractioned on a denaturing SDS polyacrylamide gel and interrogated with another HNF4α (H−1415, Fig 4.6, lower panel) antibody or an HNF4γ antibody (B6502A, Fig 4.6, upper panel). These procedures were also performed using mixtures of recombinant mouse HNF4 proteins to serve as positive controls. The specificity of the antibodies employed in these studies is demonstrated by the failure of anti-4α pAb to precipitate HNF4γ recombinant protein (compare lanes 3 and 10 in upper panel). Likewise the anitibodies used for immunoblotting are selective and fail to detect the other HNF4 subtype (HNF4γ antibody detects no HNF4α recombinant protein or tissue endogenous protein, lanes 1 and 6 of upper panel; HNF4α antibody detects no signal for HNF4γ recombinant protein or tissue endogenous protein, lanes 3 and 7 of lower panel). When the precipitated protein complexes were blotted with antibody against HNF4γ, signals were clearly evident in the mixture of recombinant HNF4α and γ (lane 9), mouse islets and the beta-cell lines (lanes 11 and 12) and intestine (lane 14) which indicated the presence of HNF4α/HNF4γ complexes in these samples. Note the complete absence of HNF4γ signal in the liver sample despite the very efficient immunoprecipitation of HNF4α from this tissue source

(compare lane 13 of upper panel and lower panel in Fig 4.6). We also consistently detected an HNF4γ-immunoreactive band of a higher molecular weight in mouse intestine samples to suggest that there may be additional isoforms or modified variants of HNF4γ in this tissue (Fig 4.6, upper panel, lane 7 and 14).

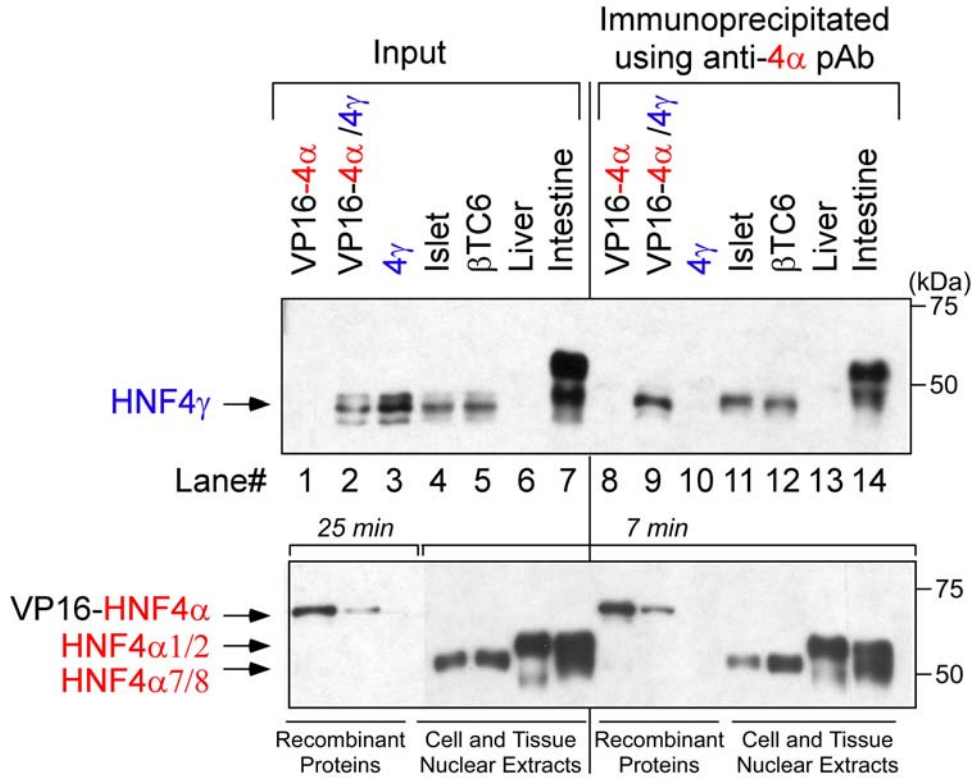

Figure 4.6. Detection of endogenous HNF4α/4γ heterodimers in mouse tissues by coimmunoprecipitation (upper panel lanes 11, 12, and 14). Nuclear extracts were prepared from mouse tissues, islets or the beta-cell line, βTC6, and recombianant HNF4proteins were generated by IVTT. 5µg of extracts and 1µl of IVTT samples were evaluated directly for the presence of HNF4 proteins (Input, left). 50µg of extracts and 5µl of IVTT samples were also subjected to immunoprecipitation using an HNF4α-specific antibody (pAb-SC6556, right). The input and the precipitated proteins were analyzed by immunoblotting using an HNF4γ-antibody (mAb-B6502A, upper panel) or another HNF4α antibody (mAb-H1415, lower panel). The identification of HNF4α isoforms is based on predicted molecular mass and is consistant with the RNA levels of these species measured by qPCR.

Interaction of transcriptional co-factors with HNF4α and HNF4γ

The transcriptional activity of nuclear receptors are heavily dependent on the recruitment of accessory factors including coactivators and corepressors (reviewed in (Xu, Glass et al. 1999)). Several cofactors have been previously reported to regulate the activity of liver HNF4α (4α1 and 4α2). However, very little is known about which cofactors may regulate the activity of pancreatic HNF4α (4α7 and 4α8) , HNF4γ, and HNF4α/γ heterodimers.

The amino acid sequence of HNF4γ shows the highest degree of similarity in DNA binding domain (94%) and in LBD (80%) toward HNF4α. The amino terminal (A/B domain) and carboxy terminal region (F domain) of HNF4γ is rather diverse when comparing to that of HNF4α (23% for A/B and 32% for the F domain) (Taraviras, Mantamadiotis et al. 2000). The A/B domain and the F domain of HNF4 proteins have been reported to participate in the recruitment of cofactors to modulate transcription activity. Based on these observations, we hypothesized that the difference in the A/B and F domains between HNF4α and HNF4γ may result in the differential recruitment of cofactors and contribute to the functional differences between HNF4 dimers (4α/4α, 4γ/4γ. and 4α/4γ).

Using a candidate-based approach, the mRNA levels of several cofactors including PPARγ coactivator 1α (PGC1α), PPARγ coactivator 1β (PGC1β), receptor-interacting protein 140 (RIP140), and SHP were examined by qPCR to establish their presence in various mouse tissues (Fig 4.7). Our results demonstrate that PGC1α is expressed in mouse islets (Ct=27.5). Adding this coactivator to our cell reporter assay

resulted in a potent enhancement in luciferase activity for liver HNF4α variants (20-fold for HNF4α1 and 23-fold for HNF4α2). It is less potent in activating islet HNF4α variants (4.6-fold for HNF4α7 and 7.3-fold for HNF4α8). Interestingly, we found that PGC1α is a stronger coactivator for HNF4γ (41-fold). PGC1β is also present in the mouse islet (Ct=28.1) and does not interact with any of the HNF4α variants but showed a modest increase in activity for HNF4γ (1.6-fold). RIP140 (Ct=25.5 in mouse islets) suppresses the activity of liver HNF4α variants by half (51% for HNF4α1 and 55% for HNF4α2), and is less effective in decreasing the activity of islet HNF4α variants (26% for HNF4α7 and 24% for HNF4α8). RIP140 can also interact with HNF4γ and is a very strong repressor of its activity (93% decreased). SHP (Ct=30.1 in mouse islets) also represses the activity of liver HNF4α variants by 50%, and suppresses islet HNF4α variants by 13% (4α8) to 30% (4α7), but did not exhibit any effect on HNF4γ.

In summary, we identified PGC1α, PGC1β, and RIP140 as potential cofactors for HNF4γ that may regulate the activity of HNF4γ in the pancreatic islet cells. We also demonstrated that HNF4α variants and HNF4γ interact with these cofactors differently. Together, these results suggested that different HNF4 dimers formed in the pancreatic beta-cells may be able to modulate the transcription activity of downstream genes by recruiting different co-factors.

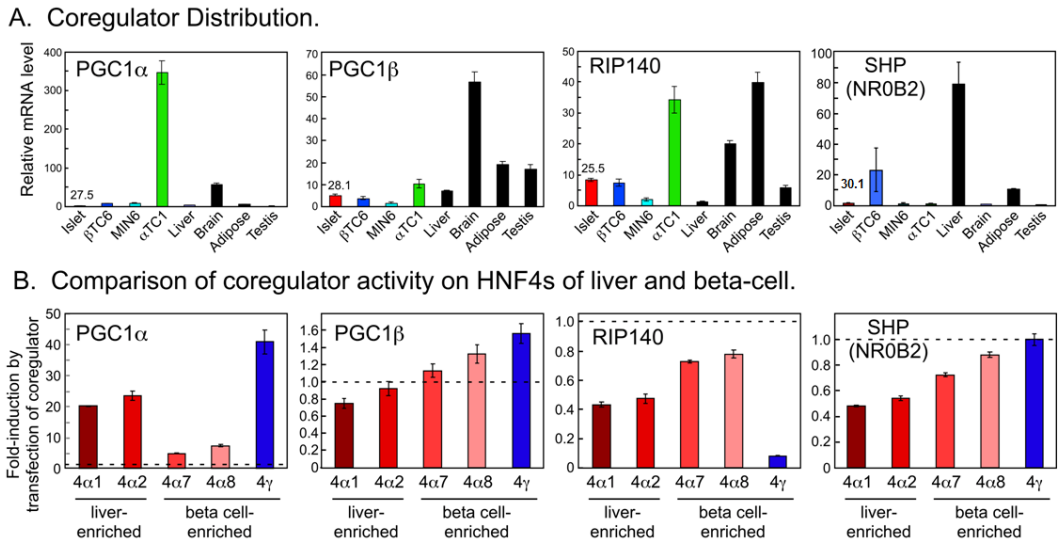

Figure 4.7. Coactivator/corepressor interaction with HNF4s
Panel A. Expression of selected cofactors in cells of the endocrine pancreas. Relative mRNA expression levels of these co-factors were measured by qPCR. C_T number is provided for islet samples.
Panel B. PGC1α increases the transcriptional activity of HNF4γ to a greater extent than for all liver and islet isoforms of HNF4α (~40-fold for 4γ, ~20-fold for liver HNF4αs, and ~5-fold for islet HNF4αs). PGC1β does not induce significant activity for all HNF4 tested. RIP140 acts as a corepressor for the HNF4s with strongest repression for HNF4γ (>90% repression for HNF4γ, ~60% for liver HNF4αs, and ~20% for islet HNF4αs). SHP does not affect the transcriptional activities of HNF4γ, although this vector causes transcriptional repression of liver HNF4α isoforms (~50%) and islets HNF4α isoforms (~20%). Hela cells and the consensus reporter were used in these assays.

Discussion

In this study, we first provide biochemical and cell-biological evidence to demonstrate that HNF4α and HNF4γ not only form homodimers, but also form a functional heterodimer. Furthermore, we were able to detect the endogenous HNF4α/HNF4γ heterodimers in islets, β-cell lines and intestine. The physiological significance of this novel heterodimer is currently under investigation. There are two possibilities regarding

how the HNF4 heterodimer can affect the regulation of HNF4 target genes in the cell. The first possibility is that HNF4α/HNF4γ heterodimers bind to a subset of target genes that are distinct from those recognized by HNF4α homodimers and HNF4γ homodimers. To identify such genes, a CHIP-re-chip experiment could be performed. After two runs of chromatin immunoprecipitation using antibodies for HNF4α and HNF4γ sequentially, the DNA fragments that are co-precipitated should be HNF4α/HNF4γ heterodimer-specific sequences and would be labeled and used to interrogate a promoter microarray to identify target gene(s) regulated selectively by the HNF4α/HNF4γ heterodimer.

The second possibility is that all HNF4 dimers (4α/4α, 4γ/4γ. and 4α/4γ) share the same target genes and the relative abundance of the HNF4α and HNF4γ proteins determines which dimer occupies the promoter elements regulating these genes. Different coregulator recruitment and transcriptional activity of these dimers would then affect target expression. This proposal is supported by the high degree of sequence similarity (94%) in the DNA binding domains of HNF4α and HNF4γ. In addition, our results from EMSA suggest that the HNF4 homodimers and heterodimers interact with all HNF4 response elements tested thus far (Fig 4.3). Finally, our reporter assay results demonstrate that several cofactors that are expressed in beta-cells show different interaction toward HNF4α and HNF4γ (Fig 4.6).

Together, we propose that the regulation of target genes by HNF4 proteins in different tissues is dependent on the cellular context of HNF4 proteins. In liver, we see no evidence of HNF4γ expression (Fig 4.1) which agrees with previous reports (mouse liver (Taraviras, Mantamadiotis et al. 2000); human liver or HepG2 cell line (Drewes, Senkel

et al. 1996) and http://www.nursa.org/10.1621/datasets.02004), and consequently the target genes of HNF4 in this tissue are soley regulated by the HNF4α homodimer. In intestine, both HNF4α and HNF4γ are present and form homodimers and heterodimers (Fig 4.6), and hence the relative abundance of 4α/4α, 4α/4γ, 4γ/4γ dimers will determine which dimer occupies the promoter element of target genes. In the beta-cells of pancreatic islet, HNF4γ may affect HNF4α activity with the same mechanism and thus may play a role in regulating beta-cell function.

CHAPTER 5

Conclusions and Recommendations

5.1 Conclusions and implications

The National Diabetes Education Program (NDEP) estimated that 24 million (~8%) Americans have been diagnosed with diabetes. A study reported by the Centers for Disease Control and Prevention (CDC) in the 67th ADA Scientific session showed the prevalence of diabetes has risen 5% annually since 1990 and this trend is likely to worsen in coming years. According to the American Diabetes Association, diabetes is the 6th leading cause of death in the U.S. and claims more than 200,000 deaths per year. The total estimated medical cost of diabetes in 2007 was 174 billion and people with diagnosed diabetes spend an average of $11,744 per year, ~2.3 times higher than what medical expenditures would be in the absence of diabetes (2008).

The progression of diabetes is coupled to pancreatic β cell dysfunction at every stage (Weir and Bonner-Weir 2004). The preservation of islet function and prevention of islet cell death therefore are considered to be therapeutic approaches to improve the diabetic phenotype. The proper function of islets relies on their ability to sense and respond to many environmental signals. We believed that gaining knowledge of the sensor systems in the islet may provide novel therapeutic targets to improve islet function.

5.1.1 Nuclear receptors in the islet

One primary aim of our studies was to reveal novel modulators of islet function. By taking advantage of the high sensitivity of qPCR, we completed a comprehensive survey of the expression of nuclear receptor family members in isolated mouse islets and representative alpha- and beta-cell lines. These data provide useful information for future studies that aim to reveal the role of nuclear receptors in regulating endocrine pancreas development and in regulating endocrine cell function in the adult. In addition, by comparing the NR expression patterns in the whole islet with that from cultured alpha- and beta-cell lines, we tentatively identified cell-type enriched nuclear receptors. These cell-type enriched NRs may also play roles in cell lineage determination during development. We also identified several nuclear receptors with altered expression levels in mouse islets when cultured under different glucose concentrations.

We believe that our data should provide useful information for researchers that study the regulation of endocrine pancreas development, cell lineage specification, and beta-cell regeneration.

5.1.2 LXR and ChREBP in regulating islet function

In this study, we performed experiments to uncover the potential roles of LXR in the pancreatic islets. By discovering that activation of LXR in the islets enhanced GSIS, we showed that LXR is involved in the regulation of carbohydrate homeostasis not only in liver and white adipose tissue but also in the endocrine pancreas. In addition, we identified the novel LXR target gene, ChREBP, a glucose-sensitive transcription factor that is indispensible for proper GSIS. Together, our data suggest that the LXR-ChREBP axis plays an important role in regulating islet function.

5.1.3 HNF4

Since HNF4α was originally discovered and characterized in the liver where HNF4γ is not expressed, it has been long believed that HNF4α works as a homodimer to regulate target gene expression. When HNF4γ was discovered several years later, because of the similarity between HNF4α and HNF4γ, it was proposed that HNF4γ similarly works as a homodimer. However, when we compared the amino acid sequences of HNF4α and HNF4γ within the region that are responsible for dimerization, and found that they have identical key amino acids. This observation led to the hypothesis that a novel heterodimer can be formed between HNF4α and HNF4γ when both are present in the same cell type. In this study, we provided both biochemical and cell biological evidence to demonstrate that in the beta-cell of the endocrine pancreas, HNF4α and HNF4γ are both expressed and indeed form a heterodimer. Based on our tissue distribution data of HNF4s, beta-cells in the islet and epithelial cells in the intestine are the only two cell types that express similar levels of HNF4α and HNF4γ RNA and thus are likely to harbor HNF4α/HNF4γ heterodimers. By endogenous Co-IP experiments, we do detect HNF4α/HNF4γ heterodimer in the islets and intestine but not in the liver.

Mutations of HNF4α in human have been shown to cause MODY1, a rare form of monogenic diabetes. Although HNF4γ is also abundantly expressed in the islet, its function is still largely unknown. Our study suggests that it may participate in regulating islet function by forming a heterodimer with HNF4α.

5.2 Recommedations for future studies

5.2.1 Regarding NRs in the islet

In the current study, we completed the NHR profiling in healthy islets from adult mice. These data reflect the basal expression of nuclear receptors under normal physiological conditions. To gain a better understanding of which nuclear receptors may be involved in islet development and/or regeneration, it would be interesting to compare the expression of NHRs in embryonic endocrine pancreas with the expression in adult. Also, by evaluating the expression of NHRs in islets from mouse models of dibetes, the NHRs that are altered under pathological conditions can be identified.

In addition, we noticed that the expression pattern of NHRs in adult human islets is distinct from the pattern of NHRs in mouse islets. The most profound difference was observed for LRH-1. This suggests that LRH-1 may be far more important in human islet development and/or function.

5.2.2 Regarding LXR

In our study, we showed that the LXR-ChREBP axis plays a role in the positive regulation of GSIS. However, our results also suggested that there are other LXR target genes that might contribute to the beneficial effects of LXR activation on GSIS. This observation was extended to human islets, and microarray data provides us with additional candidates to identify novel modulators (Supplementary table 3.2). One particularly interesting candidate is *ghrelin*, a gene that encodes an appetite-controlling

peptide that is predominantly produced in the stomach upon fasting. Several studies suggest that islet cells also express and produce ghrelin, which may work in a paracrine manner to regulate the secretion of hormones from other islet cells (Qader, Hakanson et al. 2008). The molecular mechanisms that control the expression of ghrelin are not yet fully understood.

The specificity of LXR in regulating ghrelin should be tested using LXR null islets. Based on the time-frame that we applied the treatment (16 hours), it is possible that *ghrelin* is regulated by LXR either in a direct or indirect manner. This issue can also be addressed by multiple ways. First, a time-course experiment can be performed to see how early ghrelin can be activated by an LXR ligand. Secondly, a translational blockade can be imposed while treating islets with the LXR agonist to rule out the possibility that a secondary transcription factor is required. In addition, cell based reporter assays can be performed to test if LXR can directly regulate the *ghrelin* promoter. It would also be interesting to test if the expression of *ghrelin* in the A-like cells of the stomach is also subject to the regulation of LXR.

The other interesting candidate for further analysis is *sulf1*, a sulfatase that removes the sulfate from heparin sulfate proteoglycan (HSPG). HSPG is a component of the extracellular matrix and is a coreceptor for many heparin-binding growth factors. It has been shown that dysregulation of HSPG can lead to islet amyloid deposition which is observed in 90% of patients with Type 2 diabetes mellitus (TIIDM). In addition, the sulfate status of HSPG has been shown to be a mechanism that regulates the interaction between growth factors and receptors.

Our preliminary data suggested that *sulf1* is down-regulated by LXR activation in the islets and this effect is LXR dependent since it is not observed in LXR null islets treated with T1317 (data not shown). Interestingly, the expression of *sulf1* in the LXR null islets is 10-fold higher when compared to the expression in wild-type islets. This further supports our observed LXR-regulation of *sulf1*. It is not clear yet whether *sulf1* is a direct target of LXR. Also, it is not clear for now what the consequences of *sulf1* regulating by LXR may be in islet physiology.

5.2.3 Regarding HNF4 heterodimer

We proposed that the HNF4α/HNF4γ heterodimer in the islets can serve as a novel way to modulate the expression of HNF4 target genes in the beta-cells of the islet. It is unclear how HNF4α/HNF4γ heterodimers participate in the regulation of gene expression in the islets at the present time. There are two possible mechanisms regarding how HNF4α/HNF4γ heterodimer may control the expression of target genes. First, there might be a subset of HNF4 target genes that can only be regulated by HNF4α/HNF4γ heterodimer but not homodimer of HNF4α or HNF4γ. This possibility can be tested by a ChIP-re Chip study using our specific antibodies for HNF4α and HNF4γ to perform two rounds of immunoprecipitation from islet samples and perform non-biased binding site identification on promoter microarrays. This approach will lead to the identification of novel heterodimer specific targets in the islet and reveal the functional significance of HNF4α/HNF4γ heterodimer.

Alternatively, it is possible that all three HNF4 dimer species (4α/4α, 4γ/4γ, and 4α/4γ) bind to target gene promoters in a similar fashion. The relative abundance of HNF4α and HNF4γ protein would therefore determine the relative amount of each dimer species. By competition, the most abundant dimer would bind to the promoter of target genes, and selective transcription co-factors could be recruited and contribute to differences in the expression of target genes.

Finally, the functional significance of HNF4γ-containing dimers in beta-cells of the mouse islet can be further revealed by characterizing the phenotype of HNF4γ -/- mice, which have been recently described (Gerdin, Surve et al. 2006). The offspring from heterozygote parents were produced with the expected Mendelian ratio (1:2:1 for -/- : +/- : +/+). HNF4γ-/- animals are heavier (10%) than wild type littermates when examined at 7 weeks of age. This report also indicated that HNF4γ-/- mice have lower locomotor activity, energy expenditure, and respiratory exchange ratio (RER) than wild type control mice. Food and water intake was significantly lower in the HNF4γ-/- animals. These data suggested that HNF4γ may participate in energy homeostasis. The authors did not perform experiments to measure parameters of glucose homeostasis or insulin secretion in HNF4γ-/- mice. Glucose tolerance tests and insulin tolerance tests using these animals together with blood glucose/insulin parameters would contribute to an understanding of HNF4γ's role in carbohydrate homeostasis. Additionally, characterization of isolated islets from these HNF4γ-/- mice would pinpoint the functional importance of HNF4γ in the beta-cell.

APPENDIX A

KD3010, a potent and selective PPARδ agonist, potentiates glucose stimulated insulin secretion from mouse islets

Abstract

KD3010 is a synthetic PPARδ agonist that has been shown to reduce visceral adiposity, plasma triglyceride and non-esterified fatty acids when orally administrated to high fat diet-fed mice. In addition, it also improves insulin resistance and hyperinsulinemia. Based on our previous NHR profiling study, we learned that PPARδ is abundantly expressed in the mouse islets. However, the consequence of PPARδ activation in the islet is still largely unknown. The present study was performed to investigate the effect of PPARδ agonist, KD3010, on the regulation of insulin secretion from isolated mouse islets. qPCR analysis of PPAR target genes demonstrates that KD3010 is a potent agonist for PPAR in the islets. When challenged with 17.5 mM glucose, KD3010 treated islets secreted more insulin compared to vehicle treated islets. In addition, we tested the specificity of KD3010 toward PPARδ by showing that it is still capable of enhancing GSIS in PPARα -/- islets. In summary, our data suggest that the activation of PPARδ in the isolated islets may affect the lipid handing and thus contribute to the regulation of insulin secretion.

Introduction

PPAR nuclear receptor subfamily has three members, PPARα, PPARγ, and PPARδ (also called β). These receptors were first discovered to be orphan members in the nuclear receptor superfamily that are involved in peroxisome proliferation (Issemann and Green

1990). Later on, PPARα was identified to be a molecular target of fibrates, a class of drugs used to treat hyperlipidemia (Issemann, Prince et al. 1993; Green and Wahli 1994; Vu-Dac, Schoonjans et al. 1995) . PPARγ, on the other hand, was found to be the target of thiazolidinediones (TZDs) (Lehmann, Moore et al. 1995) which have been used for correction of insulin resistance in type II diabetes. Endogenously, fatty acids and derivatives have been shown to be ligands for PPARs.

Among the three members in the PPAR subfamily, PPARδ remains the least characterized. However, studies suggested that like PPARα and PPARγ, PPARδ is also involved in the regulation of lipid and glucose metabolism (Grimaldi 2005; Barish, Narkar et al. 2006). Activation of PPARδ in adipose tissue and skeletal muscle has been shown to induce fatty acid oxidation and increase energy expenditure (Tanaka, Yamamoto et al. 2003; Wang, Lee et al. 2003). Synthetic ligands for PPARδ are thus considered to be candidates for improving lipid and glucose homeostasis. In addition to adipose tissue and muscle, PPARδ is also present in the β cells of the islet although the consequences of PPARδ activation in the islets are not clear.

KD3010 is a selective and potent agonist for PPARδ that shows ~1000-fold selectivity over PPARα and PPARγ. Animal experiment data suggests that administration of this compound can decrease diet-induced obesity (DIO) and can reverse hyperinsulinemia as well as insulin resistance (Guha, Deng et al. 2006). However, it is not clear that if the activation of PPARδ in the islet also contributes to the beneficial effects of this compound. In this study, we aim to address the functional consequences of activating PPARδ by KD3010 in isolated mouse islets.

Materials and Methods

RNA measurement

RNA was isolated from tissue samples or cultured cells using RNA STAT-60 (Tel-Test Inc.) and 2 μg of total RNA was treated with RNase-free DNase (Roche). Then theRNA was reverse-transcribed with random hexamers using SuperScript II (Invitrogen), as previously described in detail (Kurrasch, Huang et al. 2004).

Quantitative real-time PCR (qPCR) was performed using an Applied Biosystem Prism 7900HT sequence detection system and SYBR-green chemistry (Kurrasch, Huang et al. 2004; Valasek and Repa 2005). Gene-specific primers were designed using Primer Express Software (PerkinElmer Life Sciences) and validated by analysis of template titration and dissociation curves. Primer sequences are provided in supplementary table Appendix A.1. 10 μl qPCR reactions contained 25ng of reverse-transcribed RNA, 150 nM of each primer and 5 μl of 2X SYBR Green PCR master mix (Applied Biosystems). Results of the qPCR were evaluated by the comparative Ct method (user bulletin No.2, Perkin Elmer Life Sciences) using cyclophilin as the invariant control gene.

Islets isolation and insulin secretion experiment

Islets were isolated by liberase digestion and cultured in INS-1 medium at 11.1 mM glucose. After overnight recovering, islets were treated with either DMSO or PPAR agonists (10 μM) for 16 hours. For static incubation experiments, 5-10 islets were plated pre well within a 24-well culture plate, in Secretion Assay Buffer (SAB, containing 0.114 M NaCl, 4.7 mM KCl, 1.2 mM KH_2PO_4, 1.16 mM $MgSO_4$, 12.75 mM $NaHCO_3$, 25 mM $CaCl_2$, 20 mM HEPES and 0,2% BSA, pH 7.4) without glucose for 1 hour. Then, the

islets groups were stimulated with 5 or 17.5 mM glucose for 1 hour and secreted insulin was measured using radioimmunoassay (RIA, Linco Diagnosis). For perifusion experiments, islets were transferred onto a nitrocellulose filter (Millipore) in a plastic perifusion chamber (Millipore). The experiments were performed in duplicate with 100 islets in each chamber. Culture media of varying glucose concentration was warmed to 37^0C and applied to the chamber by peristaltic pump at a flow of 0.5 ml/min while effluent fractions were collected for insulin measurement by RIA.

Results

Activation of PPAR target genes in islets by KD3031

In the mouse islet, PPARδ is the most abundant isoform among the three PPAR isoforms and is present in both α cells and β cells (Chapter 2, Fig 2.4). To test if the synthetic ligand of PPARδ, KD3010, can activate PPARδ in the islets, we treated isolated islets from A129/svj mice with DMSO or KD3010 (10 μM) for 16 hours and RNA was extracted for qPCR analysis. Several known target genes of PPARs that are involved in lipid handling and oxidation were upregulated by KD3010 treatment as expected (Fig Appx. A.1). These results demonstrated that PPARδ is present and functional in the mouse islets. In addition, these data also suggested that the synthetic ligand, KD3010, is effective in activating PPARδ in the islet cells.

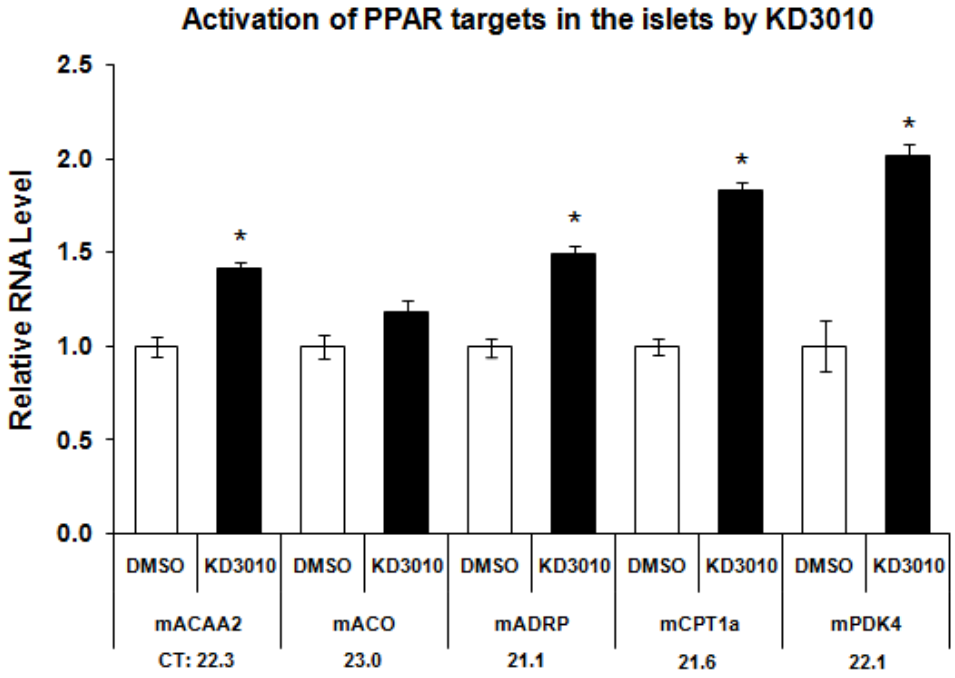

Figure Appx.A.1. Activation of known PPAR target genes in islets by synthetic PPARδ ligand KD3010. Mouse islets were treated with 10 μM KD3010 for 16 hours and RNA levels of known PPAR target genes were measured by qPCR using cyclophiline as the invariant housekeeping gene. The values depicted reveal the fold change observed with KD3010 treatment (* $p<0.05$, as compared to vehicle). Ct values (vehicle treated samples) were provided for each gene and the full name of each gene is available in Table App.A.1.

KD3010 enhances GSIS from isolated mouse islets

Next, we determined if the activation of PPARδ in the isolated islets by KD3010 would affect insulin secretion. Under static incubation, KD3010 treated islets secret more insulin (~64%) comparing to vehicle (DMSO) treated islets when stimulated with high glucose (17.5 mM). For comparison, a synthetic ligand for PPARα was included in this experiment and also increased GSIS by ~30% (Fig Appx.A.2, panel A). Basal insulin secretion under 5mM glucose was not altered when islets were treated with KD3010 or

PPARAα agonist. When insulin secretion was measured in a perifusion system, KD3010 treated islets also showed enhanced insulin secretion compared to vehicle treated islets (Fig Appx.A.2, panel B). These data suggest that the activation of PPARAδ in the cells of islets by KD3010 sensitized the β cell and enhanced insulin secretion upon glucose stimulation.

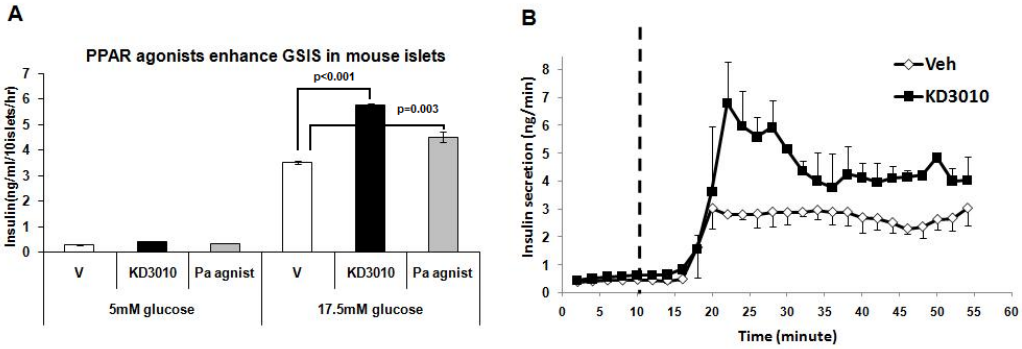

Figure Appx.A.2. KD3010 enhances GSIS from isolated mouse islets.
Glucose-stimulated insulin secretion is increased in KD3010 treated (16 hours) mouse islets. ***(A)*** Glucose-induced insulin secretion from isolated islets was measured under static incubation condition at a glucose concentration of 5 mM (basal) or 17.5 mM (stimulatory). Both PPARδ and PPARα agonist increased insulin secretion under stimulatory glucose condition. ***(B)*** Glucose-induced insulin secretion in perifusion experiments. The perfusate was collected at 2-minute intervals, and insulin levels were determined by using RIA. KD3010 treated islets (filled square) displayed increased insulin secretion when compared with control (open diamond). High glucose (17.5 mM) was introduced into the perifusion system at 10 minute as indicated.

KD3010 enhances GSIS from isolated mouse islets in a PPARδ selective manner

In order to test the specificity of KD3010 toward PPAR isoforms, islets from wild type and PPARα null mice were isolated and subjected to KD3010 or WY (a PPARα agonist) treatments. Both PPARα and PPARδ ligands enhanced insulin secretion from islets of wild type mice (Fig Appx.A.3, panel A). However, PPARα ligand (WY) failed to

enhanced insulin secretion from PPARα null islets while PPARδ agonists (KD3010) was still effective in the absence of PPARα (Fig Appx.A.3, panel B). These data demonstrated that the effect of KD3010 is independent of PPARα.

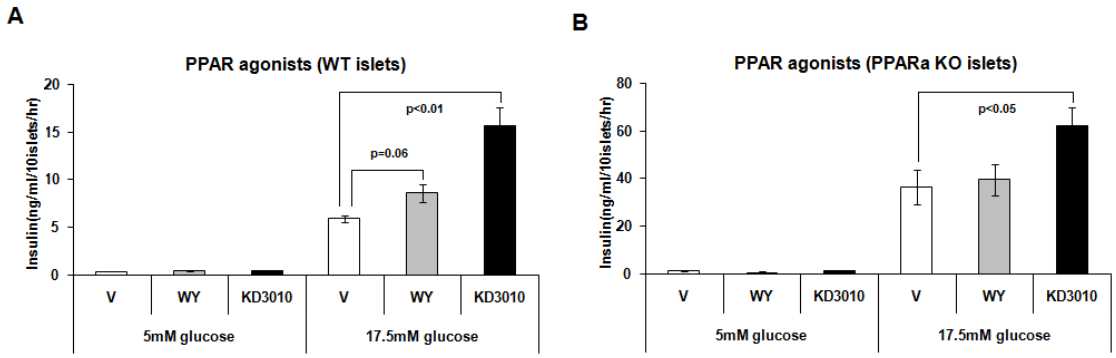

Figure Appx.A.3. KD3010 enhances GSIS in a PPARδ selective manner.
Glucose-induced insulin secretion from isolated islets was measured under static incubation at a glucose concentration of 5 mM (basal) or 17.5 mM (stimulatory). **(*A*)** Both PPARδ (KD3010) and PPARα agonist (WY) increased insulin secretion at a stimulatory glucose concentration. **(*B*)** PPARα agonist (WY) failed to induces GSIS in islets from PPARα null mice while PPARδ agonist (KD3010) was still effective.

Discussion

Accumulating studies suggest that PPARδ is a powerful metabolic regulator that controls fatty acid catabolism, uncoupling of energy, and triglyceride storage in tissues including muscle, adipose tissue, and the heart (reviewed in (Barish, Narkar et al. 2006)). In addition, activation of PPARδ has also been shown to modulate inflammatory responses (Takata, Liu et al. 2008) and decrease hepatic glucose output (Lee, Olson et al. 2006). These features of PPARδ make high-affinity PPARδ synthetic agonists ideal therapeutic targets for metabolic syndrome. Compared to other tissues, the effects of activating

PPARδ in the islets cells are less understood despite the fact that PPARδ is abundantly present in the islet. Here we describe the beneficial effects of a high affinity synthetic ligand for PPARδ on regulating GSIS from isolated mouse islets. This observation strengthens the potential of using PPARδ agonists in the metabolic syndrome. However, more experiments are required to address the long term effects of chronic activation of PPARδ in the islets.

Table Appx A. qRT PCR primer sequences for measurement of PPAR targets RNA levels

symbol	Gene name	Accession no.	Primer sequence 5'-3'	
mACAA2	*acetyl-Coenzyme A acyltransferase 2*	NM_177470	QF	GGATTTGATAGACGTGAACGAA
			QR	AAGATCCAGGGCCTTCTGAAC
mACO	*acyl-Coenzyme A oxidase*	NM_015729	QF	CTGCTCAGCAGGAGAAATGG
			QR	TGGGCGTAGGTGCCAATTA
mADRP	*adipose differentiation related protein*	NM_007408	QF	GACCTCTGCGGCCATGAC
			QR	GTATTGGCAACCGCAATTTGT
mCPT1a	*carnitine palmitoyl transferase 1a*	NM_013495	QF	CAAAGATCAATCGGACCCTAGAC
			QR	CGCCACTCACGATGTTCTTC
mPDK4	*pyruvate dehydrogenase kinase*	NM_013743	QF	CAAAGACGGGAAACCCAAGC
			QR	CGCAGAGCATCTTTGCACAC
m36B4	*acidic ribosomal phosphoprotein P0*	NM_007475	QF	CACTGGTCTAGGACCCGAGAAG
			QR	GGTGCCTCTGAAGATTTTCG

APPENDIX B

Expression of GPCR and RGS in the islet cells

Abstract

G protein-coupled receptors (GPCRs) are membrane receptors that regulate many physiological and disease processes. Regulators of G-protein signaling (RGS) and G protein-coupled receptor kinases (GRKs) are negative regulators of GPCRs that control the potency and duration of their signals. Cells in the pancreatic islets are subjected to the regulation of numerous environmental signals many of which signal through GPCRs. The roles of several GPCRs, such as receptors for GLP-1 and GIP, have been examined in the islets and proposed to be therapeutic targets to improve islet function. However, much is still unknown about the expression and function of many other GPCRs. In addition, the roles of GRKs and RGS in the islets have been neglected and must be studied to fully understand the activity of GPCRs in the islets. To reveal potential modulators of islet function, we performed qRT-PCR to quantify the expression of members of GPCRs, RGSs, and GRKs in the mouse islets and representative α and β cell lines. By comparing the expression profiles in the islets with that of α cell line (αTC1) and β cell lines (βTC6 and MIN6), we found several GPCRs and RGS that showed cell type enriched expression patterns. In addition, we found that acute activation of GPR119, a novel GPCR and TGR5 by synthetic ligands enhanced the GSIS from isolated mouse islets.

Introduction

The heterotrimeric guanine nucleotide-binding proteins (G proteins) are signal transducers that integrate signals from many extracellular stimuli. G proteins are a

complex containing three subunits called Gα, β, and γ. Specialized receptors on the surface of cells called G-protein-coupled receptors (GPCR) sense the external environment and activate the Gα subunit of G-proteins, which then initiates intercellular responses.

Upon ligand binding to the GPCRs, coupled G proteins are activated and can signal through downstream effectors such as adenylyl cyclases, phospholipases, and ion channels. These effectors then regulate a broad range of cellular responses including transcription, mobility, secretion, and motility.

The activation of G proteins is usually short lived. Downstream signals have to be terminated shortly after activation to prevent over-activation and also to enable the system to reset for the next cycle of activation. There are two major negative regulator systems to inactivate GPCR pathway, GRK-arrestin mediated receptor internalization and regulators of G protein signaling (RGS). The first system involves the addition of phosphates to activated GPCR by GRKs, members of the kinase family. The phosphorylated receptors are then internalization by arrestin to decrease the numbers of available receptors on the membrane. The second system, the RGS proteins, works by accelerating the hydrolysis of GTP on the active Gα subunits and terminate the signals. There are seven GRKs, two arrestins, and about twenty RGS proteins in the mammalian genome.

Several GPCRs are expressed in the islet cells and are involved in the regulation of islet function. Glucagon receptor (GCGR) is abundantly expressed on the membrane of β cells and is important for the paracrine effect of glucagon. Incretines such as GLP-1 and GIP are gastrointestinal hormones that increase the secretion of insulin from islets.

These incretins modulate islet function through GLP-1R and GIPR, both are members of GPCR family. There are also several GPCRs that have recently been identified as fatty acids receptors and can be involved in the regulation of insulin secretion. However, the roles of many other GPCR family members are still poorly understood.

In this study, our goal is to examine the expression of members of GPCRs, GRKs, and RGSs in the mouse islets and to reveal potential players in islet function. We used real time PCR to survey the expression of novel GPCRs, RGSs, GRKs in islets and several other mouse tissues.

Materials and Methods

RNA measurement

RNA was isolated from tissue samples or cultured cells using RNA STAT-60 (Tel-Test Inc.) and 2 μg of total RNA was treated with RNase-free DNase (Roche). Then the RNA was reverse-transcribed with random hexamers using SuperScript II (Invitrogen), as previously described in detail (Kurrasch, Huang et al. 2004).

Quantitative real-time PCR (qPCR) was performed using an Applied Biosystem Prism 7900HT sequence detection system and SYBR-green chemistry (Kurrasch, Huang et al. 2004; Valasek and Repa 2005). Gene-specific primers were designed using Primer Express Software (PerkinElmer Life Sciences) and validated by analysis of template titration and dissociation curves. Primer sequences are provided in Appendix table B.1. 10 μl qPCR reactions contained 25ng of reverse-transcribed RNA, 150 nM of each primer and 5 μl of 2X SYBR Green PCR master mix (Applied Biosystems). Results of

qPCR were evaluated by the comparative Ct method (user bulletin No.2, Perkin Elmer Life Sciences) using cyclophilin as the invariant control gene.

Islets isolation and insulin secretion experiment

Islets were isolated by liberase digestion and cultured in INS-1 medium at 11.1 mM glucose. After overnight recovering, islets were used for static incubation insulin secretion experiments. 5-10 islets were plated per well within a 24-well culture plate in Secretion Assay Buffer (SAB, containing 0.114 M NaCl, 4.7 mM KCl, 1.2 mM KH_2PO_4, 1.16 mM $MgSO_4$, 12.75 mM $NaHCO_3$, 25 mM $CaCl_2$, 20 mM HEPES and 0,2% BSA, pH 7.4) without glucose for 1 hour. Then, the islet groups (6 independent wells for each condition) were stimulated with 5 or 17.5 mM glucose together with DMSO or GPR119 ligand (10 μM) for 1 hour. Secreted insulin was measured using radioimmunoassay (RIA, Linco Diagnosis).

Results

Expression of GPCRs in the mouse endocrine pancreas

Inorder to examine the expression of GPCRs in the mouse islets and the representative islet cell lines, primers for qPCR were generated for a panel of GPCRs of our interest. The results were plotted to show the relative abundance of a given GPCRs between tissue/cell types (Fig Appx.B.1). The expressions of GPCRs can be also plotted to get a ranking of expression levels in the tissue/cell lines being examined (Fig Appx.B.4) to provide information regarding the relative abundance of GPCRs in a given tissue.

β cells abundant GPCRs in the mouse endocrine pancreas

Among the GPCR that we examined, GLP-1R is the most abundant in the islet sample (with Ct of 17.5) and is much more abundantly expressed in the β cells compared to α-cells.

Several other GPCRs showed a β cell selective expression pattern like GLP-1R. These GPCR include ADRA2A, CCKAR, CCKBR, GPR39, GPR40, GPR41, GPR43, P2RY1, GPRC6A, and GIPR. A description of what is known about each of these GPCR's follows:

ADRA2A (α2-adrenergic receptor) is expressed in the islets with Ct of 22.3. Noradrenaline, the ligand for ADRA2A has been shown to regulate insulin secretion (Ahren 2000) and a mutation on ADRA2A has been shown to be associated with obesity and metabolic alterations (Lima, Feng et al. 2007).

CCKAR and CCKBR, receptors for cholecystokinin (CCK) are expressed in islets with Ct of 24.9 and 29 respectively. The roles of these two GPCRs for islet function remain to be established.

GPR39 has been proposed to be receptor for obestatin (Zhang, Ren et al. 2005) and its function remains unclear.

GPR40 (Fujiwara, Maekawa et al. 2005), GPR41, and GPR43 (Brown, Goldsworthy et al. 2003) are FFA receptors and have been proposed to involved in the regulation of β cell function.

P2RY11 (Purinergic receptor subtype Y) is a receptor for extracellular adenine nucleotides such as ATP and ADP (Leon, Hechler et al. 1997). It is abundantly expressed

in the islet with Ct of 23.3 and shows a β cell enriched pattern. Activation of P2YR1 has been reported to regulate intracellular calcium and thus is likely to have an effect on insulin secretion.

GPRC6A has been proposed to be receptor for osteocalcin (Pi, Faber et al. 2005), a bone derived hormone that may regulate islet function [202]. The function of this GPCR in islet is not clear as well.

α cells abundant GPCRs in the mouse endocrine pancreas

On the other hand, several GPCR members such as SSTR2, GPR54, GPR55, and P2RY14 show an α-cell selective expression pattern, which are described below:

SSTR2 (Somatostatin receptor 2) has been shown to be required for somatostatin to inhibit insulin and glucagon secretion. SSTR2-/- mice have hyperglucagonemia and hyperglycemia (Singh, Grotzinger et al. 2007). SSTR2 thus may be a potential therapeutic target to lower glucagon in T2DM patients.

GPR55 is a newly identified cannabinoid receptor (Lauckner, Jensen et al. 2008) and the functions remain to be characterized in the islet.

P2RY14 (Purinergic receptor subtype Y14) is a receptor for sugar nucleotides such as UDP-glucose (Freeman, Tsui et al. 2001). The roles of this receptor in the islets cells are also not clear for the time being. It is likely to play an important role in regulating α cell function based on the exclusive expression pattern we observed.

GPCRs in both α and β cells the mouse endocrine pancreas

Several GPCRs appear to be present in both α and β cells in the islets, which are described below:

GPR119 and GPR 120 are both fatty acid binding GPCRs. GPR119 has been shown to regulate GSIS and has been proposed to be therapeutic target for T2DM. The effects of a synthetic agonist for GPR119 will be addressed later in this chapter. GPR120 has been proposed to regulate GLP-1 releasing and thus can regulate islet function indirectly (Hirasawa, Tsumaya et al. 2005). However, our data show that it is also expressed in the islet cells and may have direct effects on islet function.

GPR54 (Kisspeptin receptor) has been proposed to mediate the effect of kisspeptins in regulating islets insulin secretion (Hauge-Evans, Richardson et al. 2006) although the detailed role of this GPCR in islet physiology remains to be revealed.

TGR5, a putative bile acid receptor on the cell membrane (Kawamata, Fujii et al. 2003) is also present in the islets. This surprising observation led us to test the effect of TGR5 activation in the islets, which will be addressed later.

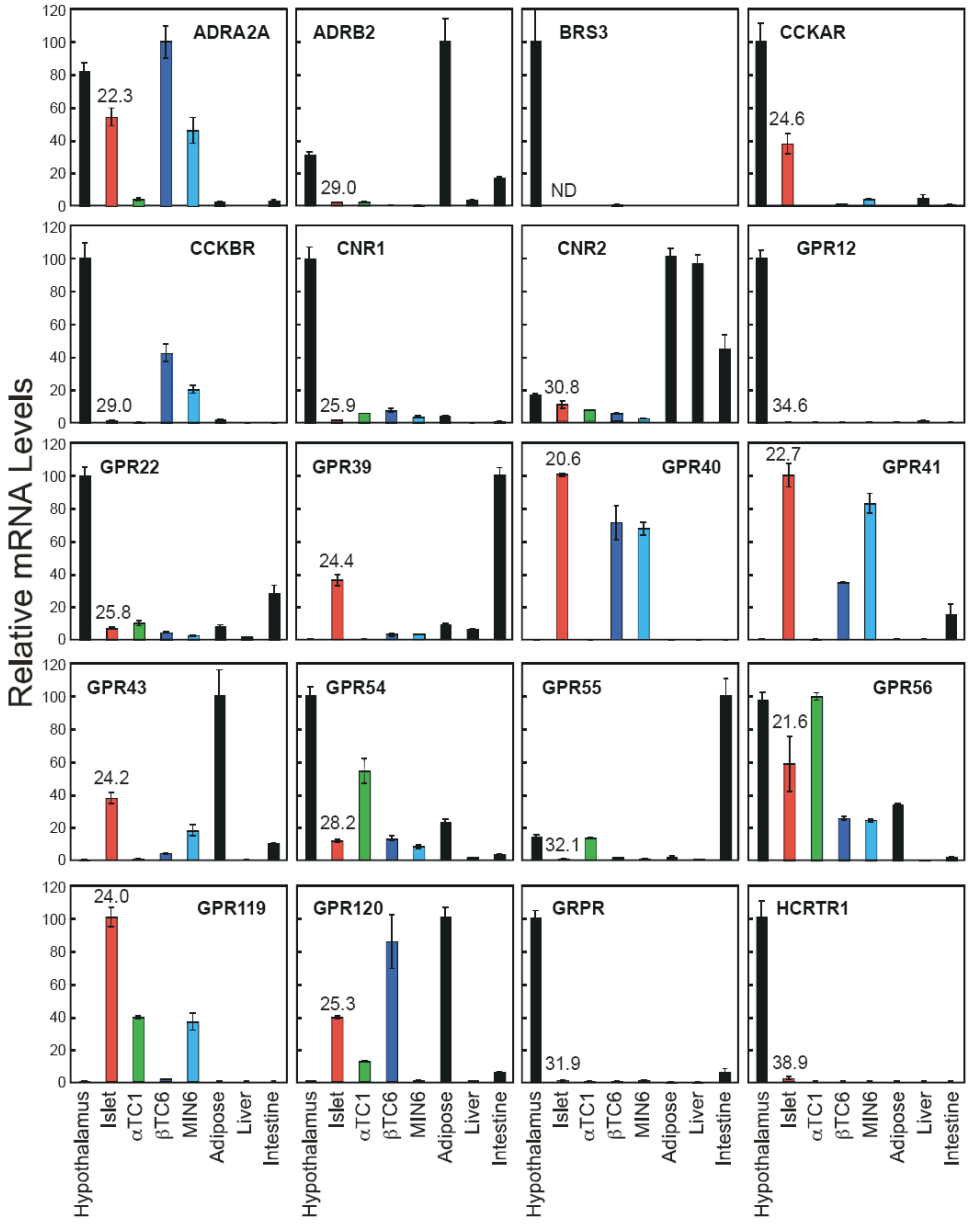

Fig. Appx. B.1. Expressions of selected GPCRs in the mouse endocrine pancreas
All values are expressed relative to cyclophilin, and arithmetically adjusted to depict the highest-expressing sample as a unit of 100. Values represent the means and SEM of three independent samples for each tissue or cell line, thus portraying biologic variance. Note that as this data is portrayed, comparisons can only be made between different tissues for a single GPCR, not between various receptors (see Figure App. B.4).

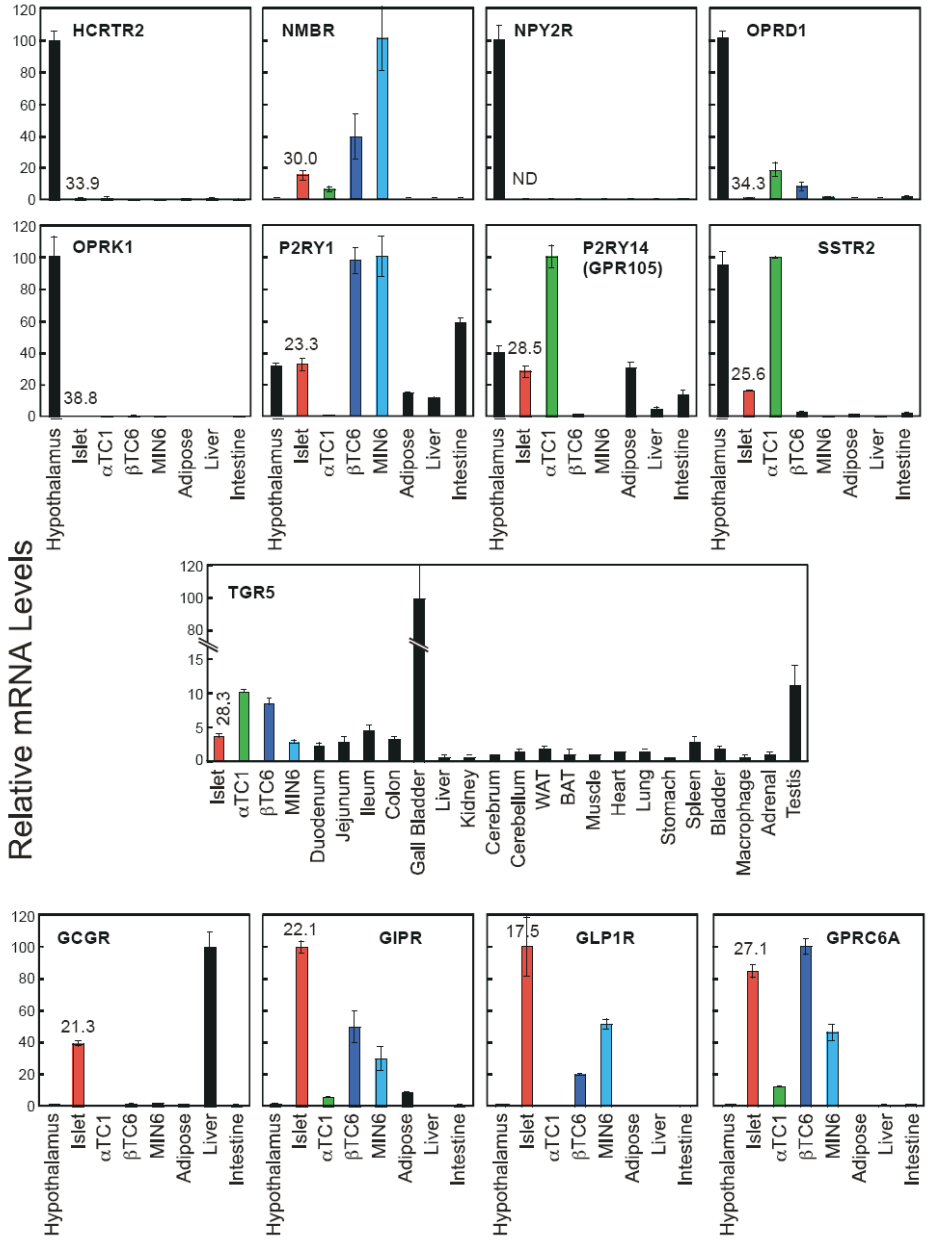

.

Fig. Appx.B.1 continued.

Expression of GRK/Arrestins in the mouse endocrine pancreas

GRK2 and arrestin beta 1 **(**ARRB1) have been proposed to modulate GIP-mediated insulin secretion. Overexpression of GRK2 enhances agonist induced GIPR phosphorylation, inhibits cAMP production, and attenuates GIP-stimulated insulin secretion (Tseng and Zhang 2000). However, the expression and the potential roles of other RGKs in the endocrine pancreas have not been addressed.

We used qPCR to get an expression profile of all GRKs and two arrestins in the mouse islets and α/β cell lines **(**Fig Appx.B.2). GRK1, also known as rod cell GRK, is exclusively expressed in rod/cone cells in the retina (Zhao, Huang et al. 1998) and was not detected in the mouse islets. GRK2, 3, 5, and 6 are present in the islets at comparable levels (Ct between 20.6 to 23.6). GRK4 is also expressed in the islet although with a lower abundance (Ct=27.4).

ARRB1 and ARRB2 are both present in the mouse islet, and ARRB2 is more abundantly expressed (ARRB2: Ct=22.8, ARRB1: Ct=25). There is no cell selective expression pattern observed.

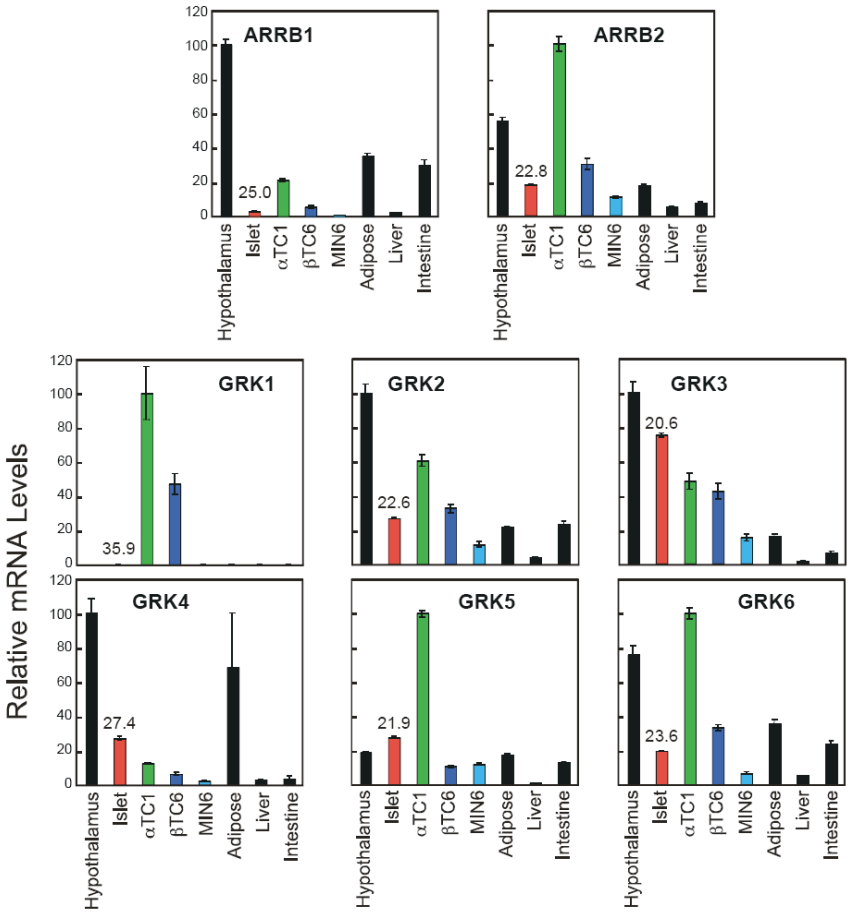

Fig. Appx.B.2. Expressions of GRKs and arrestins in the mouse endocrine pancreas. All values are expressed relative to cyclophilin, and arithmetically adjusted to depict the highest-expressing sample as a value of 100. Values represent the means and SEM of three independent samples for each tissue or cell line, thus portraying biological variance.

Expression of RGS in the mouse endocrine pancreas

Very few studies have attempted to address the function of RGS in the islets so far. One study has shown that GIP-induced insulin secretion is repressed by RGS2 (Tseng and Zhang 1998). Another study showed that prostaglandin E (PGE1) inhibits both cAMP

production and insulin secretion through a Gαz dependent manner while RGS17 blocked the inhibitory effect of PGE1 (Kimple, Nixon et al. 2005). These examples made us to believe that RGS proteins can be important in islet function, so we decided to examine the expression of RGS in the islet.

The expression of RGS in the pancreatic islets was examined and compared among several other tissues as well as among RGS (Fig Appx.B.3 and Appx.B.5). The high expressors (Ct<25) in the islet include RGS4, 16, 11, 17, 3, 5, 2, 7, and RGS9. The medium expressors (25<Ct<30) are RGS10, 19, 12, 1, 8, and RGS20. The low expressors (30<Ct<33) include RGS18, 13, 6, and RGS14.

RGS4 is the most abundant RGS expressed in the islets and appears to be expressed in both α cells and β cells (Ct=17.0 for islet, 18.3 for αTC1, and 19.3 for MIN6 cell).

The expression of RGS9 in the islet seems to be β cell selective (Ct=23.9 for islet, 22.1 for βTC6, 21.7 for MIN6, and not detectable in αTC1 cells).

On the other hand, some RGS appear to be α cell enriched. These RGS include RGS5 (Ct=22.9 for islet, 21.4 for αTC1, 31.1 for βTC6, and 28.9 for MIN6 cell), RGS6, RGS16.

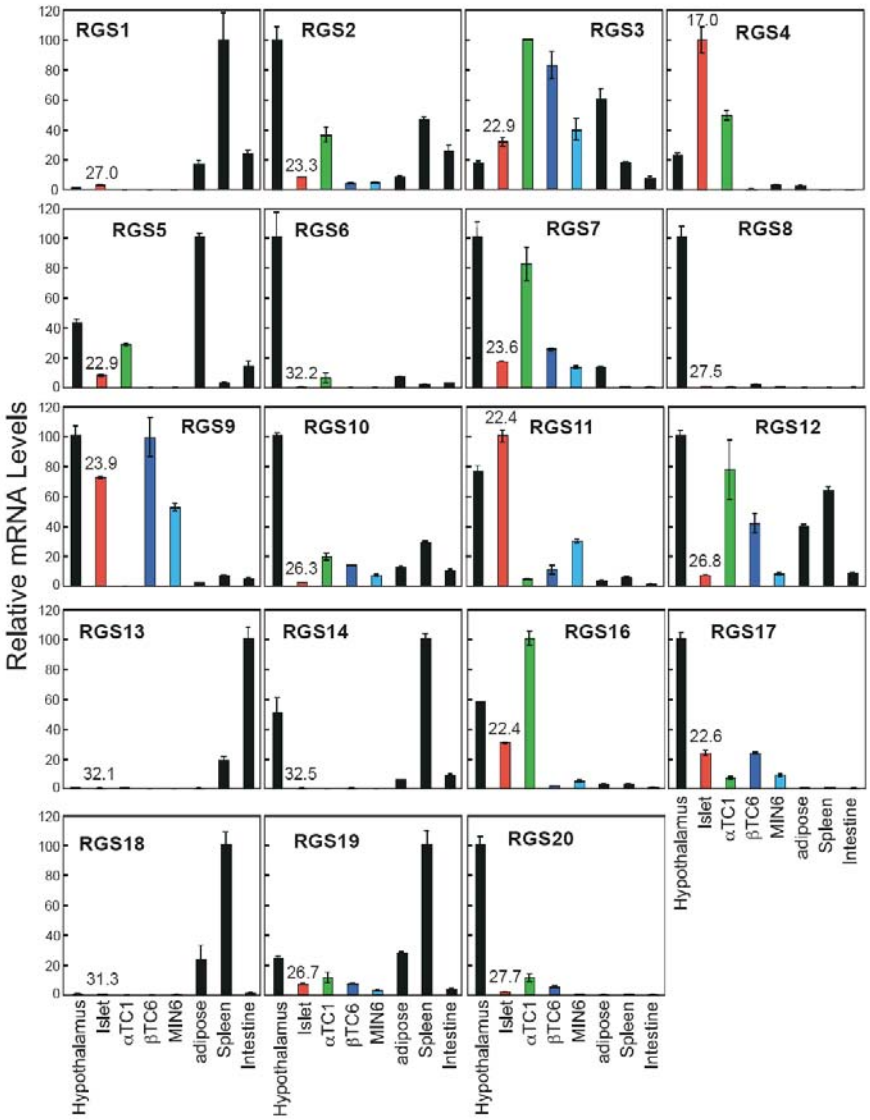

Fig. Appx.B.3. Expression of RGSs in the mouse endocrine pancreas
All values are expressed relative to cyclophilin, and arithmetically adjusted to depict the highest-expressing sample as a value of 100. Values represent the means and SEM of three independent samples for each tissue or cell line, thus portraying biologic variance.

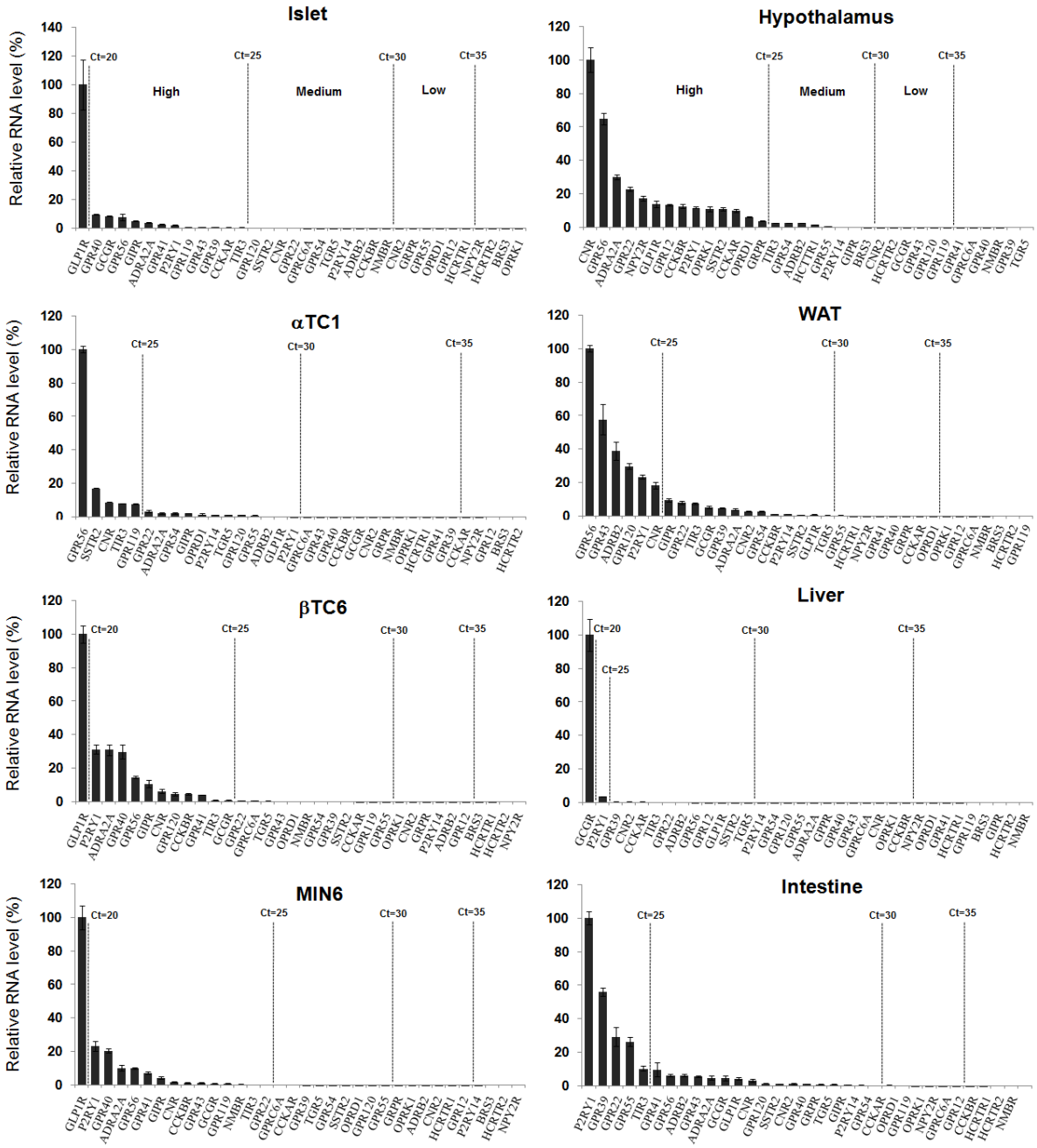

Fig. Appx.B.4. **Comparative expression levels of selected GPCRs for mouse islets, cell lines and several other tissues.**
All values are expressed relative to cyclophilin, and arithmetically adjusted to depict the highest-expressed GPCR for each tissue/cell line as a value of 100. Values represent the means and SEM of three independent samples for each tissue or cell line.

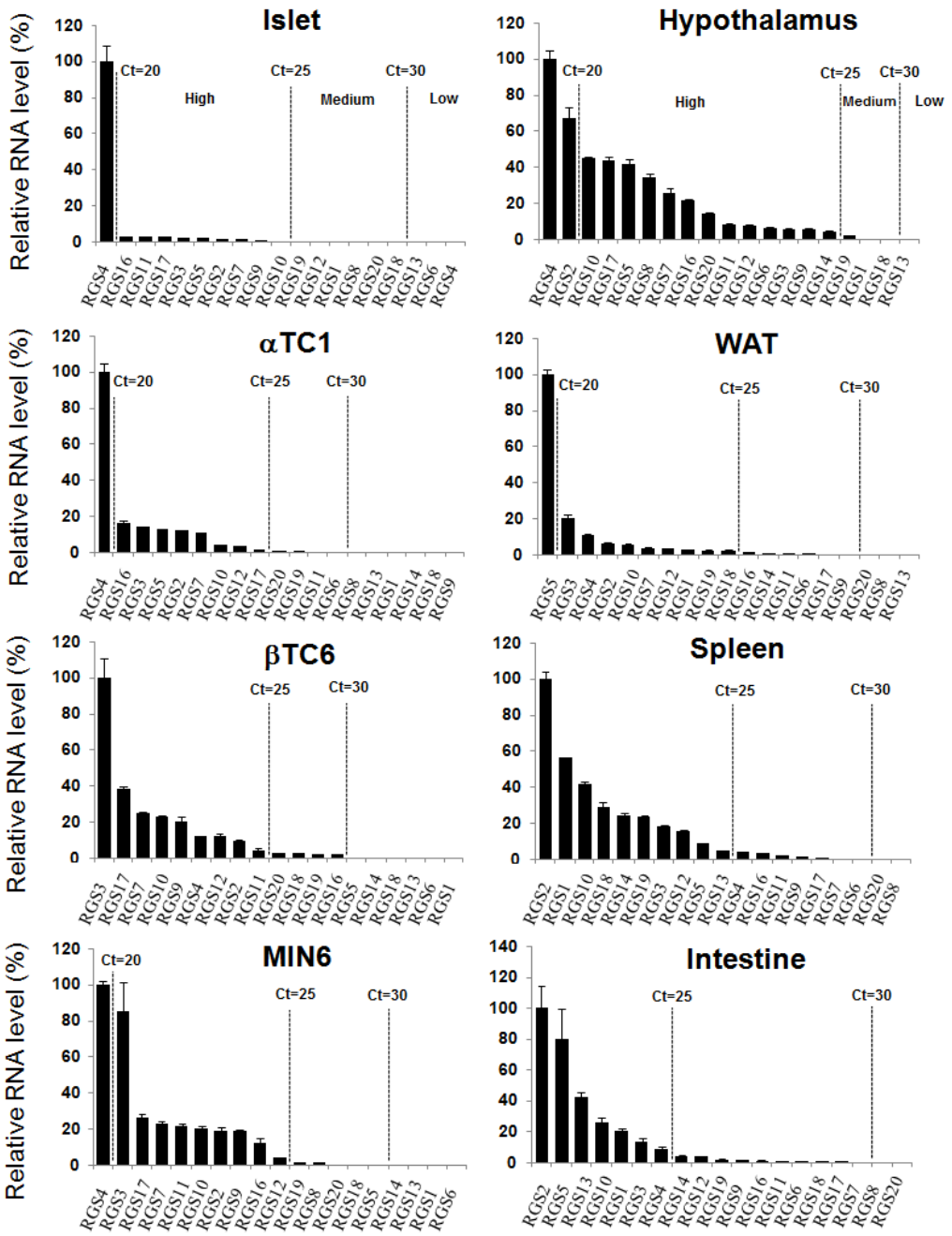

Fig. Appx.B.5. **Comparative expression levels of RGS for mouse islets, cell lines and several other tissues.**

All values are expressed relative to cyclophilin, and arithmetically adjusted to depict the highest-expressed RGS for each tissue/cell line as a value of 100. Values represent the means and SEM of three independent samples for each tissue or cell line.

Activation of GPR119 increases GSIS

GPR119 is a newly identified GPCR that is predominantly expressed in the islets compared to other tissues (Fig App B.1, and (Sakamoto, Inoue et al. 2006)). It has been shown that activation of GPR119 by lysophosphatidylcholine (LPC) and oleoylethanolamide (OEA) enhance GSIS through increasing cAMP (Soga, Ohishi et al. 2005; Overton, Babbs et al. 2006; Sakamoto, Inoue et al. 2006). GPR119 therefore is considered to be a therapeutic target for obesity, diabetes, and related metabolic diseases.

Here we tested a synthetic ligand of GPR119, Klys0011, to see if the acute activation of GPR119 by this synthetic ligand in the islets will lead to the increase of insulin secretion. DMSO or three concentrations (400 nM, 2 μM, and 10 μM) of Klys0011 were applied to islets together with either 5 mM or 17.5 mM glucose during GSIS experiments. Klys0011 did not have effects on insulin secretion under low glucose conditions (5 mM), however under high glucose (17.5 mM) insulin secretion was increased by Klys0011 in a dose dependent manner (Fig Appx B.6, a 72% increase with 2 μM Klys0011, and 3.4 -fold increase with 10 μM Klys0011).

Interestingly, we also detect the expression of GPR119 in the αTC1 cell. It is currently unknown whether GPR119 plays a role in regulating glucagon secretion.

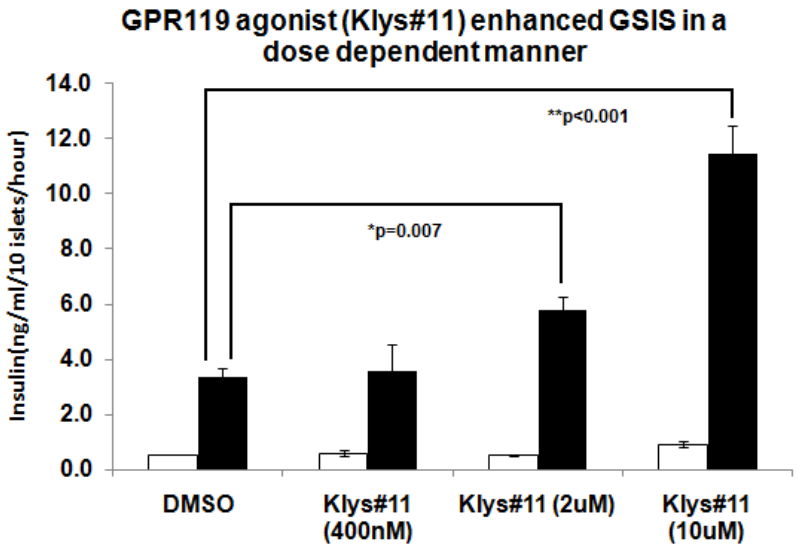

Figure Appx.B.6. GPR119 agonist enhances GSIS from isolated mouse islets.
Glucose-stimulated insulin secretion is enhanced in mouse islets that are treated with synthetic ligand for GPR119 (Klys0011, 1 hour). Islets were incubated with a glucose concentration of 5 mM (basal) or 17.5 mM (stimulatory) with DMSO or GPR119 ligand (400 nm, 2 μM, or 10 μM). Under 5 mM glucose (white bars), KLY did not induce insulin secretion while under 17.5 mM glucose (black bars) it increased insulin secretion in a dose dependent manner.

Activation of TGR5, the membrane bile acid receptor in islets leads to increased GSIS

Bile acids are known to regulate the expression of various enzymes and transporters that are required for bile acid metabolism through the binding and activation of farnesoid X receptor (FXR) (Makishima, Okamoto et al. 1999). In addition to these well established genomic effects, bile acids are also reported to elicit a non-genomic and acute response which is coupled with the activation of cAMP (Potter, Sellin et al. 1991). This non-genomic effect of bile acids is mediated by a membrane GPCR for bile acids named TGR5 (Maruyama, Miyamoto et al. 2002; Kawamata, Fujii et al. 2003). Activation of TGR5 by bile acids has been shown to regulate macrophage function (Kawamata, Fujii et

al. 2003), modulate GLP-1 release from the intestine (Katsuma, Hirasawa et al. 2005), and control energy expenditure in brown adipose tissue (Watanabe, Houten et al. 2006).

In our GPCR profiling study, we found that TGR5 is present in the isolated mouse islets and cultured α/β cell lines (Fig Appx B.1). Since an increase of cAMP in the β cell of islets has been known to induce insulin secretion, we proposed that the activation of TGR5 will likely lead to the increase of insulin secretion from islet. When isolated islets were incubated with a synthetic ligand for TGR5 (Klys0013, EC_{50}=70 nM), insulin secretion under high glucose was increased by more than 3-fold (Fig Appx B.7, panel A).

Next, we wanted to address if bile acids, the endogenous ligands for TGR5 can have effects on islet GSIS. Chenodeoxycholic acid (CDCA), cholic acid (CA), and lithocholic acid (LCA) were tested during a GSIS experiment. CDCA appears to have no effect on insulin secretion. CA increases GSIS modestly (30%), and LCA enhances GSIS by 60% (Fig Appx B.7, panel B). Interestingly, when TGR5 was first reported to be a membrane receptor for bile acids, LCA was one of stronger ligands among several bile acids tested for binding affinity (Kawamata, Fujii et al. 2003). Our GSIS results with LCA being most effective in enhancing GSIS agree with this binding affinity report.

It has been shown that bile acid levels increase after meal not only in the liver and intestine but also in the systemic circulation (from ~5 μM to 15 μM in humans) due to the spillover from the enterohepatic recirculation in the portal vein (Ho 1976; Engelking, Dasher et al. 1980; Everson 1987). Based on these observations, concentrations of bile acids in the islets are likely to be increased after meals as well. It is

thus tempting to hypothesis that bile acids can serve as signaling molecules to inform islets that a meal has been ingested.

FXR is a nuclear receptor that senses bile acids and according to our nuclear receptor profiling data, FXRα is expressed in the islet (Fig.2.1). We wanted to determine whether bile acids also modulate insulin secretion through the activation of FXR. Islets were treated with synthetic FXR agonist (GW4064, 10 μM) for 16 hours and GSIS experiments were performed. The data showed that the activation of FXR by GW4064 did not change GSIS despite the activation of many well known target genes of FXR after the treatment (data not shown). This observation suggests that the effect of bile acids on insulin secretion is an acute response after meal through the activation of the GPCR, TGR5, but not through the nuclear receptor, FXR.

In summary, our data showed that TGR5, the membrane BAs sensor is expressed in islet cells and that that activation of this GPCR by either a synthetic ligand or endogenous BAs can positively regulate GSIS.

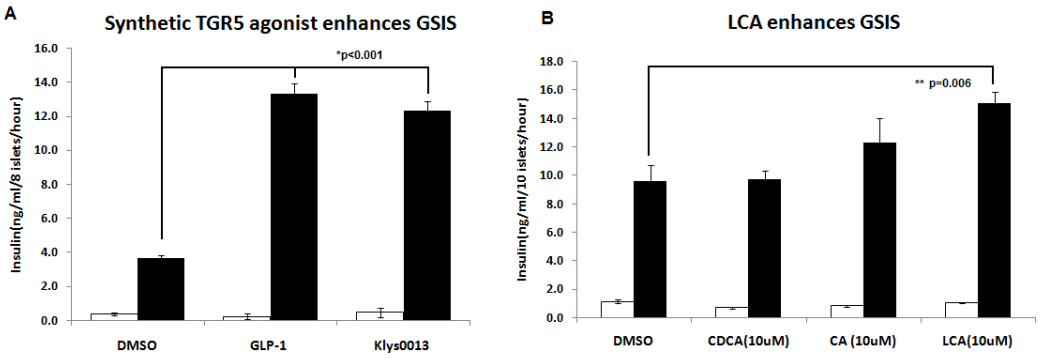

Figure Appx.B.7. TGR5 ligands enhance GSIS from isolated mouse islets.
(*A*) Glucose-stimulated insulin secretion is enhanced in mouse islets that are treated with synthetic ligand for TGR5 (Klys0013, 1 hour). Islets ware incubated with a glucose concentration of 5 mM

(basal, white bars) or 17.5 mM (stimulatory, black bars) with DMSO or 10μM TGR5 ligand. A potent incretin, GLP-1(50 nM) is used as a positive control. **(*B*)** Several endogenous ligands of TGR5 were tested for their effects on GSIS. Isolated mouse islets were incubated with Chenodeoxycholic acid (CDCA, 10 μM), cholic acid (CA, 10 μM), or lithocholic acid (LCA, 10 μM) for 1 hour during the GSIS experiment.

Discussion

The most important function of the pancreatic islets is to secrete hormones in response to physiological needs. Glucose acts as the fundamental trigger for the release of hormones from islet cells. Beside glucose itself, many environmental factors are also involved in the regulation of hormone secretion from islets. As previously discussed, we believed that members in the nuclear receptor family are intracellular sensors that monitor the abundance of lipid signaling molecules and control the expression of target genes that may participate in the secretion of hormones from the islet. We consider this sensor system a relatively long term modulator of islet function since gene transcription and translation are required. On the other hand, GPCRs are membrane sensors that can regulate the secretion of hormones from islets acutely by activation of effectors such as cAMP, IP3, and Ca^{2+} that serve as a direct link to secretory vesicles of islet cells.
The strength and duration of the GPCR signals are tightly controlled by the actions of GRKs and RGS, regulators that control the membrane GPCR recycling and inactivate Gα protein respectively. We believed that many members in the GPCR, GRK, and RGS families are potential novel regulators of islet function and have not been addressed.
In this study, we started with a comprehensive quantification of the expression of GPCRs, GRKs, and RGSs in the mouse islets and several tissues using q-PCR technique.

These data provide a useful database for identifying potential GPCR/RGS/GRK as functional regulators in each tissue.

We also demonstrated that activation of GPR119 and TGR5 in the islets by synthetic ligands lead to the increase of GSIS. These data confirmed the potential of probing novel GPCR as therapeutic targets for improving islet function. To our knowledge, this is the first report to demonstrate that TGR5, the membrane receptor for bile acids, is present in the islets and can regulate insulin secretion. This observation leads to an intriguing hypothesis that bile acids in the circulation may play a novel role in regulating islet functions.

In summary, our data should provide valuable directions for the future studies regarding the functional significance of a given GPCR, GRK, or RGS in different cell types in the mouse islet.

To date, very little has been done regarding the potential roles of RGS and GRKs in regulating islets function. RGS2 and GRK2 have been proposed to modulate GIP mediated GSIS (Tseng and Zhang 2000),(Tseng and Zhang 1998). More studies will be needed to uncover this complicated regulatory system in the islets.

Beside islets cells, the roles of the RGS and GRKs in other tissues involved in metabolic control are also interesting to us. Among these tissues, hypothalamus is the most attractive because neurons in hypothalamus are heavily regulated by neurotransmitters which signal through GPCRs. The potential role of RGS and GRKs in the hypothalamus is intriguing and our data do provide several candidates for further study.

Table Appx B. qRT PCR primer sequences for mouse GPCRs, GRKs, and RGSs.

Gene Abbrev.	Gene Name	Accession Number	Sequence of Primers (5' to 3')
Arrestins			
Arrb1	Arrestin, beta 1	NM_177231	F: GCACCCCAAGCCTAAGGA R: CCGCTGGCGAGCAAAG
Arrb2	Arrestin, beta 2	NM_145429	F: CAAGACCGTCAAGAAGATCAGAGT R: CTGCGCGGTGCTGAAG
G Protein-coupled receptor kinases			
GRK1	GPCR kinase 1	NM_011881	F: 5'CGCTTCGGGCAAACG R: 5'GAATGTTCTTGGCATAGACAGTCCTA
GRK2	GPCR kinase 2 (Adrbk1)	NM_130863	F: GACTGGCAGATGGTCTTCTTACA R: AAAGCGTCAGCTGCATTCAC
GRK3	GPCR kinase 3 (Adrbk2)	NM_177078	F: AGAAACAGGTGACGGCTACACTT R: ACTCCACGTTCTTCCACTGACA
GRK4	GPCR kinase 4	NM_019497	F: GCAAATATGTTAGATCCACCTTTCA R: GAGAACTGCCCAATATCCAAGAT
GRK5	GPCR kinase 5	NM_018869	F: AAGGGCTGTTCCACAGACTCTT R: GGTGGTTACAACTGGTCTTAGGAGTA
GRK6	GPCR kinase 6	NM_001038018	F: CGTAGCGAACACGGTGCTA R: GCGCCATTTCTTGCTCTTG
Regulator of G-protein signaling			
RGS3	RGS3	NM_019492	F : TGCTACAACTGAATGAGAGACCCG R: CAGGATGATCTCGCTAGGACAG

The rest of the RGS primers are listed in previous publication (Kurrasch, Huang et al. 2004).

Table Appx B. Continued.

Gene Abbrev.	Gene Name	Accession Number	Sequence of Primers (5' to 3')
G Protein Coupled Receptors - CLASS A			
ADRA2A	Adrenergic receptor 2, type a	NM_007417	F: CATCTCCTCGTCCATCGGTTC R: CTTGGCGATCTGGTAAATACG
ADRB2	Adrenergic receptor B2	NM_007420	F: TGATGGTCTTTGTCTATTCCCG R: GGGCGTGGAATCTTCCTTCAG
BRS3	Bombesin-like receptor 3	NM_009766	F: CACCCTGAACATACCGACTGA R: CAATTCTCTTCCGGGATTCAA
CCKAR	Cholecystokinin receptor A	NM_009827	F: CCCCAACCTGCTCAAGGATT R: GCCCATGAAGTAGGTGGTAGTCTT
CCKBR	Cholecystokinin receptor B	NM_007627	F: TCTCTGGCCCAGTGAACGT R: CGGGATGAAGAACAGCAGTATT
CNR1	Cannabinoid receptor 1	NM_007726	F: CACAAGCACGCCAATAACACA R: ACAGTGCTCTTGATGCAGCTTTC
CNR2	Cannabinoid	NM_009924	F: GAACATGGCCGTGCTCTATATTA

	receptor 2		R: AACAGGTACGAGGGCTTTCTG
GPR12	G Protein-coupled receptor 12	NM_008151	F: ACTGTGGACCGCTACCTCTCG R: GGTGACGGTCCTCTCGGAGT
GPR22	G Protein-coupled receptor 22	NM_175191	F: GCCTCTGAACCACAGACTACCAGA R: GGATGCTGTCAGCTTGTTCCG
GPR33	G Protein-coupled receptor 33	Nm_008159	F: CATCAAACACTAGGGCAATGGA R: CAGAAGGAAACCCAGCAAGAA
GPR39	G Protein-coupled receptor 39	BC085285	F: CAGACCATCATATTCCTGAGACTGA R: ATCCGTCGGATCTGATTGG
GPR40	G Protein-coupled receptor 40 (Ffar1)	AF539809	F: CATTTCCTTCTGTGGGCCTT R: GAATGTCACAACTGGCGTTC
GPR41	G Protein-coupled receptor 41 (Ffar3)	NM_001033316	F: CCTGCCTGTACGACTAGAGATGG R: GGCGACTGTAGCAGTAACTCG
GPR43	G Protein-coupled receptor 43 (Ffar2)	NM_146187	F : GGGGAAGAAGAGGAATGCCG R: GATGGGAGCCCTGTGTGTTG
GPR54	G Protein-coupled receptor 54 (Kiss1r)	NM_053244	F : CATGTGCAAATTCGTCAACTACAT R : CACACTCATGGCCGTCAGA
GPR55	G Protein-coupled receptor 55	NM_001033290	F: GGGACAGAAGTGTGACCAAATC R: ACGGAATCGAATGAGCAGTTG
GPR56	G Protein-coupled receptor 56	NM_018882	F: GCCAAGAGGCTCCTGGTAGTAG R: CACCCAGGACTTGGCTAGAATT
GPR84	G Protein-coupled receptor 84	NM_030720	F:TGTTTACTGAAGACAAGTGTGAAAACTG R: GCAGGAGAAGTTGGCATCTGA
GPR119	G Protein-coupled receptor 119	NM_181751	F : GCCATCCGGAGCTCGAT R : CAGAAGGATATGTGATTGCATGTTC
GPR120	G Protein-coupled receptor 120	NM_181748	F : GTCATTGTGATCAGTTACTCCAAAATT R : AGTATGCCAAGCTCAGCGTAAG
GRPR	Gastrin-releasing peptide receptor	NM_008177	F: CATGTCAAGAAGCAGATCGAATC R: AGGCCCACAAACACCAGTACT
HCRTR1	Orexin receptor 1	NM_198959	F : TGCCTGAGCTAGCCAATCG R : TGAAAAAGCAGCTGTGATAGATCTT
HCRTR2	Orexin receptor 2	NM_198962	F : GTGCTAAAGAGAGTATTTGGGATGTT R : GCCAATGAGAAAAAGTGAACCA
NMBR	Neuromedin B receptor	NM_008703	F: TTGCTGTGGACCAGTTTGAAG R: TCAGGGACCGCCAACAA
NPY2R	Neuropeptide Y receptor Y2	NM_008731	F : GGAACGCGCAAGAGTCAATA R : TCTCATCTGCCTCTGCACCTA
OPRD1	Opioid receptor, delta 1	NM_013622	F : GGGCTTCTGGGCAACGT R : TGGCGGTCTTCAATTTGGT
OPRK1	Opioid receptor, kappa 1	NM_011011	F: GGTGGGCTTAGTGGGCAAT R: TGGTTGCGGTCTTCATCTTC
P2RY1	Purinergic receptor P2Y	NM_008772	F: TGCGAGCACGGTTGGAT R: GGCATAAACCCTGTCGTTGAA
P2RY14	Purinergic receptor P2Y14 (GPR105)	NM_133200	F : CCTGCTGTCCTCCAGACACA R: AAGAGAGAATTCCAGACACATTGC
SSTR2	Somatostatin receptor 2	NM_009217	F: ACCCCAGCCCTGAAAGG R: CGCAGCTGTTGGCATAGGT

TGR5	G protein-coupled bile acid receptor 1	Nm_174985	F: TCCTGCCTCCTTCTCCACTT R: ATGCACCAGCAGCAGATTG
G Protein Coupled Receptors - CLASS B			
GCGR	Glucagon receptor	NM_008101	F: GGGTGGTGGTCAAGTGTCTGT R: CACCAGATTCCCATGTTGTCA
GIPR	Gastric inhibitory polypeptide receptor	NM_001080815	F : GCAGGGCAGCTGTGTCAGT R : TGGGCTTCAGTCCAAGTCAGT
GLP1R	GLP-1 receptor	NM_021332	F : CTTTCTTTCTCCGCCTTGGT R : GGTGCAGTGCAAGTGTCTGA
G Protein Coupled Receptors – CLASS C			
GPRC6A	G-Protein coupled receptor 6A	NM_153071	F: TCTGCCACGCCCTTAACTTT R: GGTCTGCCTGGTCTTGCA

APPENDIX C

Role of Syt7 in regulating islet function

Abstract

Vertebrates express at least 15 different synaptotagmins with the same domain structure but diverse localizations and tissue distributions. Synaptotagmin-1,-2, and -9 act as calcium sensors for the fast phrase of neurotransmitter release, and synaptotagmin-12 acts as a calcium-independent modulator of release. The exact functions of the remaining 11 synaptotagmins, however, have not been established. Analogous to the role of synaptotagmin-1, -2, and -9 in neurotransmission, these other synaptotagmins may serve as Ca^{2+} transducers regulating other Ca^{2+}-dependent membrane processes, such as insulin secretion in pancreatic β-cells. By qPCR, we determined the expression of synaptotagmins in the cells of mouse islet and found that synaptotagmin-7 is one of the most abundant in pancreatic β-cells. To determine whether synaptotagmin-7 regulates Ca^{2+}-dependent insulin secretion, we analyzed synaptotagmin-7 null mutant mice for glucose tolerance and insulin release. Here, we show that synaptotagmin-7 is required for the maintenance of systemic glucose tolerance and glucose-stimulated insulin secretion. The mutant mice have normal insulin sensitivity, insulin production, islet architecture, ultrastructural organization, and metabolic and calcium responses, but they exhibit impaired glucose-induced insulin secretion, indicating a calcium-sensing defect during insulin-containing secretory granule exocytosis. Taken together, our findings show that synaptotagmin-7 functions as a positive regulator of insulin secretion and may serve as a calcium sensor controlling insulin secretion in pancreatic β cells.

Introduction

The rising of intracellular [Ca^{2+}] is a critical step in signaling cascades that leads to the exocytosis of insulin-containing granules from the islet β cells. Many proteins including the SNARE complex and several synaptotagmins are involved in this vesicle trafficking pathway (Jahn and Sudhof 1999; Gao, Reavey-Cantwell et al. 2000; Gerber and Sudhof 2002; Iezzi, Kouri et al. 2004). Studies using genetically modified mice have shown that synaptotagmin-1,-2, and-9 are calcium sensors for the first phase of neuron transmitter release (Xu, Mashimo et al. 2007). However, the slow phase of the release remains intact, which suggests that other proteins are responsible for the releasing process in the absense of synaptotagmin-1,-2, and-9. Here, we determined the expression of all known synaptotagmins in the islets of the pancreas by qPCR. We found that synaptotagmin-7, a high affinity Ca^{2+} sensor is abundantly expressed in the islets. We also found that synaptotagmin-7 null mice have abnormal glucose tolerance and insulin secretion responses. In addition, islets from synaptotagmin-7 null mice exhibit impaired insulin secretion. These data suggest that synaptotagmin-7, a Ca^{2+}sensor, is a positive regulator of insulin secretion from the β-cells.

Materials and Methods

RNA measurement

RNA was isolated from tissue samples or cultured cells using RNA STAT-60 (Tel-Test Inc.) and 2 μg of total RNA was treated with RNase-free DNase (Roche). The RNA was then reverse-transcribed with random hexamers using SuperScript II (Invitrogen) as previously described in detail (Kurrasch, Huang et al. 2004).

with development and circadian rhythm in other organs, are likewise expressed in the adult mouse islet. This suggests that these, and perhaps additional, nuclear hormone receptors of this family play critical roles in islet function.

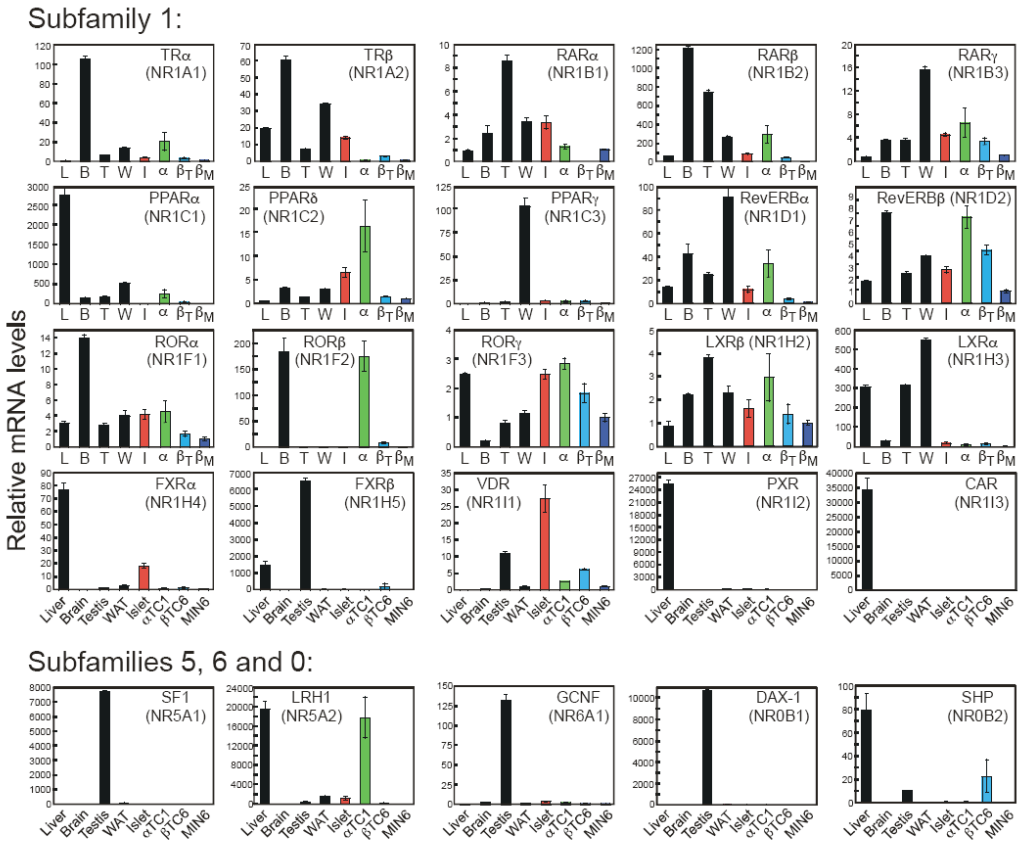

Fig. 2.1 Nuclear receptors expressed in the mouse endocrine pancreas: subfamilies 1, 5, 6 and 0. The relative mRNA levels are depicted for mouse liver (L), brain (B), testis (T) epididymal white adipose tissue (W, WAT), islets (I, red), alpha-cells (αTC1 cell line, green) and beta-cells (βTC6, light blue and MIN6, dark blue). All values are expressed relative to cyclophilin, and arithmetically adjusted to depict the lowest-expressing sample as a unit of 1. Values represent the means and SEM of three independent samples for each tissue or cell line, thus portraying biologic variance, and the results shown are representative of two independent studies. Note that as these data are portrayed, comparisons can only be made between different tissues for a single NHR, not between various receptors (see Figure 2.4 for this comparison).

Nuclear hormone receptor subfamily 2 (Fig. 2.2)

Quantitative real-time PCR (qPCR) was performed using an Applied Biosystem Prism 7900HT sequence detection system and SYBR-green chemistry (Kurrasch, Huang et al. 2004; Valasek and Repa 2005). Gene-specific primers were designed using Primer Express Software (PerkinElmer Life Sciences) and validated by analysis of template titration and dissociation curves. Primer sequences are provided in supplementary table Appendix C.2. 10 µl qPCR reactions contained 25 ng of reverse-transcribed RNA, 150 nM each of the primer and 5 µl of 2X SYBR Green PCR master mix (Applied Biosystems). Results of qPCR were evaluated by the comparative Ct method (user bulletin No.2, Perkin Elmer Life Sciences) using cyclophilin as the invariant control gene.

Synaptotagmin-7null mice

The synaptotagmin-7 mutant mice were generated on C57BL/6 background as described (Maximov, Lao et al. 2008). Synaptotagmin-7 heterozygous mice were used for breeding to generate homozygous mutant and littermate controls. All mice used in this study were bred and housed in our animal facility. All experiments involving animals were reviewed and approved by the University of Texas Southwestern Medical Center and A*STAR Institutional Animal Care and Use Committees.

Body composition measurement

Body compositions of age-matched 14- to 16-week-old synaptotagmin-7 mutant and control littermates were measured with an EchoMRI 100 (Echo Medical Systems) according to manufacturer's instructions. Briefly, unanesthetized mice were weighed first

before they were put in a mouse holder and inserted in MR analyzer. Readings of body fat mass and body lean mass were given within ≈1 min.

Glucose and Insulin Tolerance Test

For IPGTT, mice were fasted overnight (16-18 h) with free access to water, after which they were weighed and blood samples were collected to determine glucose and insulin levels. After glucose injection (2 mg/g of body weight), blood samples (4 μl per time point) were collected from the tail vein at 15, 30, 60, 90, and 120 min. Blood glucose concentrations were determined by using Accu-Check Advantage glucometer (Roche). Plasma for insulin measurement was obtained from ≈35 μl of blood collected from the tail vein at 8, 15, 30, and 60 min after the glucose challenge. Blood samples were mixed with 2 μl of 0.5 M EDTA on ice and centrifuged at 10,000 × *g* for 10 min. Plasma insulin concentrations were determined by using Ultrasensitive Mouse Insulin ELISA (Mercodia, detection range 0.025-6.4 μg/liter). For ITT, Actrapid (1 unit per kilogram of body weight) was given i.p., and blood glucose levels were determined before and at 15, 30, and 60 min after the injection.

Islets isolation and insulin secretion experiment

Islets were isolated by liberase digestion and cultured for 24 h in INS-1 medium with 11.1 mM glucose. Subsequent experimental handling was performed with Krebs-Ringer medium supplemented with 1 mg/ml BSA, 3 mM D-glucose, and 20 mM Hepes (pH 7.4). For analysis of islet secretory responses, similar-sized islets from a single mouse (5 islets

per dish) were first incubated at 37°C for 60 min in a flow chamber under continuous perifusion with KRH medium. They were then stimulated with 20 mM glucose for 40 min. Fractions of the medium were collected every 3 min, starting at 6 min before stimulation. Insulin concentration in each fraction was measured using mouse insulin ELISA kit (Mercodia, detection range 0.18-7.4 μg/liter).

Results

Expression of Synaptotagmins in the endocrine pancreas

To examine the relative expression of all synaptotagmins in the islets, qPCR was performed on samples from mouse islet, beta-cell lines (βTC6 and MIN6), and alpha-cell line (αTC1). In the islets, several of the synaptotagmins we examined are abundantly expressed (Fig Appx.C.1). The high expressors (Ct<25) include Syt2, Syt3, Syt4, Syt7, Syt9, Syt11, and Syt13. The medium expressors (25<Ct<30) are Syt1, Syt5, Syt6, and Syt12. The low expressors (Ct>30) are Syt8 and Syt10.

Synaptotagmin-7 is abundantly expressed in the islets (Ct=21.2). In the cell lines samples, α cell line (Ct=19.9) expresses higher level of synaptotagmin-7 than both β-cell lines (Ct=21.1 for βTC6 and 20.1 for MIN6, Fig Appx.C.1).

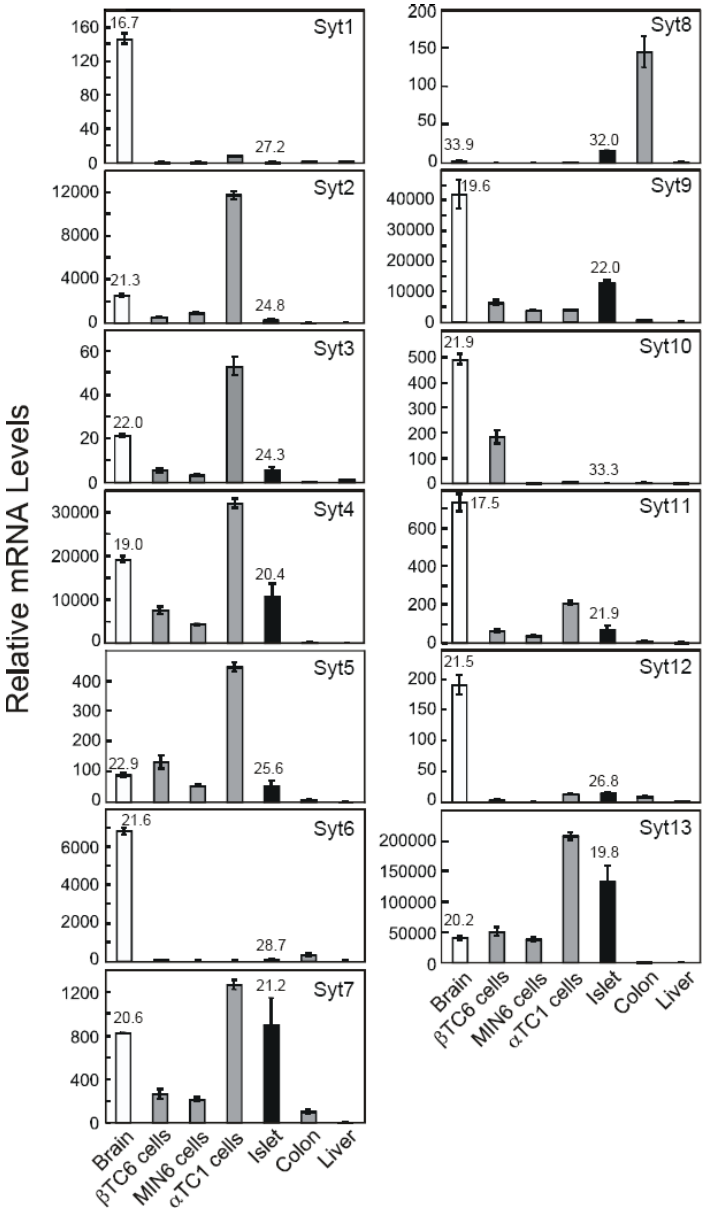

Fig. Appx.C.1. Expression profile of synaptotagmin mRNA in cells of the mouse endocrine pancreas. RNA was isolated from brain, islets and other tissues of male 129SvJ mice or from the insulinoma cell lines MIN6 or βTC-6, and the glucagonoma cell line, αTC1. Results of qPCR were evaluated using cyclophilin as the invariant control gene. Values depict the means and SEM of three independent samples, each analyzed in duplicate. The cycle number at threshold is provided for brain and islet samples to allow comparison of RNA abundance among the synaptotagmins for those two tissues.

Characterization of glucose homeostasis in Syt7-/- mice

To study the effects of synaptotagmin-7 deletion on systemic glucose homeostasis and insulin release *in vivo*, we performed i.p. glucose tolerance tests (IPGTT) on overnight-fasted synaptotagmin-7 null mice and their control littermates. An i.p. glucose challenge (2 g per kilogram of body weight) revealed an impaired glucose tolerance in male, but not female synaptotagmin-7 null mice. Females were less prone to insulin resistance and diabetes than males, possibly because of hormonal differences, which could render hormone-related phenotypes difficult to detect. Therefore, we focused our studies on male mice. In IPGTT, synaptotagmin-7 -/- mice showed delayed glucose clearance with glucose levels higher than control mice at 15, 30, and 60 min after injection (Fig Appx.C.2, panel A). Basal glucose levels were not different between fed or fasted synaptotagmin-7 -/- and control animals (Table Appx.C.1). Insulin concentrations were also measured during the glucose tolerance test. Synaptotagmin-7 null mice showed lower insulin levels at 8 and 30 min after glucose injection (Fig Appx.C.2, panel B). Insulin levels after overnight fasting were also lower in synaptotagmin-7 -/- mice but similar in fed animals (Table Appx.C.1).

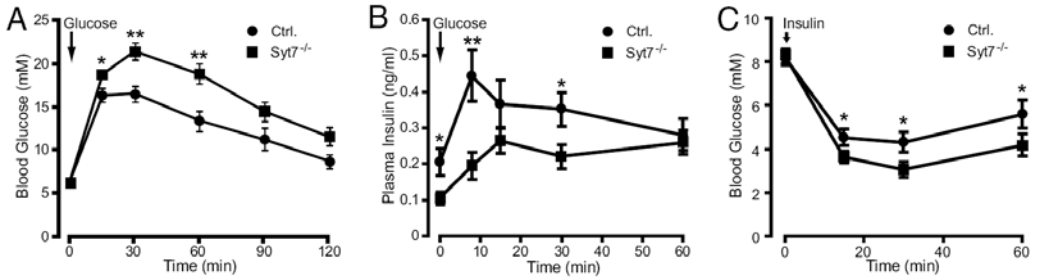

Fig. Appx. C. 2. Impaired glucose tolerance and insulin secretion, but normal insulin sensitivity in synaptotagmin-7 mutant mice. (*A*) An i.p. glucose tolerance test (IPGTT) was performed on overnight-fasted synaptotagmin-7 mutants and wild-type control mice. Blood glucose levels before and at 15, 30, 60, 90, and 120 min after glucose injection (2 mg per gram of body weight) were measured. Synaptotagmin-7 mutant ($Syt7^{-/-}$) mice (filled square, $n = 13$) exhibited glucose intolerance as evidenced by higher glucose concentration after injection and delayed clearance of glucose. $*$, $P < 0.02$, $**$, $P < 0.005$ vs. control (filled circle, $n = 17$). **(*B*)** Plasma insulin levels in control and synaptotagmin-7 mutant mice before and at 8, 15, 30, and 60 min of IPGTT were determined. Synaptotagmin-7 mutant mice showed insulin-secretory deficiency, especially in the first 15 min, upon glucose challenge. $n = 10$ for control (filled circle) and 11 for mutant (filled square). $*$, $P < 0.05$, $**$, $P < 0.005$. **(*C*)** Blood glucose levels were measured in 2-h-fasted control and mutant mice before and at 15, 30, and 60 min after injection of 1 unit/kg insulin. Synaptotagmin-7 mutant mice appeared to have higher insulin sensitivity than the wild-type controls. $*$, $P < 0.03$, $n = 17$.

Table Appx C.1 Physiological characterization of body composition, glucose and insulin levels, and ultrastructural analysis of $Syt7^{-/-}$ and control mice

	Control mice		$Syt7^{-/-}$ mice		
Characteristic	Mean ± SEM	No.	Mean ± SEM	No.	Statistics
Body weight, g	30 ± 0.5	41	27 ± 0.5	44	$P < 0.001$
Body fat, %	11.3 ± 0.7	9	7.6 ± 0.6	13	$P < 0.001$
Body lean, %	74.9 ± 0.7	9	78.3 ± 0.6	13	NS
Fasting glucose, mmol/liter	6.2 ± 0.4	13	6.2 ± 0.3	17	NS
Resting glucose, mmol/liter	8.3 ± 0.4	17	8.4 ± 0.3	17	NS
Fasting insulin, ng/ml	0.27 ± 0.07	14	0.16 ± 0.03	16	$P < 0.05$
Resting insulin, ng/ml	1.02 ± 0.16	12	0.74 ± 0.14	15	NS
Islet area (×1,000 μm^2)	16.6 ± 4.9	36	17.4 ± 2.8	26	NS
Cell number per 100 μm^2 of islet area	55 ± 3	23	53 ± 2	25	NS

NS, not significant.

Glucose induced insulin secretion is impaired in syt7-/- islets

To determine the time course of glucose-induced insulin secretion in control and synaptotagmin-7 -/- mice, we first incubated batches of isolated and cultured islets in 3 mM glucose for 60 min, then perifused in 3 mM glucose for an additional 30 min at 37°C before switching perifusion to 20 mM glucose. Perifusion medium was collected every 3 min starting from 6 min before stimulation (Fig Appx.C.3, panel A). There was no difference in insulin release between synaptotagmin-7 -/- and control mouse islets during the 6 min before the stimulation started. In control islets, elevation of glucose concentration from 3 to 20 mM caused ~10-fold enhancement of secretion, which showed two peaks: The first started at the 0- to 3-min interval and reached its maximum at 6–9 min, and the second occurred at 21–24 min. In synaptotagmin-7 -/- mouse islets, the insulin secretion curve had a similar biphasic pattern; however, the first phase of insulin release was significantly reduced, and the second phase was also impaired. Net insulin secretion by glucose stimulation was calculated as the sum of corresponding fractions after baseline subtraction. Total amount of net insulin secretion, which was the sum of all fractions over the entire stimulation period, was lower in islets from synaptotagmin-7 -/- mice than from controls (Fig Appx.C.3, panel B). Net insulin secretion during the first 15 min of stimulation, corresponding to the first phase, was reduced by >40% in synaptotagmin-7 null islets compared with controls.

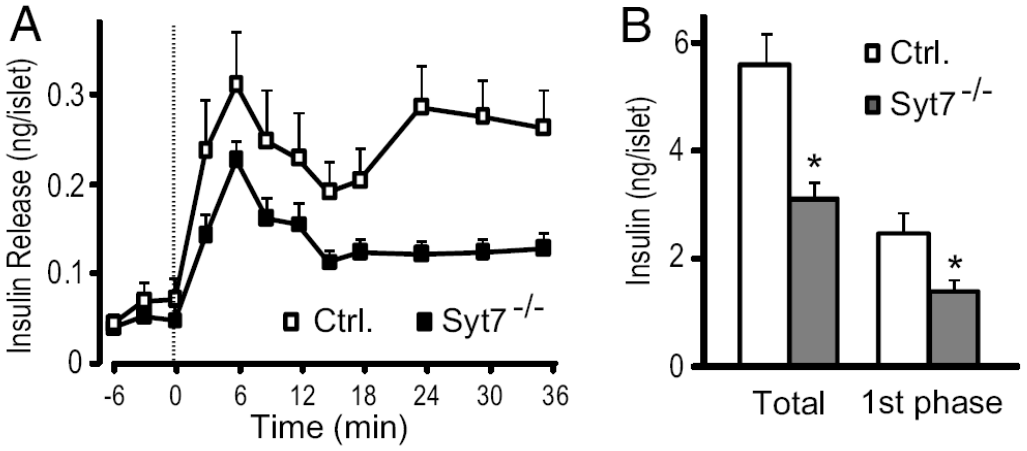

Fig. Appx. C.3. GSIS is reduced in islets isolated from synaptotagmin-7 null mice. (*A*) Glucose-induced insulin secretion from isolated islets was measured in perifusion experiments at a glucose concentration of 3 mM (basal) or 20 mM (stimulatory). The perfusate was collected in 3-min intervals, and insulin levels were determined by using ELISA. Synaptotagmin-7 mutant islets ($Syt7^{-/-}$, filled square) displayed impaired insulin secretion when compared with control (open square). **(*B*)** Glucose-induced insulin secretion for the entire stimulation period (Total) or the first phase (during the first 15 min after stimulation) in the perifusion experiments was lower in isolated islets from mutant (gray bar) than from control (white bar). Insulin secretion was calculated by integrating the area under each curve in *A* after baseline subtraction. Data are presented as mean ± SEM. $n = 9$ for mutant and 10 for control. $* P < 0.05$.

Discussion

In this study, we showed that several synaptotagmins including synaptotagmin-7 are abundantly expressed in the endocrine pancreas. We also characterized glucose homeostasis in the synaptotagmin-7 null mice and showed that they have reduced insulin secretion and consequent glucose intolerance. The impairment of insulin secretion can be pinpointed to the failure of synaptotagmin-7 -/- islets to respond to glucose elevation demonstrated by GSIS experiments using isolated islets. The morphological characteristics of synaptotagmin-7 -/- islets in the pancreas appear to be normal and the

level of insulin mRNA and protein are not different from that of wild type islets (data not shown). These data suggested that the impairment of insulin secretion is likely caused by a defect in the Ca^{2+} sensing due to the loss of synaptotagmin-7 as a calcium sensor in the β-cells of islet.

In the islets, synaptotagmin-7 is not only expressed in the β-cells but appears to be also present in the α-cells (Figure Appx.C.1). As compared to what is known about insulin secretion from β-cells, the molecular mechanisms involved in the glucagon secretion from α cells are less understood (Gromada, Franklin et al. 2007). However, the release of glucagon- containing granules is also Ca^{2+} dependent. In addition, synaptotagmin 5, another member of the synaptotagmin family localizes to glucagon containing vesicles in the α-cells and is involved in the regulation of glucagon exocytosis (Saegusa, Fukuda et al. 2002). Based on what we have learned about synaptotagmins in the β-cells, it is tempting to speculate that synaptotagmin-7 may also participate in the regulation of glucagon secretion from α-cells.

Table Appx C.2. qRT PCR primer sequences for measurement of mouse synaptotagmin RNA levels

symbol	Gene name	Accession no.	Primer sequence 5'-3'	
mSyt1	*Synaptotagmin I*	NM_009306	QF	CAAAAGTCCACCGGAAAACC
			QR	TTGCCACCTAATTCCGAGTATG
mSyt2	*Synaptotagmin II*	NM_009307	QF	GGCGGCGAGATGTGATACT
			QR	GGGTGTCTATGATGGCATCAA
mSyt3	*Synaptotagmin III*	NM_016663	QF	CGAACTGCGGATCAGAGGAT
			QR	GGACGATGCCACAGAATGTC

mSyt4	*Synaptotagmin IV*	NM_009308	QF	TGAATCTGCCCGGAGTTCTT
			QR	TGGTGATAGGAGCCATGTTTTC
mSyt5	*Synaptotagmin V*	NM_021889	QF	CCTTTGGAAGGATATCGAGTATGTC
			QR	TGGAAGATAGCAGAGTGAAAACATAA
mSyt6	*Synaptotagmin VI*	NM_018800	QF	CAAGTGTCGAAATCTCAAAGCAAT
			QR	CAGCCTCCGTCCATCACA
mSyt7	*Synaptotagmin VII*	NM_018801	QF	ACCTCGTCAACTCCCTTACCA
			QR	GGGCCTCATCCTCCTCAGA
mSyt8	*Synaptotagmin VIII*	NM_018802	QF	CCTCCAAGAAAGGCACGACTA
			QR	GCTGGCTAACGGGAACCA
mSyt9	*Synaptotagmin IX*	NM_016908	QF	CCCTGAATCCACACTTTGGA
			QR	CAGCACTCTGCCCCCTAGTT
mSyt10	*Synaptotagmin IX*	NM_018803	QF	GCAAACAACCGAGCCTACGT
			QR	GACATTCATTTGCCTTGGTAGGT
mSyt11	*Synaptotagmin XI*	NM_018804	QF	GACACTTGCCGAAGATGGATATC
			QR	TGCGTTTTCTGCCGTAGTAGA
mSyt12	*Synaptotagmin XII*	NM_134164	QF	GTGGTGAAAGCCAAGAATCTCAT
			QR	TCCCATCCTGCAGCAGGTAT
mSyt13	*Synaptotagmin XIII*	NM_030725	QF	CTCCTTAAGTTCCCGGACATCT
			QR	AGGTGTAGTCTGCGTAGTTGATGAC
mCyclo	*Cyclophilin*	NM_011149	QF	TGGAGAGCACCAAGACAGACA
			QR	TGCCGGAGTCGACAATGAT

BIBLIOGRAPHY

(2008). "Economic costs of diabetes in the U.S. In 2007." Diabetes Care **31**(3): 596-615.

Ahren, B. (2000). "Autonomic regulation of islet hormone secretion--implications for health and disease." Diabetologia **43**(4): 393-410.

Allenby, G., M. T. Bocquel, et al. (1993). "Retinoic acid receptors and retinoid X receptors: interactions with endogenous retinoic acids." Proc Natl Acad Sci U S A **90**(1): 30-4.

Amacker-Francoys, I., S. Mohanty, et al. (2005). "The metabolisable hexoses D-glucose and D-mannose enhance the expression of IRS-2 but not of IRS-1 in pancreatic β-cells." Experimental and Clinical Endocrinology of Diabetes **113**: 423-429.

Ashcroft, F. M., P. Proks, et al. (1994). "Stimulus-secretion coupling in pancreatic beta cells." J Cell Biochem **55 Suppl**: 54-65.

Bailey, C. J. and H. Ahmed-Sorour (1980). "Role of ovarian hormones in the long-term control of glucose homeostasis. Effects of insulin secretion." Diabetologia **19**(5): 475-81.

Barish, G. D., M. Downes, et al. (2005). "A nuclear receptor atlas: macrophage activation." Molecular Endocrinology **19**: 2466-2477.

Barish, G. D., V. A. Narkar, et al. (2006). "PPAR delta: a dagger in the heart of the metabolic syndrome." J Clin Invest **116**(3): 590-7.

Barseghian, G. and R. Levine (1980). "Effect of corticosterone on insulin and glucagon secretion by the isolated perfused rat pancreas." Endocrinology **106**(2): 547-52.

Becker-Andre, M., E. Andre, et al. (1993). "Identification of nuclear receptor mRNAs by RT-PCR amplification of conserved zinc-finger motif sequences." Biochemical & Biophysical Research Communications **194**(3): 1371-1379.

Benoit, G., A. Cooney, et al. (2007). "International Union of Pharmacology. LXVI. Orphan nuclear receptors." Pharmacological Reviews **58**: 798-836.

Bihan, H., C. Rouault, et al. (2005). "Pancreatic islet response to hyperglycemia is dependent on peroxisome proliferator-activated receptor alpha (PPARα)." FEBS Letters **579**: 2284-2288.

Bono, H., K. Yagi, et al. (2007). "Systematic expression profiling of the mouse transcriptome using RIKEN cDNA microarrays." Genome Research **13**: 1318-1323.

Bookout, A. L., Y. Jeong, et al. (2006). "Anatomical profiling of nuclear receptor expression reveals a hierarchical transcriptional network." Cell **126**: 789-799.

Bourlon, P.-M., B. Billaudel, et al. (1999). "Influence of vitamin D deficiency and 1,25 dihydroxyvitamin D_3 on *de novo* insulin biosynthesis in the islets of the rat endocrine pancreas." Journal of Endocrinology **160**: 87-95.

Briancon, N. and M. C. Weiss (2006). "*In vivo* role of the HNF4α AF-1 activation domain revealed by exon swapping." EMBO Journal **25**: 1253-1262.

Brown, A. J., S. M. Goldsworthy, et al. (2003). "The Orphan G protein-coupled receptors GPR41 and GPR43 are activated by propionate and other short chain carboxylic acids." J Biol Chem **278**(13): 11312-9.

Brunham, L. R., J. K. Kruit, et al. (2008). "Cholesterol in islet dysfunction and type 2 diabetes." J Clin Invest **118**(2): 403-8.

Buckingham, R. E., K. A. Al-Barazanji, et al. (1998). "Peroxisome proliferator-activated receptor-gamma agonist, rosiglitazone, protects against nephropathy and pancreatic islet abnormalities in Zucker fatty rats." Diabetes **47**(8): 1326-34.

Cabrera, O., D. M. Berman, et al. (2006). "The unique cytoarchitecture of human pancreatic islets has implications for islet cell function." Proc Natl Acad Sci U S A **103**(7): 2334-9.

Cao, G., Y. Liang, et al. (2002). "Antidiabetic action of a liver X receptor agonist mediated by inhibition of hepatic gluconeogenesis." Journal of Biological Chemistry **278**: 1131-1136.

Cao, G., Y. Liang, et al. (2003). "Antidiabetic action of a liver x receptor agonist mediated by inhibition of hepatic gluconeogenesis." J Biol Chem **278**(2): 1131-6.

Cha, J. Y. and J. J. Repa (2007). "The liver X receptor (LXR) and hepatic lipogenesis. The carbohydrate-response element-binding protein is a target gene of LXR." J Biol Chem **282**(1): 743-51.

Chang, T. J., H. H. Lei, et al. (2000). "Vitamin D receptor gene polymorphisms influence susceptibility to type 1 diabetes mellitus in the Taiwanese population." Clin Endocrinol (Oxf) **52**(5): 575-80.

Chawla, A., J. J. Repa, et al. (2001). "Nuclear receptors and lipid physiology: opening the X-files." Science **294**: 1866-1870.

Chertow, B. S., W. S. Blaner, et al. (1987). "Effects of vitamin A deficiency and repletion on rat insulin secretion in vivo and in vitro from isolated islets." J Clin Invest **79**(1): 163-9.

Chertow, B. S., N. Q. Goking, et al. (1997). "Effects of all-trans-retinoic acid (ATRA) and retinoic acid receptor (RAR) expression on secretion, growth, and apoptosis of insulin-secreting RINm5F cells." Pancreas **15**(2): 122-31.

Choi, M. Y., A. I. Romer, et al. (2006). "A dynamic expression survey identifies transcription factors relevant in mouse digestive tract development." Development **133**: 1-11.

Clark, A. R., M. E. Wilson, et al. (1995). "Identification and characterization of a functional retinoic acid/thyroid hormone-response element upstream of the human insulin gene enhancer." Biochem J **309 (Pt 3)**: 863-70.

Clark, S. A., W. E. Stumpf, et al. (1987). "1,25-Dihydroxyvitamin D3 target cells in immature pancreatic islets." Am J Physiol **253**(1 Pt 1): E99-105.

Costrini, N. V. and R. K. Kalkhoff (1971). "Relative effects of pregnancy, estradiol, and progesterone on plasma insulin and pancreatic islet insulin secretion." J Clin Invest **50**(5): 992-9.

da Silva Xavier, G., G. A. Rutter, et al. (2006). "ChREBP binding to fatty acid synthase and L-type pyruvate kinase genes is stimulated by glucose in pancreatic β-cells." Journal of Lipid Research **47**: 2482-2491.

Dalen, K. T., S. M. Ulven, et al. (2003). "Expression of the insulin-responsive glucose transporter GLUT4 in adipocytes is dependent on liver X receptor alpha." J Biol Chem **278**(48): 48283-91.

Date, Y., M. Nakazato, et al. (2002). "Ghrelin is present in pancreatic alpha-cells of humans and rats and stimulates insulin secretion." Diabetes **51**(1): 124-9.

de Wet, J. R., K. V. Wood, et al. (1987). "Firefly luciferase gene: structure and expression in mammalian cells." Mol Cell Biol **7**(2): 725-37.

Dentin, R., F. Benhamed, et al. (2005). "Polyunsaturated fatty acids suppress glycolytic and lipogenic genes through the inhibition of ChREBP nuclear protein translocation." Journal of Clinical Investigation **115**: 2843-2854.

Dhe-Paganon, S., K. Duda, et al. (2002). "Crystal structure of the HNF4 alpha ligand binding domain in complex with endogenous fatty acid ligand." J Biol Chem **277**(41): 37973-6.

Drewes, T., S. Senkel, et al. (1996). "Human hepatocyte nuclear factor 4 isoforms are encoded by distinct and differentially expressed genes." Mol Cell Biol **16**(3): 925-31.

Driscoll, H. K., C. D. Adkins, et al. (1997). "Vitamin A stimulation of insulin secretion: effects on transglutaminase mRNA and activity using rat islets and insulin-secreting cells." Pancreas **15**(1): 69-77.

Dukes, I. D., S. Sreenan, et al. (1998). "Defective pancreatic β-cell glycolytic signaling in hepatocyte nuclear factor-1α-deficient mice." Journal of Biological Chemistry **273**: 24457-24464.

Dvorak, C. M. T., M. Hardstedt, et al. (2007). "Transcriptional profiling of stress response in cultured porcine islets." Biochemical and Biophysical Research Communications **357**: 118-125.

Eckhoff, D. E., C. A. Smyth, et al. (2003). "Suppression of the c-Jun N-terminal kinase pathway by 17beta-estradiol can preserve human islet functional mass from proinflammatory cytokine-induced destruction." Surgery **134**(2): 169-79.

Efanov, A. M., S. Sewing, et al. (2004). "Liver X receptor activation stimulates insulin secretion via modulation of glucose and lipid metabolism in pancreatic β-cells." Diabetes **53**: S75-S78.

Efanov, A. M., S. Sewing, et al. (2004). "Liver X receptor activation stimulates insulin secretion via modulation of glucose and lipid metabolism in pancreatic beta-cells." Diabetes **53 Suppl 3**: S75-8.

El Seifi, S., I. C. Green, et al. (1981). "Insulin release and steroid-hormone binding in isolated islets of langerhans in the rat: effects of ovariectomy." J Endocrinol **90**(1): 59-67.

Elayat, A. A., M. M. el-Naggar, et al. (1995). "An immunocytochemical and morphometric study of the rat pancreatic islets." J Anat **186 (Pt 3)**: 629-37.

Engelking, L. R., C. A. Dasher, et al. (1980). "Within-day fluctuations in serum bile-acid concentrations among normal control subjects and patients with hepatic disease." Am J Clin Pathol **73**(2): 196-201.

Evans, R. M. (1988). "The steroid and thyroid hormone receptor superfamily." Science **240**(4854): 889-95.

Everson, G. T. (1987). "Steady-state kinetics of serum bile acids in healthy human subjects: single and dual isotope techniques using stable isotopes and mass spectrometry." J Lipid Res **28**(3): 238-52.

Fajans, S. S., J. C. Floyd, Jr., et al. (1967). "Effect of amino acids and proteins on insulin secretion in man." Recent Prog Horm Res **23**: 617-62.

Fayard, E., K. Schoonjans, et al. (2003). "Liver receptor homolog 1 controls the expression of carboxyl ester lipase." Journal of Biological Chemistry **278**: 35725-35731.

Franke, A., J. Hampe, et al. (2007). "Systematic association mapping identifies NELL1 as a novel IBD disease gene." PLoS ONE **2**(1): e691.

Freeman, K., P. Tsui, et al. (2001). "Cloning, pharmacology, and tissue distribution of G-protein-coupled receptor GPR105 (KIAA0001) rodent orthologs." Genomics **78**(3): 124-8.

Fu, M., T. Sun, et al. (2005). "A nuclear receptor atlas: 3T3-L1 adipogenesis." Molecular Endocrinology **19**: 2437-2450.

Fujiwara, K., F. Maekawa, et al. (2005). "Oleic acid interacts with GPR40 to induce Ca2+ signaling in rat islet beta-cells: mediation by PLC and L-type Ca2+ channel and link to insulin release." Am J Physiol Endocrinol Metab **289**(4): E670-7.

Fukuchi, M., M. Shimabukuro, et al. (2002). "Evidence for a deficient pancreatic beta-cell response in a rat model of hyperthyroidism." Life Sci **71**(9): 1059-70.

Furuyama, T., K. Kitayama, et al. (2003). "Forkhead transcription factor FOX01 (FKHR)-dependent induction of PDK4 gene expression in skeletal muscle during energy deprivation." Biochemical Journal **375**: 365-371.

Gao, Z., J. Reavey-Cantwell, et al. (2000). "Synaptotagmin III/VII isoforms mediate Ca2+-induced insulin secretion in pancreatic islet beta -cells." J Biol Chem **275**(46): 36079-85.

Geisler, J. G., W. Zawalich, et al. (2002). "Estrogen can prevent or reverse obesity and diabetes in mice expressing human islet amyloid polypeptide." Diabetes **51**(7): 2158-69.

Gerber, S. H. and T. C. Sudhof (2002). "Molecular determinants of regulated exocytosis." Diabetes **51 Suppl 1**: S3-11.

Gerdin, A. K., V. V. Surve, et al. (2006). "Phenotypic screening of hepatocyte nuclear factor (HNF) 4-gamma receptor knockout mice." Biochem Biophys Res Commun **349**(2): 825-32.

Gerin, I., V. W. Dolinsky, et al. (2005). "LXRβ is required for adipocyte growth, glucose homeostasis and β cell function." Journal of Biological Chemistry **280**: 23024-23031.

Gerin, I., V. W. Dolinsky, et al. (2005). "LXRbeta is required for adipocyte growth, glucose homeostasis, and beta cell function." J Biol Chem **280**(24): 23024-31.

Germain, P., B. Staels, et al. (2006). "Overview of nomenclature of nuclear receptors." Pharmacological Reviews **58**: 685-704.

Goodman, P. A., O. Medina-Martinez, et al. (1996). "Identification of the human insulin negative regulatory element as a negative glucocorticoid response element." Mol Cell Endocrinol **120**(2): 139-46.

Gorski, J., D. Toft, et al. (1968). "Hormone receptors: studies on the interaction of estrogen with the uterus." Recent Prog Horm Res **24**: 45-80.

Green, S. and W. Wahli (1994). "Peroxisome proliferator-activated receptors: finding the orphan a home." Mol Cell Endocrinol **100**(1-2): 149-53.

Grimaldi, P. A. (2005). "Regulatory role of peroxisome proliferator-activated receptor delta (PPAR delta) in muscle metabolism. A new target for metabolic syndrome treatment?" Biochimie **87**(1): 5-8.

Gromada, J., I. Franklin, et al. (2007). "Alpha-cells of the endocrine pancreas: 35 years of research but the enigma remains." Endocr Rev **28**(1): 84-116.

Gu, G., J. M. Wells, et al. (2004). "Global expression analysis of gene regulatory pathways during endocrine pancreatic development." Development **131**: 165-179.

Guha, M., M. Deng, et al. (2006). "Abstract 3921: KD3010, a PPAR{beta}/{delta} Selective Small Molecule Agonist, Improves Hyperglycemia And Insulin Resistance while alleviating Rosiglitazone-

Induced Side Effects in Murine Models." Circulation **114**(18_MeetingAbstracts): II_843-a-.

Gupta, R. K., M. Z. Vatamaniuk, et al. (2005). "The MODY1 gene *HNF-4α* regulates selected genes involved in insulin secretion." Journal of Clinical Investigation **115**: 1006-1015.

Haataja, L., T. Gurlo, et al. (2008). "Islet amyloid in type 2 diabetes, and the toxic oligomer hypothesis." Endocr Rev **29**(3): 303-16.

Hauge-Evans, A. C., C. C. Richardson, et al. (2006). "A role for kisspeptin in islet function." Diabetologia **49**(9): 2131-5.

Heine, P. A., J. A. Taylor, et al. (2000). "Increased adipose tissue in male and female estrogen receptor-alpha knockout mice." Proc Natl Acad Sci U S A **97**(23): 12729-34.

Helleboid-Chapman, A., S. Helleboid, et al. (2006). "Glucose regulates LXRalpha subcellular localization and function in rat pancreatic beta-cells." Cell Res **16**(7): 661-70.

Herchuelz, A., P. Lebrun, et al. (1984). "Mechanism of arginine-stimulated Ca^{2+} influx into pancreatic B cell." American Journal of Physiology **246**: E38-E43.

Hirasawa, A., K. Tsumaya, et al. (2005). "Free fatty acids regulate gut incretin glucagon-like peptide-1 secretion through GPR120." Nat Med **11**(1): 90-4.

Hjelte, L., B. Ahren, et al. (1990). "Pancreatic function in the essential fatty acid deficient rat." Metabolism **39**(8): 871-5.

Ho, K. J. (1976). "Circadian distribution of bile acid in the enterohepatic circulatory system in hamsters." J Lipid Res **17**(6): 600-4.

Hohmeier, H. E., H. Mulder, et al. (2000). "Isolation of INS-1-derived cell lines with robust ATP-sensitive K^+ channel-dependent and -independent glucose-stimulated insulin secretion." Diabetes **49**: 424-430.

Hohmeier, H. E. and C. B. Newgard (2004). "Cell lines derived from pancreatic islets." Molecular and Cellular Endocrinology **228**: 121-128.

Holland, A. M., L. J. Gonez, et al. (2005). "Conditional expression demonstrates the role of the homeodomain transcription factor Pdx1 in maintenance and regeneration of β-cells in the adult pancreas." Diabetes **54**: 2586-2595.

Hopkins, A. L. and C. R. Groom (2002). "The druggable genome." Nat Rev Drug Discov **1**(9): 727-30.

Howell, S. L., M. Tyhurst, et al. (1977). "Direct effects of progesterone on rat islets of Langerhans in vivo and in tissue culture." Diabetologia **13**(6): 579-83.

Huang, B., P. Wu, et al. (2002). "Regulation of pyruvate dehydrogenase kinase expression by peroxisome proliferator-activated receptor-α ligands, glucocorticoids, and insulin." Diabetes **51**: 276-283.

Iezzi, M., G. Kouri, et al. (2004). "Synaptotagmin V and IX isoforms control Ca2+ -dependent insulin exocytosis." J Cell Sci **117**(Pt 15): 3119-27.

Iizuka, K., R. K. Bruick, et al. (2004). "Deficiency of carbohydrate response element-binding protein (ChREBP) reduces lipogenesis as well as glycolysis." Proceedings of the National Academy of Sciences USA **101**: 7281-7286.

Iizuka, K., B. Miller, et al. (2006). "Deficiency of carbohydrate-activated transcription factor ChREBP prevents obesity and improves plasma glucose control in leptin-deficient (*ob/ob*) mice." American Journal of Physiology **291**: E358-E364.

Inagaki, T., P. Dutchak, et al. (2007). "Endocrine regulation of the fasting response by PPARα-mediated induction of fibroblast growth factor 21." Cell Metabolism **5**: 415-425.

Ishii, S., K. Iizuka, et al. (2004). "Carbohydrate response element binding protein directly promotes lipogenic enzyme gene transcription." Proceedings of the National Academy of Sciences USA **101**: 15597-15602.

Issemann, I. and S. Green (1990). "Activation of a member of the steroid hormone receptor superfamily by peroxisome proliferators." Nature **347**(6294): 645-50.

Issemann, I., R. A. Prince, et al. (1993). "The peroxisome proliferator-activated receptor:retinoid X receptor heterodimer is activated by fatty acids and fibrate hypolipidaemic drugs." J Mol Endocrinol **11**(1): 37-47.

Jahn, R. and T. C. Sudhof (1999). "Membrane fusion and exocytosis." Annu Rev Biochem **68**: 863-911.

Janowski, B. A., P. J. Willy, et al. (1996). "An oxysterol signalling pathway mediated by the nuclear receptor LXR alpha." Nature **383**(6602): 728-31.

Jensen, E. V. (2004). "From chemical warfare to breast cancer management." Nat Med **10**(10): 1018-21.

Jensen, E. V. and E. R. DeSombre (1973). "Estrogen-receptor interaction." Science **182**(108): 126-34.

Jiang, G. and F. M. Sladek (1997). "The DNA binding domain of hepatocyte nuclear factor 4 mediates cooperative, specific binding to DNA and heterodimerization with the retinoid X receptor alpha." J Biol Chem **272**(2): 1218-25.

Johnson, J. A., J. P. Grande, et al. (1994). "Immunohistochemical localization of the 1,25(OH)2D3 receptor and calbindin D28k in human and rat pancreas." Am J Physiol **267**(3 Pt 1): E356-60.

Jordan, H. N. and R. W. Phillips (1978). "Effect of fatty acids on isolated ovine pancreatic islets." Am J Physiol **234**(2): E162-7.

Kadison, A., J. Kim, et al. (2001). "Retinoid signaling directs secondary lineage selection in pancreatic organogenesis." J Pediatr Surg **36**(8): 1150-6.

Kameda, N., S. Okuya, et al. (2000). "[Rosiglitazone (BRL-49653)]." Nippon Rinsho **58**(2): 401-4.

Katsuma, S., A. Hirasawa, et al. (2005). "Bile acids promote glucagon-like peptide-1 secretion through TGR5 in a murine enteroendocrine cell line STC-1." Biochem Biophys Res Commun **329**(1): 386-90.

Kawaguchi, T., M. Takenoshita, et al. (2001). "Glucose and cAMP regulate the L-type pyruvate kinase gene by phosphorylation/dephosphorylation of the carbohydrate response element binding protein." Proceedings of the National Academy of Sciences USA **98**: 13710-13715.

Kawamata, Y., R. Fujii, et al. (2003). "A G protein-coupled receptor responsive to bile acids." J Biol Chem **278**(11): 9435-40.

Kimple, M. E., A. B. Nixon, et al. (2005). "A role for G(z) in pancreatic islet beta-cell biology." J Biol Chem **280**(36): 31708-13.

Kliewer, S. A., J. M. Lehmann, et al. (1999). "Orphan nuclear receptors: shifting endocrinology into reverse." Science **284**(5415): 757-60.

Kliewer, S. A., J. M. Lenhard, et al. (1995). "A prostaglandin J2 metabolite binds peroxisome proliferator-activated receptor gamma and promotes adipocyte differentiation." Cell **83**(5): 813-9.

Kong, Y. M., R. J. MacDonald, et al. (2006). "A comprehensive survey of DNA-binding transcription factor gene expression in human fetal and adult organs." Gene Expression Patterns **6**: 678-686.

Kurokawa, R., V. C. Yu, et al. (1993). "Differential orientations of the DNA-binding domain and carboxy-terminal dimerization interface regulate binding site selection by nuclear receptor heterodimers." Genes Dev **7**(7B): 1423-35.

Kurrasch, D. M., J. Huang, et al. (2004). "Quantitative real-time polymerase chain reaction measurement of regulators of G-protein signaling mRNA levels in mouse tissues." Methods Enzymol **389**: 3-15.

Kurrasch, D. M., J. Huang, et al. (2004). "Quantitative real-time polymerase chain reaction measurement of regulators of G-protein signaling mRNA levels in mouse tissues." Methods in Enzymology **389**: 3-15.

Kwon, H.-S. and R. A. Harris (2004). "Mechanisms responsible for regulation of pyruvate dehydrogenase kinase 4 gene expression." Advances in Enzyme Regulation **44**: 109-121.

Labriji-Mestaghanmi, H., B. Billaudel, et al. (1988). "Vitamin D and pancreatic islet function. I. Time course for changes in insulin secretion and content during vitamin D deprivation and repletion." J Endocrinol Invest **11**(8): 577-84.

Laffitte, B. A., L. C. Chao, et al. (2003). "Activation of liver X receptor improves glucose tolerance through coordinate regulation of glucose metabolism in liver and adipose tissue." Proc Natl Acad Sci U S A **100**(9): 5419-24.

Laffitte, B. A., L. C. Chao, et al. (2003). "Activation of liver X receptor improves glucose tolerance through coordinate regulation of glucose metabolism in liver and adipose tissue." Proceedings of the National Academy of Sciences USA **100**: 5419-5424.

Lauckner, J. E., J. B. Jensen, et al. (2008). "GPR55 is a cannabinoid receptor that increases intracellular calcium and inhibits M current." Proc Natl Acad Sci U S A **105**(7): 2699-704.

Laudet, V., C. Hanni, et al. (1992). "Evolution of the nuclear receptor gene superfamily." EMBO J **11**(3): 1003-13.

Lee, C. H., P. Olson, et al. (2006). "PPARdelta regulates glucose metabolism and insulin sensitivity." Proc Natl Acad Sci U S A **103**(9): 3444-9.

Lee, S., S. A. Clark, et al. (1994). "1,25-Dihydroxyvitamin D3 and pancreatic beta-cell function: vitamin D receptors, gene expression, and insulin secretion." Endocrinology **134**(4): 1602-10.

Lehmann, J. M., L. B. Moore, et al. (1995). "An antidiabetic thiazolidinedione is a high affinity ligand for peroxisome proliferator-activated receptor γ (PPARγ)." Journal of Biological Chemistry **270**: 12953-12956.

Lehmann, J. M., L. B. Moore, et al. (1995). "An antidiabetic thiazolidinedione is a high affinity ligand for peroxisome proliferator-activated receptor gamma (PPAR gamma)." J Biol Chem **270**(22): 12953-6.

Lembert, N., H. C. Joos, et al. (2001). "Methyl pyruvate initiates membrane depolarization and insulin release by metabolic factors other than ATP." Biochemical Journal **354**: 345-350.

Lenhard, J. M., M. E. Lancaster, et al. (1999). "The RXR agonist LG100268 causes hepatomegaly, improves glycaemic control and decreases cardiovascular risk and cachexia in diabetic mice suffering from pancreatic beta-cell dysfunction." Diabetologia **42**(5): 545-54.

Leon, C., B. Hechler, et al. (1997). "The P2Y1 receptor is an ADP receptor antagonized by ATP and expressed in platelets and megakaryoblastic cells." FEBS Lett **403**(1): 26-30.

Liang, Y. and F. M. Matschinsky (1994). "Mechanisms of action of nonglucose insulin secretagogues." Annu Rev Nutr **14**: 59-81.

Liang, Y. and F. M. Matschinsky (1994). "Mechanisms of action of nonglucose insulin secretagogues." Annual Reviews in Nutrition **14**: 59-81.

Lima, J. J., H. Feng, et al. (2007). "Association analyses of adrenergic receptor polymorphisms with obesity and metabolic alterations." Metabolism **56**(6): 757-65.

Luckow, B. and G. Schutz (1987). "CAT constructions with multiple unique restriction sites for the functional analysis of eukaryotic promoters and regulatory elements." Nucleic Acids Res **15**(13): 5490.

Makishima, M., A. Y. Okamoto, et al. (1999). "Identification of a nuclear receptor for bile acids." Science **284**(5418): 1362-5.

Mangelsdorf, D. J., C. Thummel, et al. (1995). "The nuclear receptor superfamily: the second decade." Cell **83**(6): 835-9.

Martinez, S. C., C. Cras-Meneur, et al. (2006). "Glucose regulates Foxo1 through insulin receptor signaling in the pancreatic islet β-cell." Diabetes **55**: 1581-1591.

Maruyama, T., Y. Miyamoto, et al. (2002). "Identification of membrane-type receptor for bile acids (M-BAR)." Biochem Biophys Res Commun **298**(5): 714-9.

Matthews, K. A., W. B. Rhoten, et al. (2004). "Vitamin A deficiency impairs fetal islet development and causes subsequent glucose intolerance in adult rats." J Nutr **134**(8): 1958-63.

Maximov, A., Y. Lao, et al. (2008). "Genetic analysis of synaptotagmin-7 function in synaptic vesicle exocytosis." Proc Natl Acad Sci U S A **105**(10): 3986-91.

Minn, A. H., C. Hafele, et al. (2005). "Thioredoxin-interacting protein is stimulated by glucose through a carbohydrate response element and induces β-cell apoptosis." Endocrinology **146**: 2397-2405.

Mitro, N., P. A. Mak, et al. (2007). "The nuclear receptor LXR is a glucose sensor." Nature **445**: 219-223.

Miura, A., K. Yamagata, et al. (2006). "Hepatocyte nuclear factor-4α is essential for glucose-stimulated insulin secretion by pancreatic β-cells." Journal of Biological Chemistry **281**: 5246-5257.

Miura, A., K. Yamagata, et al. (2006). "Hepatocyte nuclear factor-4alpha is essential for glucose-stimulated insulin secretion by pancreatic beta-cells." J Biol Chem **281**(8): 5246-57.

Miyazaki, J., K. Araki, et al. (1990). "Establishment of a pancreatic beta cell line that retains glucose-inducible insulin secretion: special reference to expression of glucose transporter isoforms." Endocrinology **127**: 126-132.

Mukherjee, R., P. J. A. Davies, et al. (1997). "Sensitization of diabetic and obese mice to insulin by retinoid X receptor agonists." Nature **386**: 407-410.

Nakajima, H., I. Yoshiuchi, et al. (1996). "Hepatocyte nuclear factor-4 alpha gene mutations in Japanese non-insulin dependent diabetes mellitus (NIDDM) patients." Res Commun Mol Pathol Pharmacol **94**(3): 327-30.

Nakhei, H., A. Lingott, et al. (1998). "An alternative splice variant of the tissue specific transcription factor HNF4alpha predominates in undifferentiated murine cell types." Nucleic Acids Res **26**(2): 497-504.

Narushima, M., N. Kobayashi, et al. (2005). "A human β-cell line for transplantation therapy to control type 1 diabetes." Nature Biotechnology **23**: 1274-1282.

Nuclear Receptors Nomenclature Committee (1999). "A unified nomenclature system for the nuclear receptor superfamily." Cell **97**: 161-163.

Odom, D. T., N. Zizlsperger, et al. (2004). "Control of pancreas and liver gene expression by HNF transcription factors." Science **303**(5662): 1378-81.

Otte, K., H. Kranz, et al. (2003). "Identification of farnesoid X receptor β as a novel mammalian nuclear receptor sensing lanosterol." Molecular and Cellular Biology **23**: 864-872.

Overton, H. A., A. J. Babbs, et al. (2006). "Deorphanization of a G protein-coupled receptor for oleoylethanolamide and its use in the discovery of small-molecule hypophagic agents." Cell Metab **3**(3): 167-75.

Permutt, M. A., L. Koranyi, et al. (1989). "Cloning and functional expression of a human pancreatic islet glucose-transporter cDNA." Proc Natl Acad Sci U S A **86**(22): 8688-92.

Petkovich, M., N. J. Brand, et al. (1987). "A human retinoic acid receptor which belongs to the family of nuclear receptors." Nature **330**(6147): 444-50.

Petrescu, A. D., R. Hertz, et al. (2002). "Ligand specificity and conformational dependence of the hepatic nuclear factor-4alpha (HNF-4alpha)." J Biol Chem **277**(27): 23988-99.

Philippe, J. and M. Missotten (1990). "Dexamethasone inhibits insulin biosynthesis by destabilizing insulin messenger ribonucleic acid in hamster insulinoma cells." Endocrinology **127**(4): 1640-5.

Pi, M., P. Faber, et al. (2005). "Identification of a novel extracellular cation-sensing G-protein-coupled receptor." J Biol Chem **280**(48): 40201-9.

Picard, F., M. Wanatabe, et al. (2002). "Progesterone receptor knockout mice have an improved glucose homeostasis secondary to beta -cell proliferation." Proc Natl Acad Sci U S A **99**(24): 15644-8.

Poitout, V., L. E. Stout, et al. (1995). "Morphological and functional characterization of βTC-6 cells- an insulin-secreting cell line derived from transgenic mice." Diabetes **44**: 306-313.

Potter, G. D., J. H. Sellin, et al. (1991). "Bile acid stimulation of cyclic AMP and ion transport in developing rabbit colon." J Pediatr Gastroenterol Nutr **13**(4): 335-41.

Powers, A. C., S. Efrat, et al. (1990). "Proglucagon processing similar to normal islets in pancreatic α-like cell line derived from transgenic mouse tumor." Diabetes **39**: 406-414.

Qader, S. S., R. Hakanson, et al. (2008). "Proghrelin-derived peptides influence the secretion of insulin, glucagon, pancreatic polypeptide and somatostatin: a study on isolated islets from mouse and rat pancreas." Regul Pept **146**(1-3): 230-7.

Ravnskjaer, K., M. Boergesen, et al. (2005). "Peroxisome proliferator-activated receptor α (PPARα) potentiates, whereas PPARγ attneuates, glucose-

stimulated insulin secretion in pancreatic β-cells." Endocrinology **146**: 3266-3276.

Repa, J. J., G. Liang, et al. (2000). "Regulation of mouse sterol regulatory element-binding protein-1c gene (SREBP-1c) by oxysterol receptors, LXRalpha and LXRbeta." Genes Dev **14**(22): 2819-30.

Repa, J. J., M. Makishima, et al. (2001). Orphan nuclear receptors and the regulation of cholesterol and bile acid metabolism. The Liver: Biology and Pathobiology. I. M. Arias, J. L. Boyer, F. V. Chisariet al. Philadelphia, Lippincott Williams & Wilkins**:** 1027-1038.

Repa, J. J. and D. J. Mangelsdorf (2000). "The role of orphan nuclear receptors in the regulation of cholesterol homeostasis." Annual Reviews in Cell and Developmental Biology **16**: 459-481.

Robinson-Rechavi, M., A.-S. Carpentier, et al. (2001). "How many nuclear hormone receptors are there in the human genome?" Trends in Genetics **17**: 554-556.

Roduit, R., J. Morin, et al. (2000). "Glucose down-regulates the expression of the peroxisome proliferator-activated receptor-α gene in the pancreatic β-cell." Journal of Biological Chemistry **275**: 35799-35806.

Saegusa, C., M. Fukuda, et al. (2002). "Synaptotagmin V is targeted to dense-core vesicles that undergo calcium-dependent exocytosis in PC12 cells." J Biol Chem **277**(27): 24499-505.

Sakamoto, Y., H. Inoue, et al. (2006). "Expression and distribution of Gpr119 in the pancreatic islets of mice and rats: predominant localization in pancreatic polypeptide-secreting PP-cells." Biochem Biophys Res Commun **351**(2): 474-80.

Sandberg, M. and L. A. Borg (2007). "Steroid effects on intracellular degradation of insulin and crinophagy in isolated pancreatic islets." Mol Cell Endocrinol **277**(1-2): 35-41.

Sandberg, M. B., J. Fridriksson, et al. (2005). "Glucose-induced lipogenesis in pancreatic β-cells is dependent on SREBP-1." Molecular and Cellular Endocrinology **240**: 94-106.

Satoh, S., S. Masatoshi, et al. (2007). "Identification of *cis*-regulatory elements and *trans*-acting proteins of the rat *carbohydrate response element binding protein* gene." Archives of Biochemistry and Biophysics **on-line**.

Shalev, A., C. A. Pise-Masison, et al. (2002). "Oligonucleotide microarray analysis of intact human pancreatic islets: identification of glucose-responsive genes and a highly regulated TGFβ signaling pathway." Endocrinology **143**: 3695-3698.

Shih, D. Q., H. M. Dansky, et al. (2000). "Genotype/phenotype relationships in HNF-4α/MODY1." Diabetes **49**: 832-837.

Shih, D. Q., M. Heimesaat, et al. (2002). "Profound defects in pancreatic b-cell function in mice with combined heterozygous mutations in Pdx-1, Hnf-1a, and Hnf-3b." Proceedings of the National Academy of Sciences USA **99**: 3818-3823.

Shimabukuro, M., Y.-T. Zhou, et al. (1998). "Troglitazone lowers islet fat and restores beta cell function of Zucker diabetic fatty rats." Journal of Biological Chemistry **273**: 3547-3550.

Shyamsundar, R., Y. H. Kim, et al. (2005). "A DNA microarray survey of gene expression in normal human tissues." Genome Biology **6**: R22.

Singh, V., C. Grotzinger, et al. (2007). "Somatostatin receptor subtype-2-deficient mice with diet-induced obesity have hyperglycemia, nonfasting hyperglucagonemia, and decreased hepatic glycogen deposition." Endocrinology **148**(8): 3887-99.

Sladek, F. M., W. M. Zhong, et al. (1990). "Liver-enriched transcription factor HNF-4 is a novel member of the steroid hormone receptor superfamily." Genes Dev **4**(12B): 2353-65.

Soga, T., T. Ohishi, et al. (2005). "Lysophosphatidylcholine enhances glucose-dependent insulin secretion via an orphan G-protein-coupled receptor." Biochem Biophys Res Commun **326**(4): 744-51.

Stoeckman, A. K., L. Ma, et al. (2004). "Mlx is the functional heteromeric partner of the carbohydrate response element-binding protein in glucose regulation of lipogenic enzyme genes." J Biol Chem **279**(15): 15662-9.

Stoltzman, C. A., C. W. Peterson, et al. (2008). "Glucose sensing by MondoA:Mlx complexes: a role for hexokinases and direct regulation of thioredoxin-interacting protein expression." Proc Natl Acad Sci U S A **105**(19): 6912-7.

Su, A. I., M. P. Cooke, et al. (2002). "Large-scale analysis of the human and mouse transcriptomes." Proceedings of the National Academy of Sciences USA **99**: 4465-4470.

Suh, Y. H., S. Y. Kim, et al. (2004). "Overexpression of short heterodimer partner recovers impaired glucose-stimulated insulin secretion of pancreatic beta-cells overexpressing UCP2." J Endocrinol **183**(1): 133-44.

Takata, Y., J. Liu, et al. (2008). "PPARdelta-mediated antiinflammatory mechanisms inhibit angiotensin II-accelerated atherosclerosis." Proc Natl Acad Sci U S A **105**(11): 4277-82.

Tanaka, T., J. Yamamoto, et al. (2003). "Activation of peroxisome proliferator-activated receptor δ induces fatty acid β-oxidation in skeletal muscle and attenuates metabolic syndrome." Proceedings of the National Academy of Sciences USA **100**: 15924-15929.

Tanaka, T., J. Yamamoto, et al. (2003). "Activation of peroxisome proliferator-activated receptor delta induces fatty acid beta-oxidation in skeletal

muscle and attenuates metabolic syndrome." Proc Natl Acad Sci U S A **100**(26): 15924-9.

Taraviras, S., T. Mantamadiotis, et al. (2000). "Primary structure, chromosomal mapping, expression and transcriptional activity of murine hepatocyte nuclear factor 4gamma." Biochim Biophys Acta **1490**(1-2): 21-32.

Taraviras, S., A. P. Monaghan, et al. (1994). "Characterization of the mouse HNF-4 gene and its expression during mouse embryogenesis." Mech Dev **48**(2): 67-79.

Thomas, H., K. Jaschkowitz, et al. (2001). "A distant upstream promoter of the HNF-4alpha gene connects the transcription factors involved in maturity-onset diabetes of the young." Hum Mol Genet **10**(19): 2089-97.

Tordjman, K., K. N. Standley, et al. (2002). "PPARα suppresses insulin secretion and induces UCP2 in insulinoma cells." Journal of Lipid Research **43**: 936-943.

Tseng, C. C. and X. Y. Zhang (1998). "Role of regulator of G protein signaling in desensitization of the glucose-dependent insulinotropic peptide receptor." Endocrinology **139**(11): 4470-5.

Tseng, C. C. and X. Y. Zhang (2000). "Role of G protein-coupled receptor kinases in glucose-dependent insulinotropic polypeptide receptor signaling." Endocrinology **141**(3): 947-52.

Umesono, K., K. K. Murakami, et al. (1991). "Direct repeats as selective response elements for the thyroid hormone, retinoic acid, and vitamin D3 receptors." Cell **65**(7): 1255-66.

Uyeda, K. and J. J. Repa (2006). "Carbohydrate response element binding protein, ChREBP, a transcription factor coupling hepatic glucose utilization and lipid synthesis." Cell Metab **4**(2): 107-10.

Valasek, M. A. and J. J. Repa (2005). "The power of real-time PCR." Advances in Physiology Education **29**: 151-159.

Verga Falzacappa, C., E. Petrucci, et al. (2007). "Thyroid hormone receptor TRbeta1 mediates Akt activation by T3 in pancreatic beta cells." J Mol Endocrinol **38**(1-2): 221-33.

Vu-Dac, N., K. Schoonjans, et al. (1995). "Fibrates increase human apolipoprotein A-II expression through activation of the peroxisome proliferator-activated receptor." J Clin Invest **96**(2): 741-50.

Wagner, B. L., A. F. Valledor, et al. (2003). "Promoter-specific roles for liver X receptor/corepressor complexes in the regulation of ABCA1 and SREBP1 gene expression." Mol Cell Biol **23**(16): 5780-9.

Wang, H., G. Kouri, et al. (2005). "ER stress and SREBP-1 activation are implicated in β-cell glucolipotoxicity." Journal of Cell Science **118**: 3905-3915.

Wang, H., P. Maechler, et al. (2000). "Hepatocyte nuclear factor 4α regulates the expression of pancreatic β-cell genes implicated in glucose metabolism and nutrient-induced insulin secretion." Journal of Biological Chemistry **275**: 35953-35959.

Wang, H. and C. B. Wollheim (2002). "ChREBP rather than USF2 regulates glucose stimulation of endogenous L-pyruvate kinase expression in insulin-secreting cells." J Biol Chem **277**(36): 32746-52.

Wang, H. and C. B. Wollheim (2002). "ChREBP rather than USF2 regulates glucose stimulation of endogenous L-pyruvate kinase expression in insulin-secreting cells." Journal of Biological Chemistry **277**: 32746-32752.

Wang, L., C. Coffinier, et al. (2004). "Selective deletion of the *Hnf1β* (MODY5) gene in β-cells leads to altered gene expression and defective insulin release." Endocrinology **145**: 3941-3949.

Wang, Y. X., C. H. Lee, et al. (2003). "Peroxisome-proliferator-activated receptor delta activates fat metabolism to prevent obesity." Cell **113**(2): 159-70.

Watanabe, M., S. M. Houten, et al. (2006). "Bile acids induce energy expenditure by promoting intracellular thyroid hormone activation." Nature **439**(7075): 484-9.

Webb, G. C., M. S. Akbar, et al. (2000). "Expression profiling of pancreatic β cells: glucose regulation of secretory and metabolic pathway genes." Proceedings of the National Academy of Sciences USA **97**: 5773-5778.

Weinberger, C., S. M. Hollenberg, et al. (1985). "Identification of human glucocorticoid receptor complementary DNA clones by epitope selection." Science **228**(4700): 740-2.

Weir, G. C. and S. Bonner-Weir (2004). "Five stages of evolving beta-cell dysfunction during progression to diabetes." Diabetes **53 Suppl 3**: S16-21.

Wente, W., A. M. Efanov, et al. (2006). "Fibroblast growth factor-21 improves pancreatic β-cell function and survival by activation of extracellular signal-regulated kinase 1/2 and akt signaling pathways." Diabetes **55**: 2470-2478.

Wierup, N., H. Svensson, et al. (2002). "The ghrelin cell: a novel developmentally regulated islet cell in the human pancreas." Regul Pept **107**(1-3): 63-9.

Willy, P. J., K. Umesono, et al. (1995). "LXR, a nuclear receptor that defines a distinct retinoid response pathway." Genes Dev **9**(9): 1033-45.

Winborn, W. B., P. J. Sheridan, et al. (1983). "Estrogen receptors in the islets of Langerhans of baboons." Cell Tissue Res **230**(1): 219-23.

Winborn, W. B., P. J. Sheridan, et al. (1987). "Localization of progestin receptors in the islets of Langerhans." Pancreas **2**(3): 289-94.

Wisely, G. B., A. B. Miller, et al. (2002). "Hepatocyte nuclear factor 4 is a transcription factor that constitutively binds fatty acids." Structure **10**(9): 1225-34.

Wu, F., T. Dassopoulos, et al. (2007). "Genome-wide gene expression differences in Crohn's disease and ulcerative colitis from endoscopic pinch biopsies: insights into distinctive pathogenesis." Inflamm Bowel Dis **13**(7): 807-21.

Xu, J., J. Han, et al. (2006). "Regulation of PDK mRNA by high fatty acid and glucose in pancreatic islets." Biochemical and Biophysical Research Communications **344**: 827-833.

Xu, J., T. Mashimo, et al. (2007). "Synaptotagmin-1, -2, and -9: Ca(2+) sensors for fast release that specify distinct presynaptic properties in subsets of neurons." Neuron **54**(4): 567-81.

Xu, L., C. K. Glass, et al. (1999). "Coactivator and corepressor complexes in nuclear receptor function." Curr Opin Genet Dev **9**(2): 140-7.

Yada, T., K. Dezaki, et al. (2008). "Ghrelin regulates insulin release and glycemia: physiological role and therapeutic potential." Curr Diabetes Rev **4**(1): 18-23.

Yamagata, K., H. Furuta, et al. (1996). "Mutations in the hepatocyte nuclear factor-4alpha gene in maturity-onset diabetes of the young (MODY1)." Nature **384**(6608): 458-60.

Yang, X., M. Downes, et al. (2006). "Nuclear receptor expression links the circadian clock to metabolism." Cell **126**: 801-810.

Yoon, J. C., G. Xu, et al. (2003). "Suppression of β cell energy metabolism and insulin release by PGC-1α." Developmental Cell **5**: 75-83.

Yoshikawa, H., Y. Tajiri, et al. (2001). "Effects of bezafibrate on beta-cell function of rat pancreatic islets." Eur J Pharmacol **426**(3): 201-6.

Yoshikawa, H., Y. Tajiri, et al. (2001). "Effects of free fatty acids on beta-cell functions: a possible involvement of peroxisome proliferator-activated receptors alpha or pancreatic/duodenal homeobox." Metabolism **50**(5): 613-8.

Zhang, C., T. Moriguchi, et al. (2005). "MafA is a key regulator of glucose-stimulated insulin secretion." Molecular and Cellular Biology **25**: 4969-4976.

Zhang, J. V., P. G. Ren, et al. (2005). "Obestatin, a peptide encoded by the ghrelin gene, opposes ghrelin's effects on food intake." Science **310**(5750): 996-9.

Zhang, P., M. Bennoun, et al. (2002). "Expression of COUP-TFII in metabolic tissues during development." Mech Dev **119**(1): 109-14.

Zhang, W., Q. D. Morris, et al. (2004). "The functional landscape of mouse gene expression." Journal of Biology **3**: 21.

Zhang, Y., F. Y. Lee, et al. (2006). "Activation of the nuclear receptor FXR improves hyperglycemia and hyperlipidemia in diabetic mice." Proceedings of the National Academy of Sciences USA **103**: 1006-1011.

Zhao, H., Z. Li, et al. (2007). "Orphan nuclear receptor function in the ovary." Frontiers in Bioscience **12**: 3398-3405.

Zhao, X., J. Huang, et al. (1998). "Molecular forms of human rhodopsin kinase (GRK1)." J Biol Chem **273**(9): 5124-31.

Zhou, Y. T., M. Shimabukuro, et al. (1998). "Role of peroxisome proliferator-activated receptor alpha in disease of pancreatic beta cells." Proc Natl Acad Sci U S A **95**(15): 8898-903.